NASA
Technical
Paper
3347

May 1993

The Dynamic Phenomena of a Tethered Satellite

NASA's First Tethered Satellite Mission (TSS-1)

R. S. Ryan,
D. K. Mowery,
and D. D. Tomlin

NASA

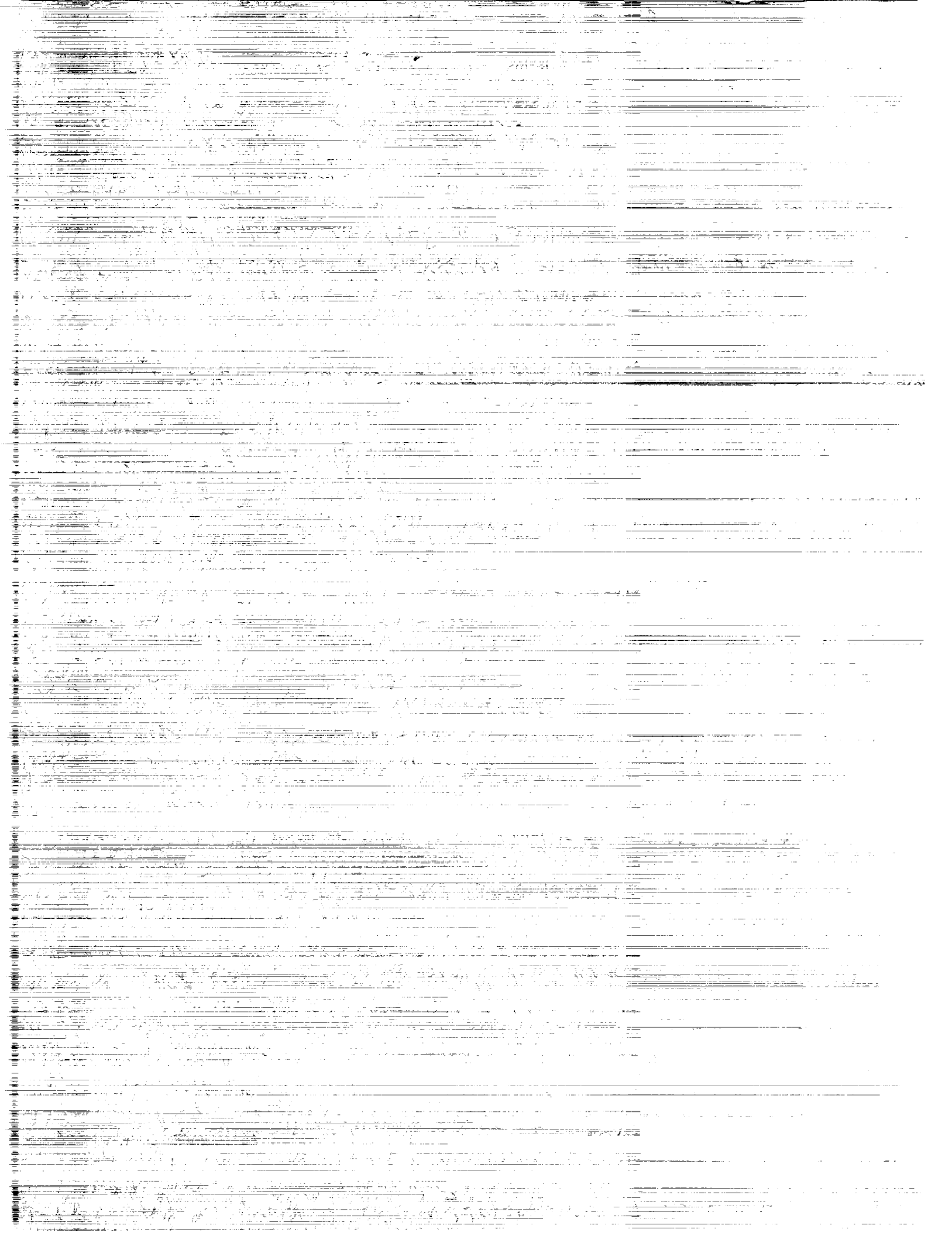

NASA Technical Paper 3347

1993

The Dynamic Phenomena of a Tethered Satellite

NASA's First Tethered Satellite Mission (TSS-1)

R. S. Ryan,
D. K. Mowery,
and D. D. Tomlin
George C. Marshall Space Flight Center
Marshall Space Flight Center, Alabama

National Aeronautics and Space Administration
Office of Management
Scientific and Technical Information Program

TABLE OF CONTENTS

LIST OF ILLUSTRATIONS

LIST OF ILLUSTRATIONS (Continued)

LIST OF ILLUSTRATIONS (Continued)

LIST OF ILLUSTRATIONS (Continued)

LIST OF ILLUSTRATIONS (Continued)

LIST OF ILLUSTRATIONS (Continued)

LIST OF TABLES

TECHNICAL PAPER

THE DYNAMIC PHENOMENA OF A TETHERED SATELLITE NASA'S FIRST TETHERED SATELLITE MISSION (TSS-1)

I. INTRODUCTION

Dynamics of a tethered satellite system are complex in that many modes exist both from a rigid-body dumbbell assumption and from an elastic phenomenon standpoint including the tether and the attached bodies. In the initial phases of the tethered satellite project, the major effort was expended on developing the satellite, understanding the basic rigid-body modes of a tethered system, and designing the deployment/retrieval mechanism, reel, tether, and other necessary components contained in the orbiter payload bay. This was no small feat, because many mechanism problems occurred during development. During this time period, it became clear that as the tether current flowed to achieved science, it created an electric field around the tether that interacted with the Earth's magnetic field, causing deflections that can evolve into a dynamic oscillation called "skiprope." The word was coined after the child's skiprope due to the parallel characteristics. The tether itself has very small inherent damping, therefore, once the oscillation started, it would continue for long periods of time. It would also grow in an angular sense when retrieved, because angular momentum is conserved, resulting in larger amplitudes as the satellite gets closer to the orbiter. This presented two potential problems: (1) skiprope could prevent docking the satellite by introducing large satellite angles due to the coupling between the satellite pendulous mode and the first lateral skiprope mode at 400-m tether length, and (2) the large skiprope amplitude could become entangled with the orbiter, especially if the satellite could not be docked and had to be cut loose from the orbiter.

A means of controlling the satellite and damping the skiprope had to be designed and baselined to ensure mission success. This was accomplished under Marshall Space Flight Center (MSFC) leadership through the Dynamics and Control Working Group (DWG) chaired by D.K. Mowery. Membership included personnel from MSFC, Johnson Space Center (JSC), Martin Marietta, the Smithsonian Astrophysical Observatory, Lang Associates, Logicon, and with occasional participation by Alenia. Implementation of the dynamic control techniques into operational procedures using the shuttle crew was accomplished by the Flight Techniques Panel chaired by Chuck Shaw, the Flight Director for TSS-1. Several members of the DWG were also members of the Flight Techniques Panel which enhanced communications.

Overall integration of the dynamics was achieved through a series of Technical Interchange Meetings (TIM's) lead by MSFC. All parties, including the flight crew, participated in these meetings. Various dynamics experts/consultants were used throughout the DWG activities.

The total project was managed by NASA MSFC through the Tethered Satellite System (TSS) Project Office. The satellite was designed and built by the Italians. All the mechanisms for transporting the satellite via the space shuttle, deploying it, and recovery by reeling it into the orbiter using the tether were designed, built, and tested by Martin Marietta Astronautics Group located in Denver, CO. JSC was responsible for the operational aspects of the mission.

Acknowledgment is due to the prime contractor, Martin Marietta, for many of the figures and most of the simulation results displayed in this document, as well as to the "Tethers in Space Handbook"[1] from which several of the figures have been taken.

II. TETHERED SATELLITE DEFINITION/CHARACTERISTICS/MISSION

A. Satellite

The satellite itself is spherical in shape, containing numerous scientific instruments, antennas, the reaction control system with appropriate sensors, and the tether attach mechanism. The basic features of the satellites are shown in figures 1 and 2. The attitude control system is composed of four rate-integrating gyros with feedback, horizon scanner (Earth scanners), accelerometer, and magnetometers, with thrusters (reaction jets) in the positions needed for attitude control, science, and tether deployment. Three gyros are aligned to the satellite axes, the fourth is skewed to preclude saturation (above 2°/s) during spin. The accelerometers were telemetered for science instrumentation as were the magnetometers which were also used as inputs to the skiprope observer. There are eight thruster groups (figs. 3 and 4). Four nozzles are in-plane (pitch), four are yaw, two are out-of-plane (roll), and four are in-line. The tension is maintained during operations by gravity/centrifugal forces and in-line thrust.

B. Support and Deployer Mechanisms

The satellite support structure and deployer are shown undeployed in figure 5. Figure 6 shows the satellite on the tip of the deployer boom. Figure 7 is an end view of the same configuration. More details of the undeployed system are shown in figure 8. Figure 9 shows the tether with Nomex core, the copper conductor covered by a 0.012-in thick insulation and wound with 10 strands of Kevlar, then braided on the outside with Nomex. Figure 10 shows the 12-m deployment boom, docking ring, U-2 tether guard, tether, concentric ring damper for damping close-in skiprope, and the satellite. Figure 11 is a more detailed schematic of the satellite support structure. Figure 12 is a schematic showing the tether control system components. The lower control and upper control mechanisms, reel assembly, and level wind mechanism are depicted. Figure 13 illustrates the reel support structure and reel, figure 14 is the lower control mechanism, figure 15 is the upper control mechanism, and figure 16 is the level wind mechanism.

The purpose of these mechanisms and structure is threefold: (1) to provide a means of transportation in the orbiter; (2) to serve as an operational base for the deployer and, through the pallet, as an interface with the orbiter; and (3) to deploy and retrieve the satellite. In order to move the deployer docking support away from the orbiter during operations, an extendible boom is used.

C. Science Objectives

The prime objective of the TSS-1 mission was to demonstrate the capability to deploy a 525-kg (1,100-lb) tethered satellite to a distance of 20 km (12 miles) above the space shuttle, acquire scientific and operational data, and return the satellite to the shuttle for reuse. In conjunction with this primary objective, several technical and scientific objectives were defined (fig. 17).

Function:

The TSS Satellite is a Spherical Multimission Payload Able to Carry Experiments With Different Mission Characteristics. The Satellite Has a Radius of 800 mm And Weighs Approximately 513 Kg.

The Satellite S-band Antenna Is in the Satellite Flight Direction.

When the Satellite is Latched, The S-band Antenna is 179° From Orbiter Flight Direction.

Distinctive Black Markings Are Painted on the White Satellite Skin to Aid Attitude Resolution for Docking.

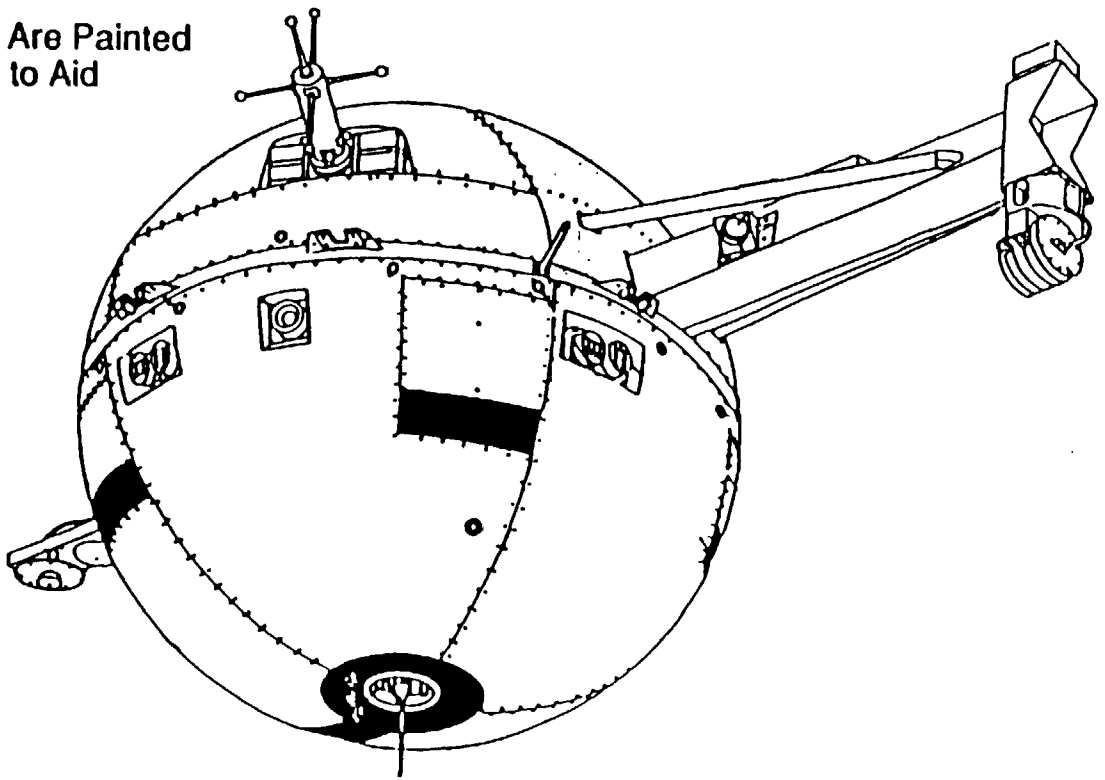

Figure 1. Tethered satellite.

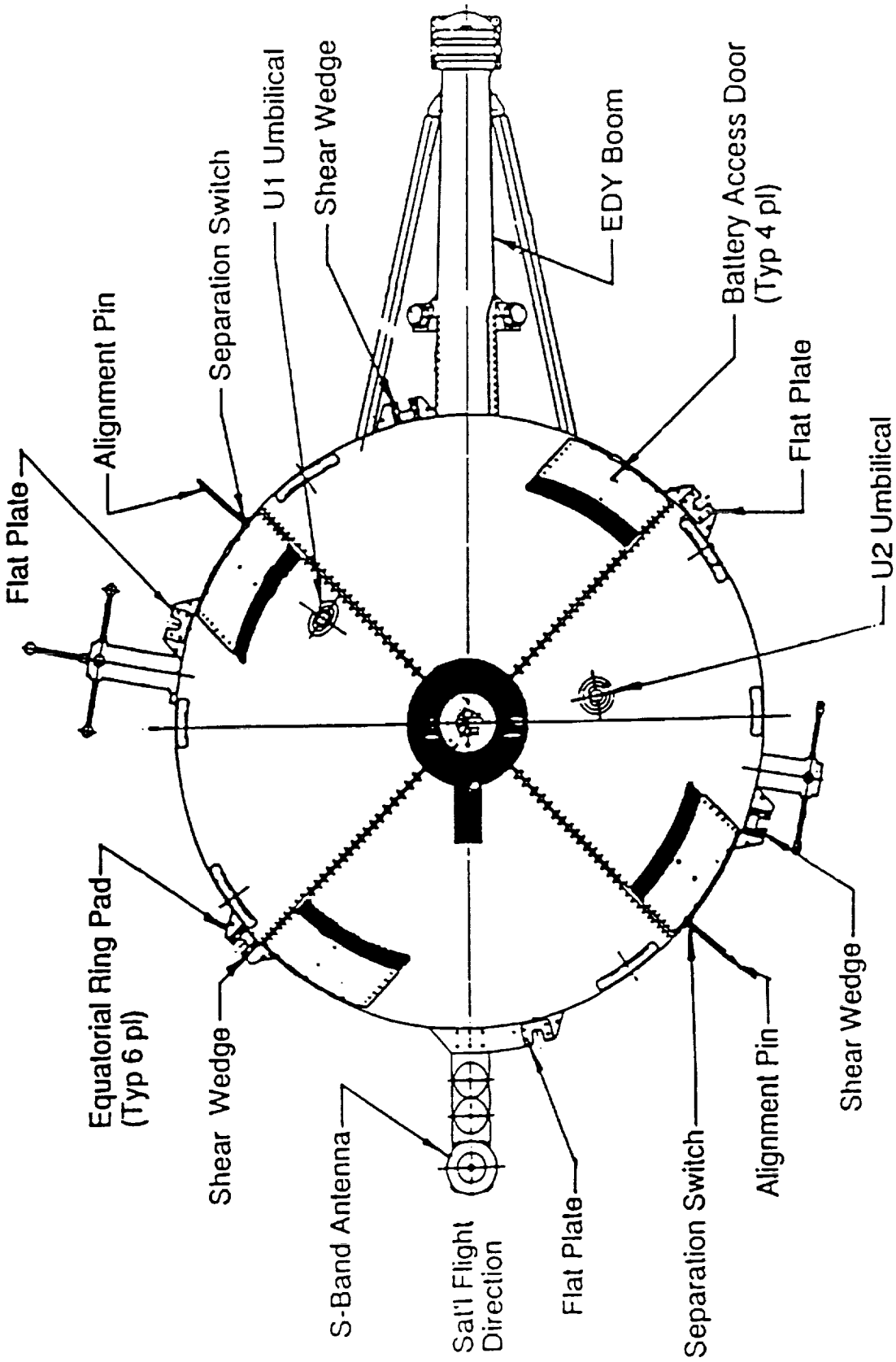

Figure 2. Tethered satellite (view from orbiter).

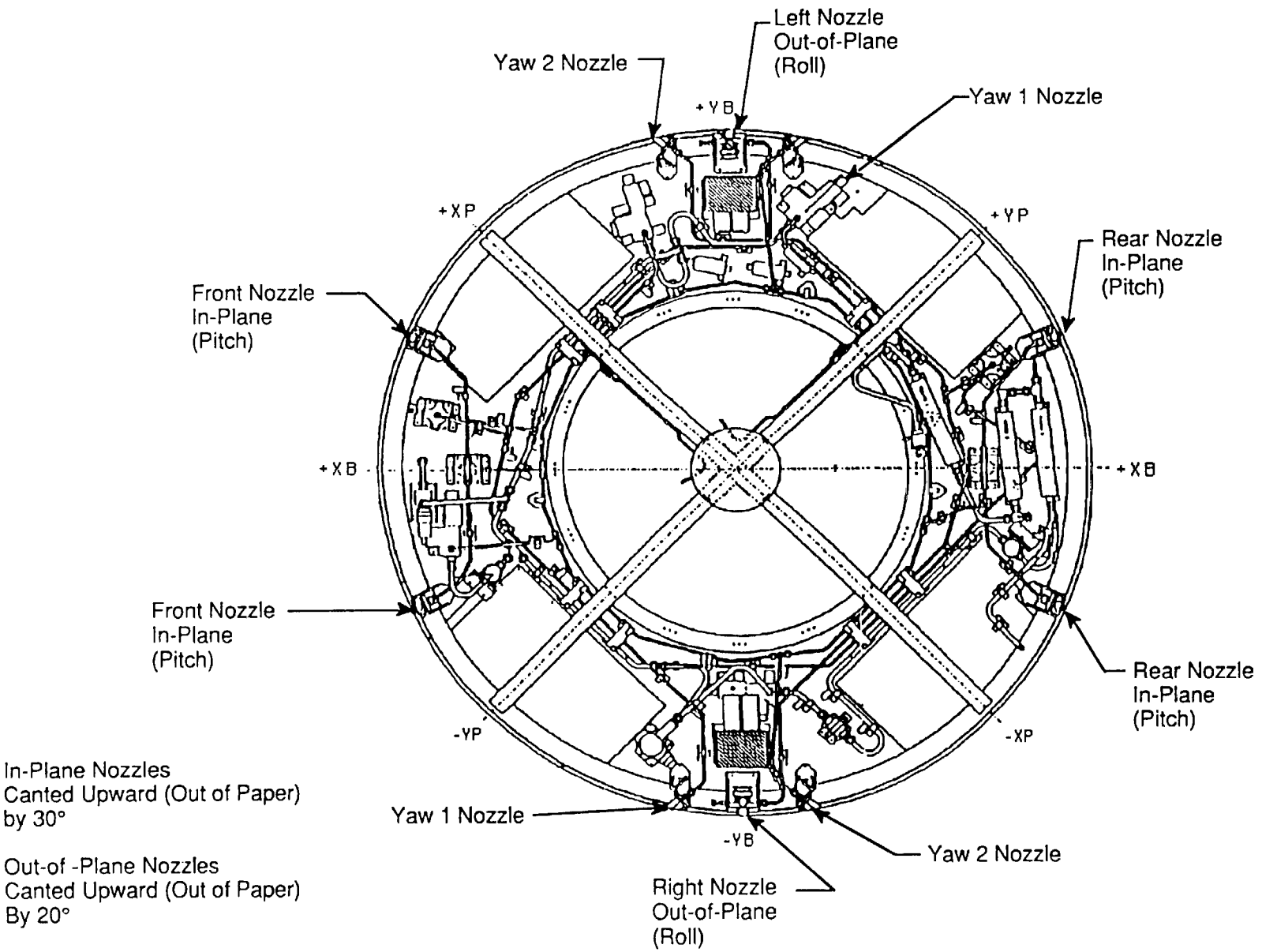

Figure 3. Tethered satellite auxiliary propulsion system.

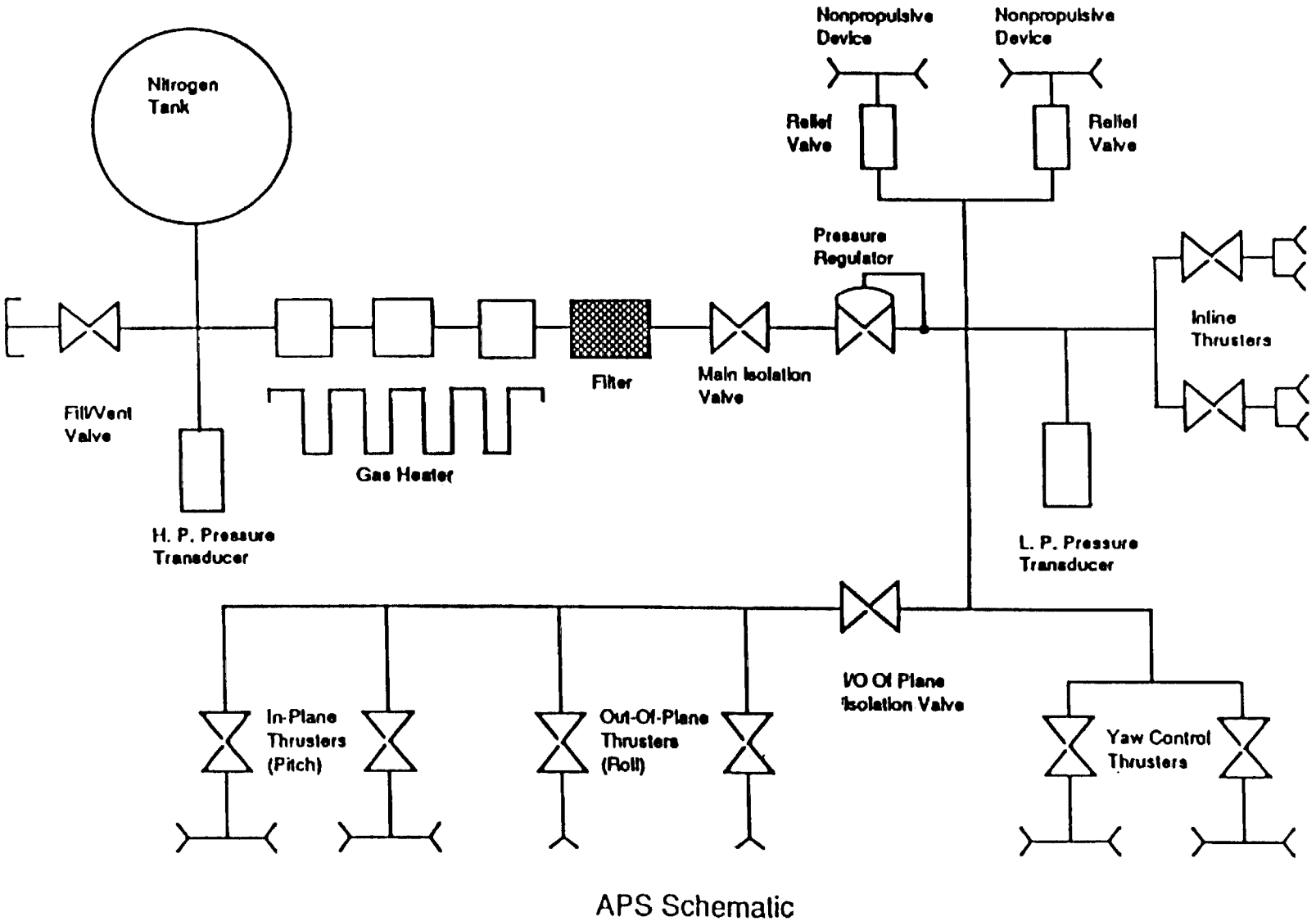

Figure 4. Tethered satellite auxiliary propulsion system schematic.

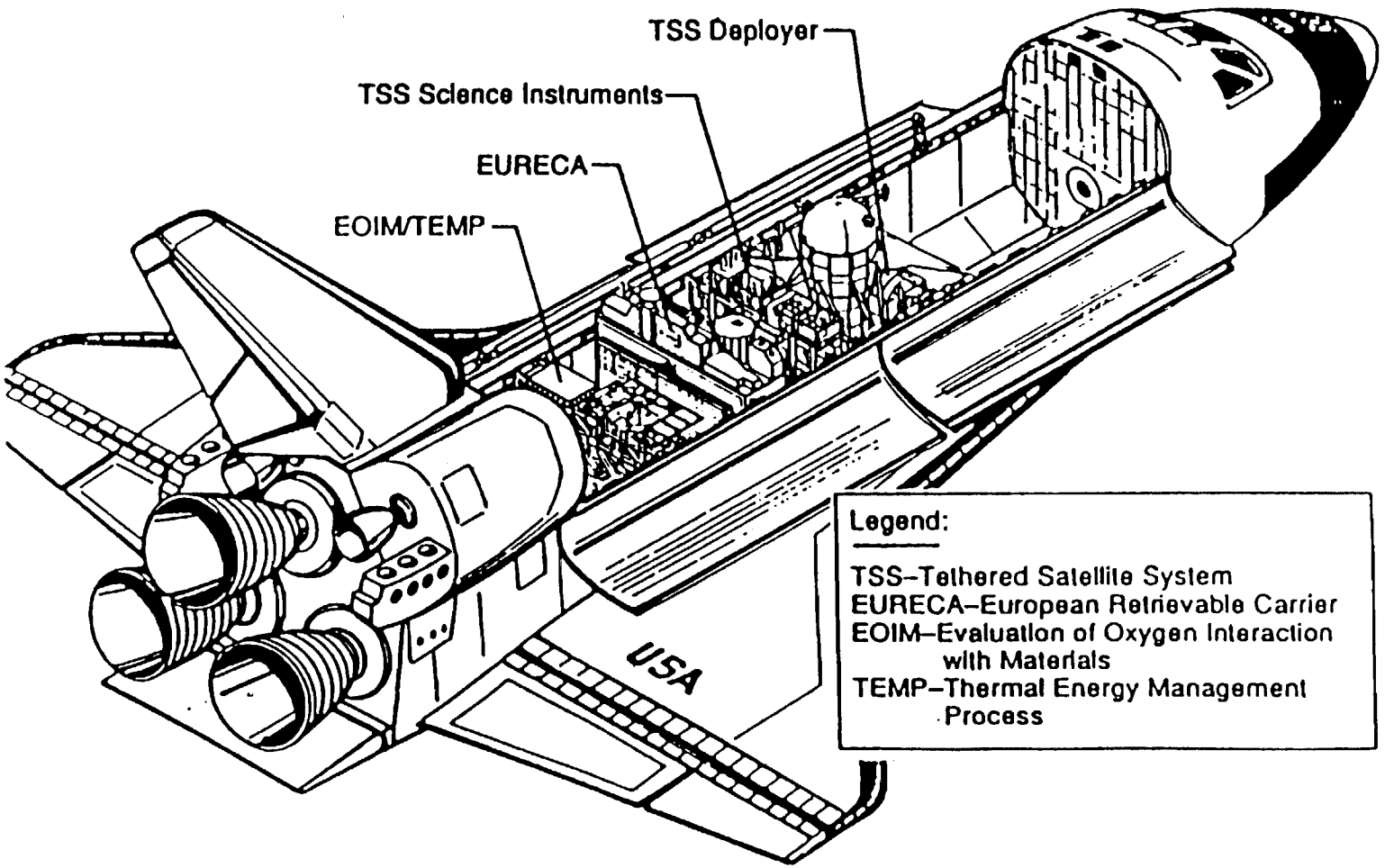

Figure 5. Cargo bay view of orbiter for TSS-1 mission.

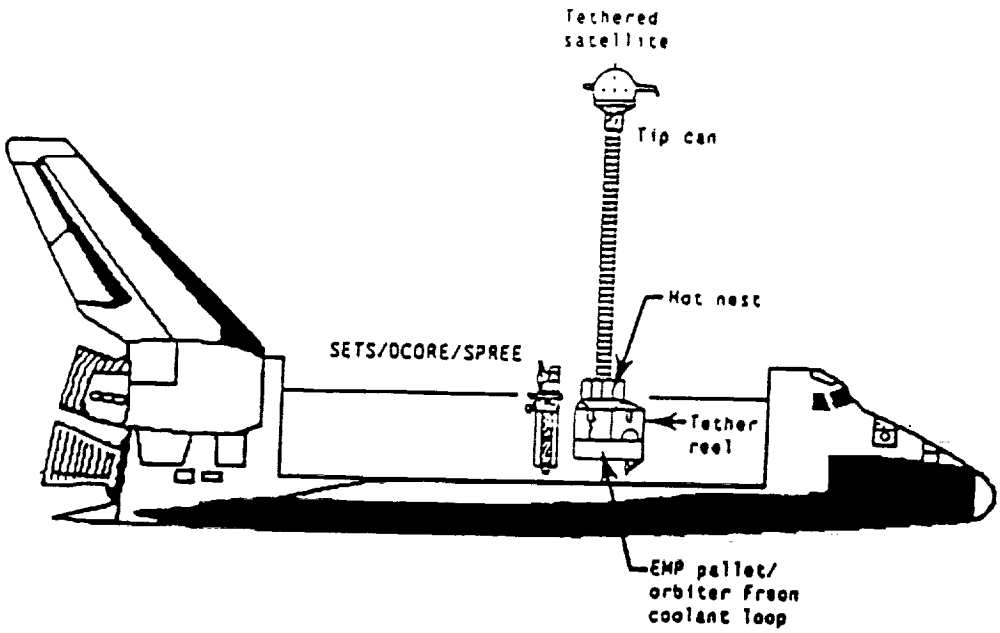

Figure 6. TSS predeploy configuration.

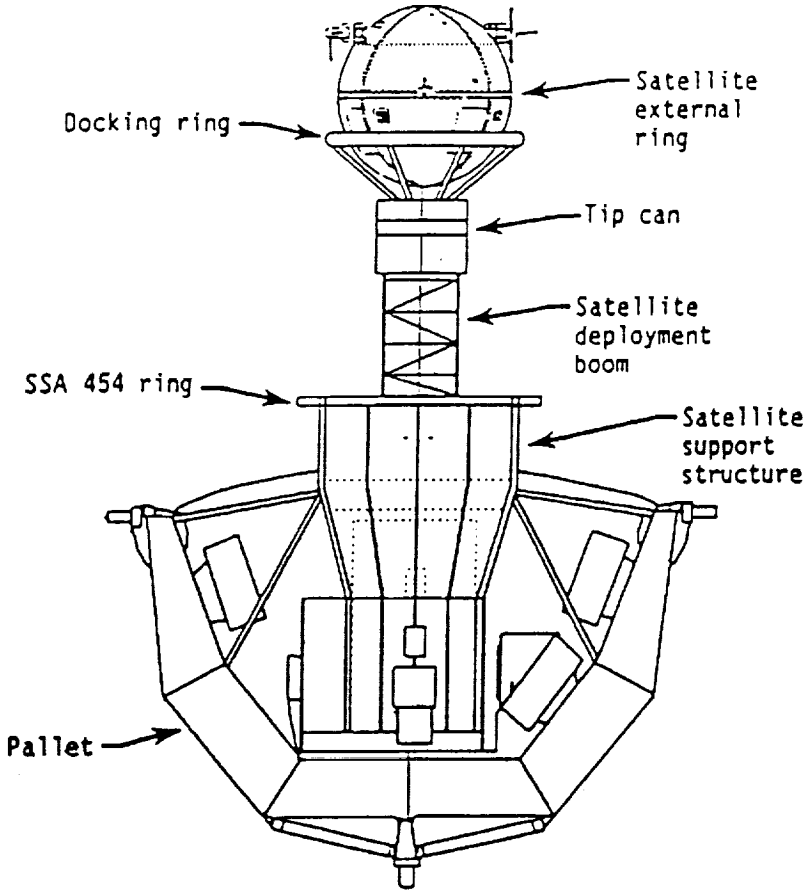

Figure 7. Satellite and deployer on enhanced multiplexer-demultiplexer pallet (EMP).

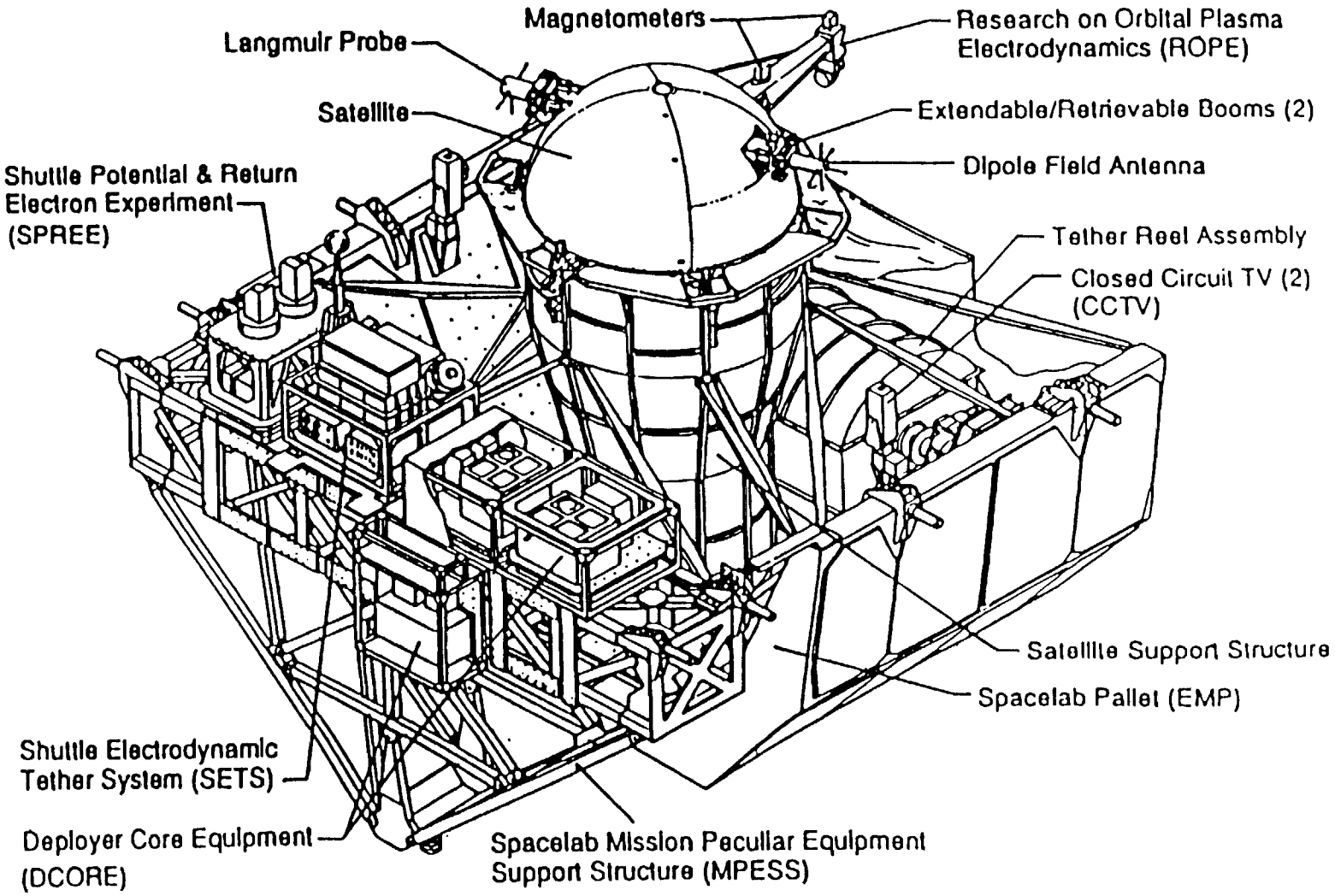

Figure 8. TSS-1 mission configuration shown with science instruments on EMPESS.

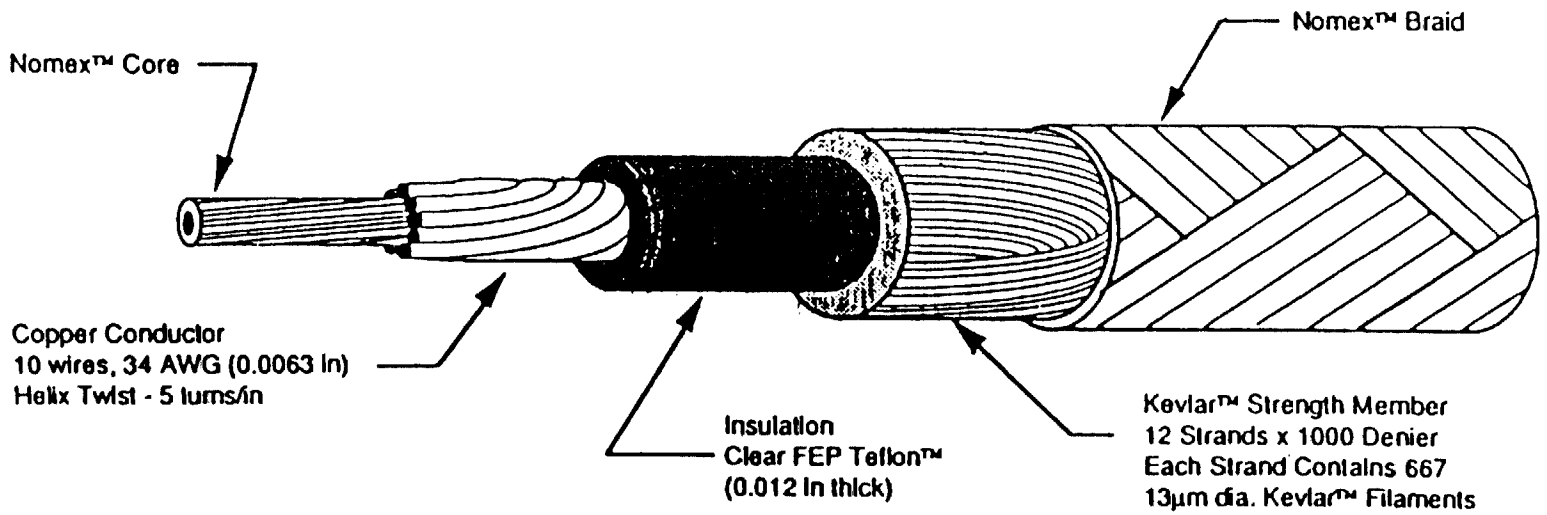

Diameter	2.54 mm (0.1 in)
Max Mass	8.2 kg/km (.0055 lb/ft or 29.0 lb/mile)
Breakstrength	1780 N (400 lb)
Temp Range	-100°C to +100°C (148°F to +257°F)
Max Elongation	5% @ 1780 N
Elec Breakdown Voltage	10 kV (specified), 15 kV (qual)
Elec Resistance	0.12 Ω/m (specified) 0.015 Ω/m (actual @ room temp)
Current Limit	5 mA (max) leakage @ 10 kVdc

Figure 9. Tether for the TSS-1 mission.

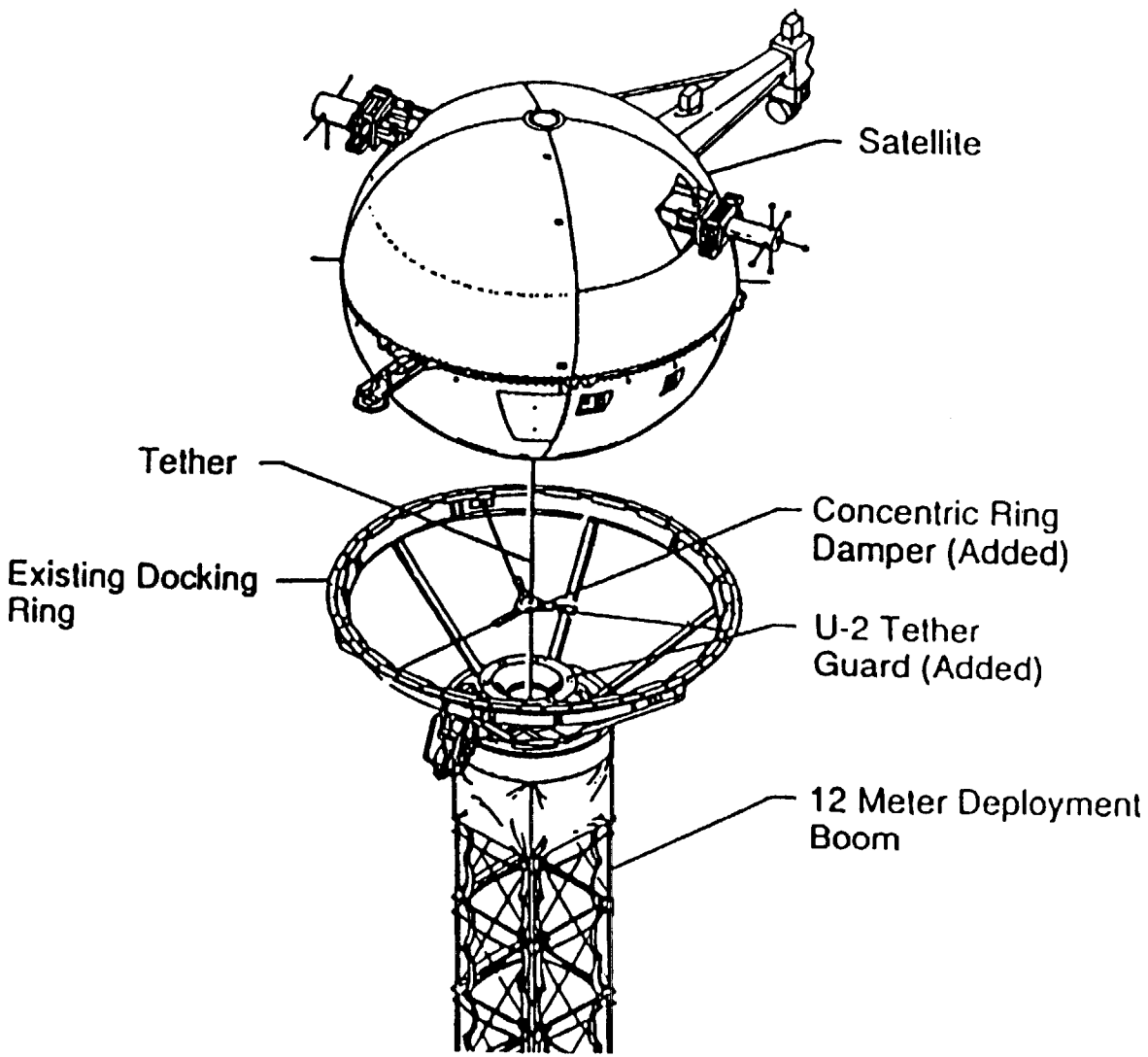

Figure 10. TSS satellite partially deployed.

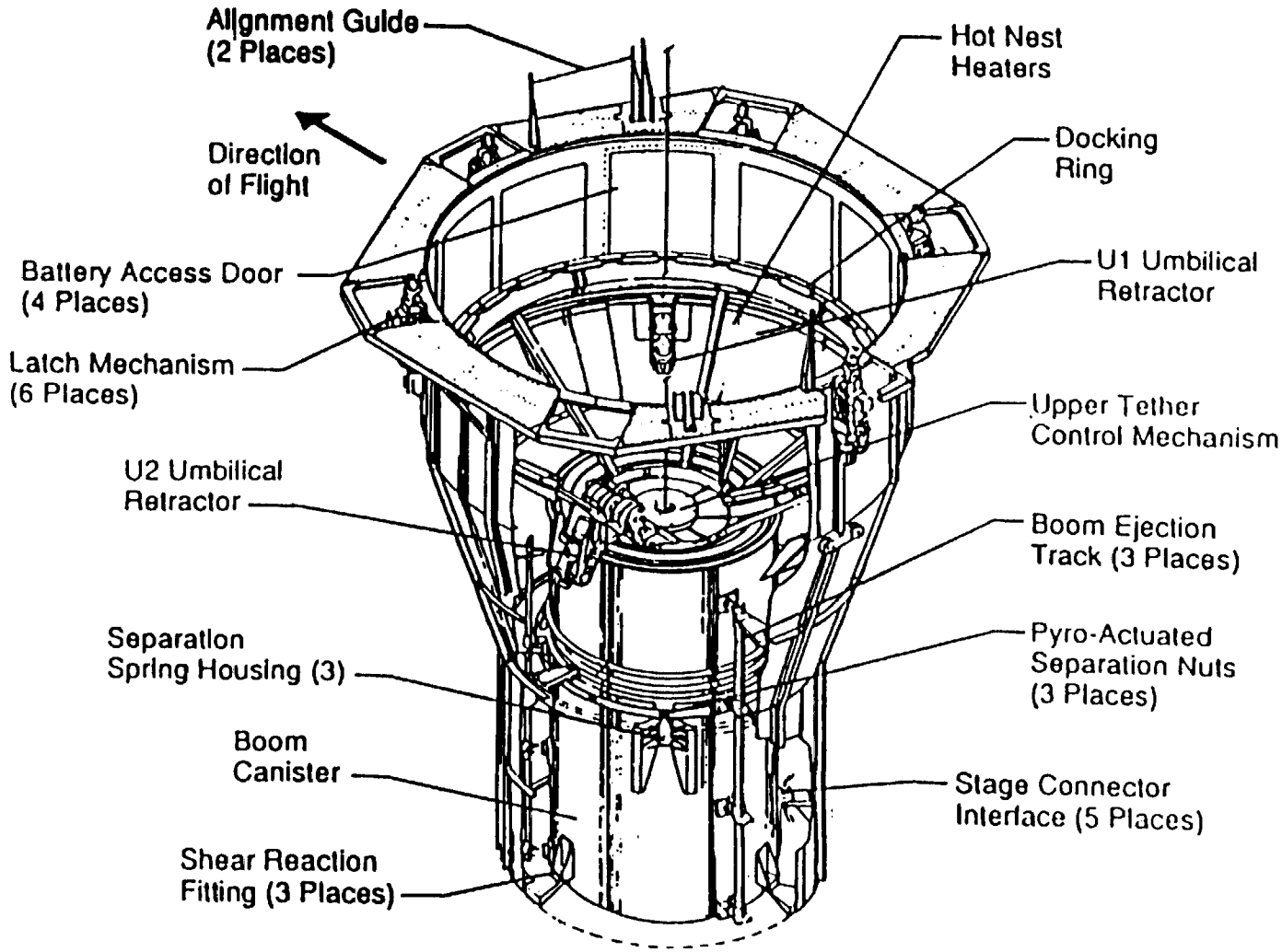

Figure 11. Satellite support structure in the satellite attachment to the pallet.

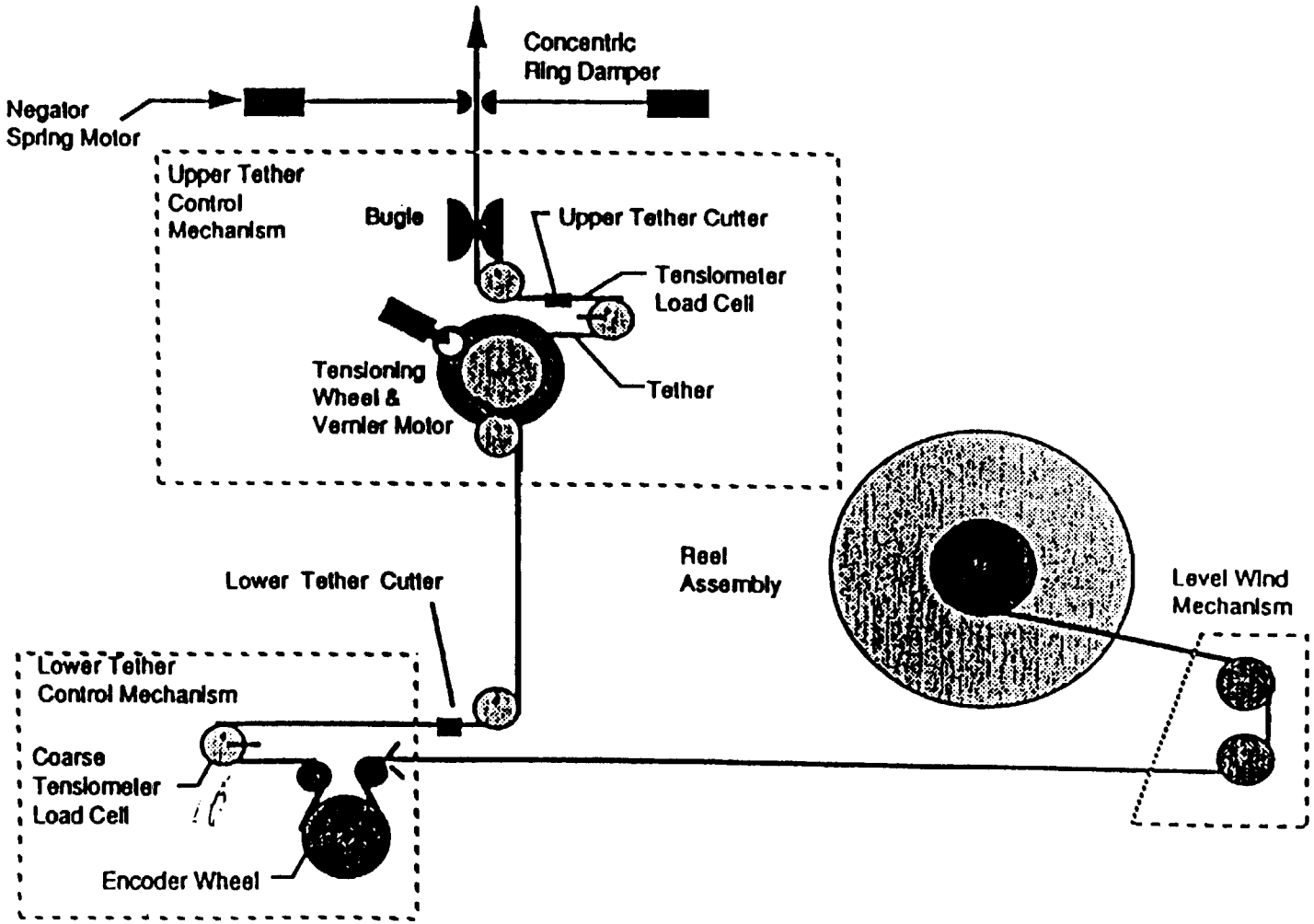

Figure 12. Tether control mechanisms schematic.

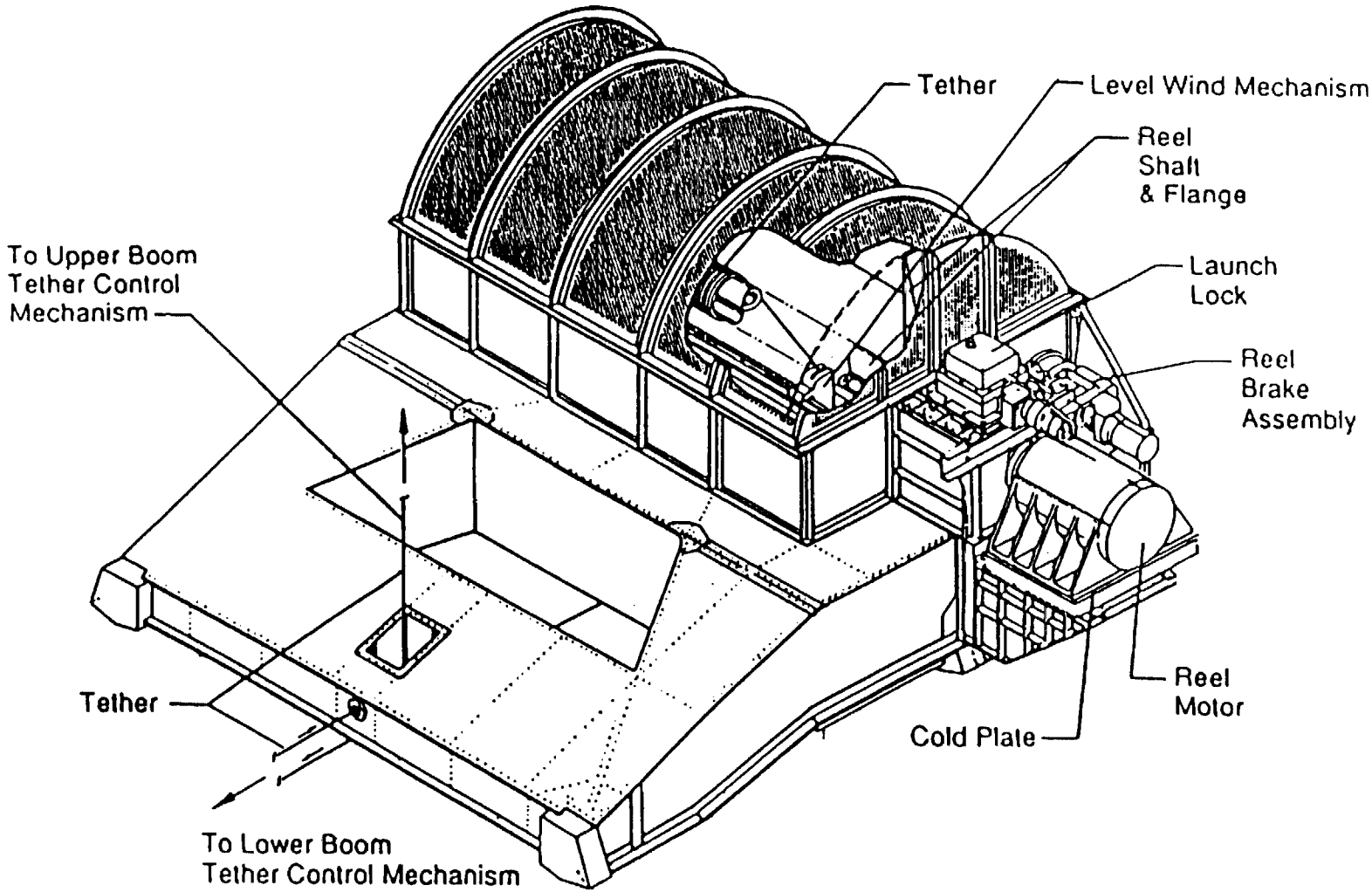

Figure 13. Reel assembly.

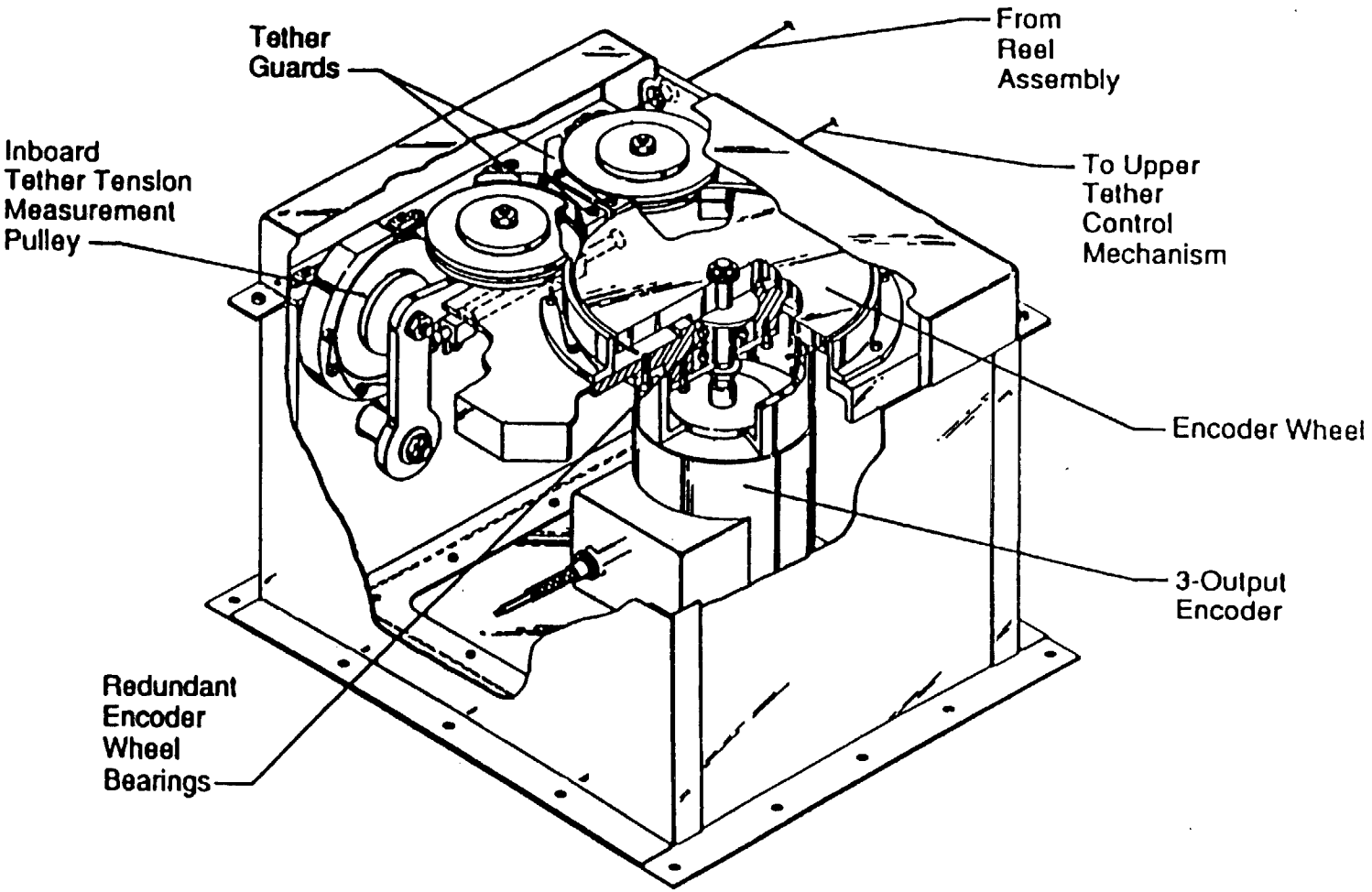

Figure 14. Lower tether control mechanism (LTCM).

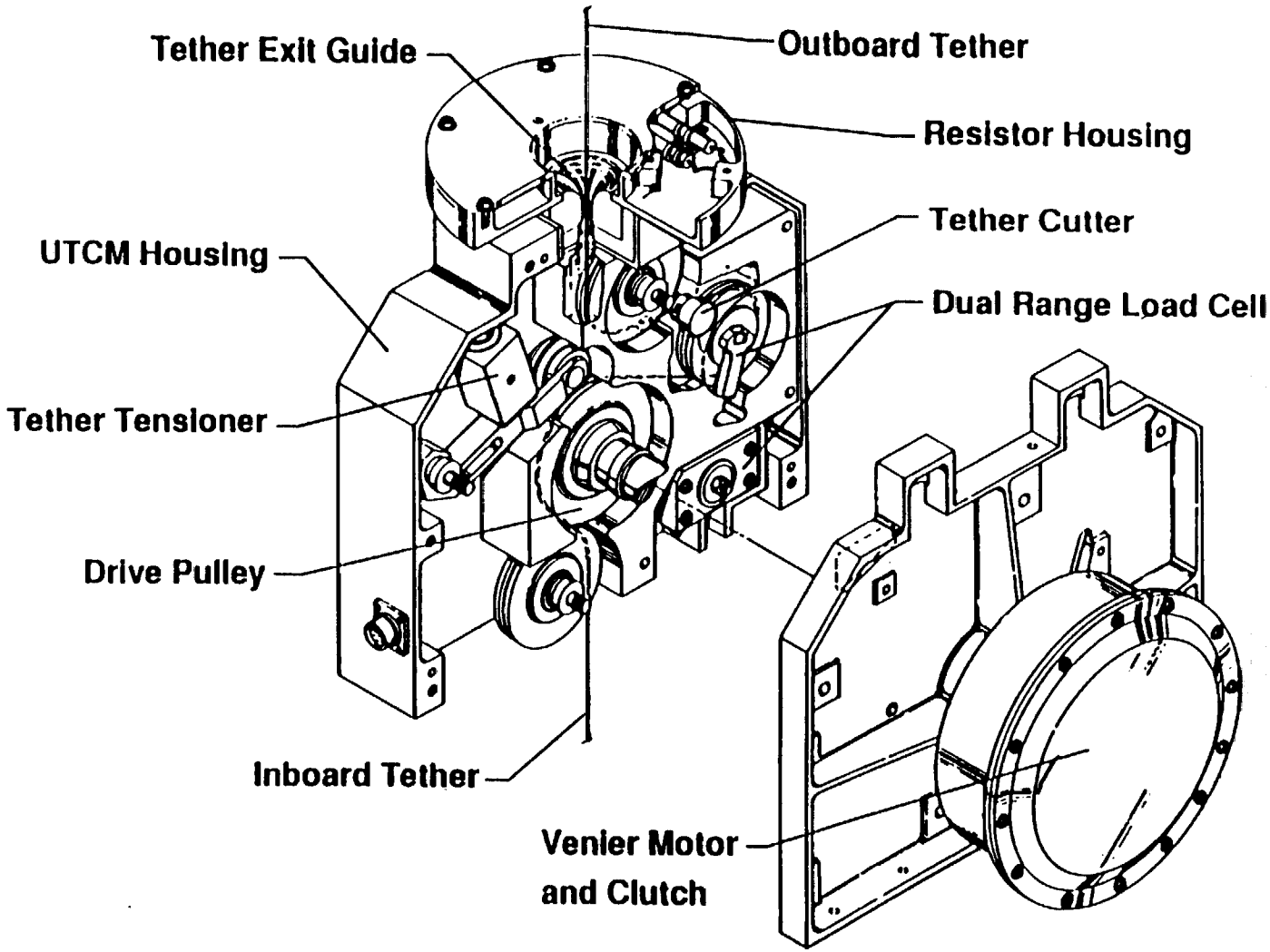

Figure 15. Upper tether control mechanism (UTCM).

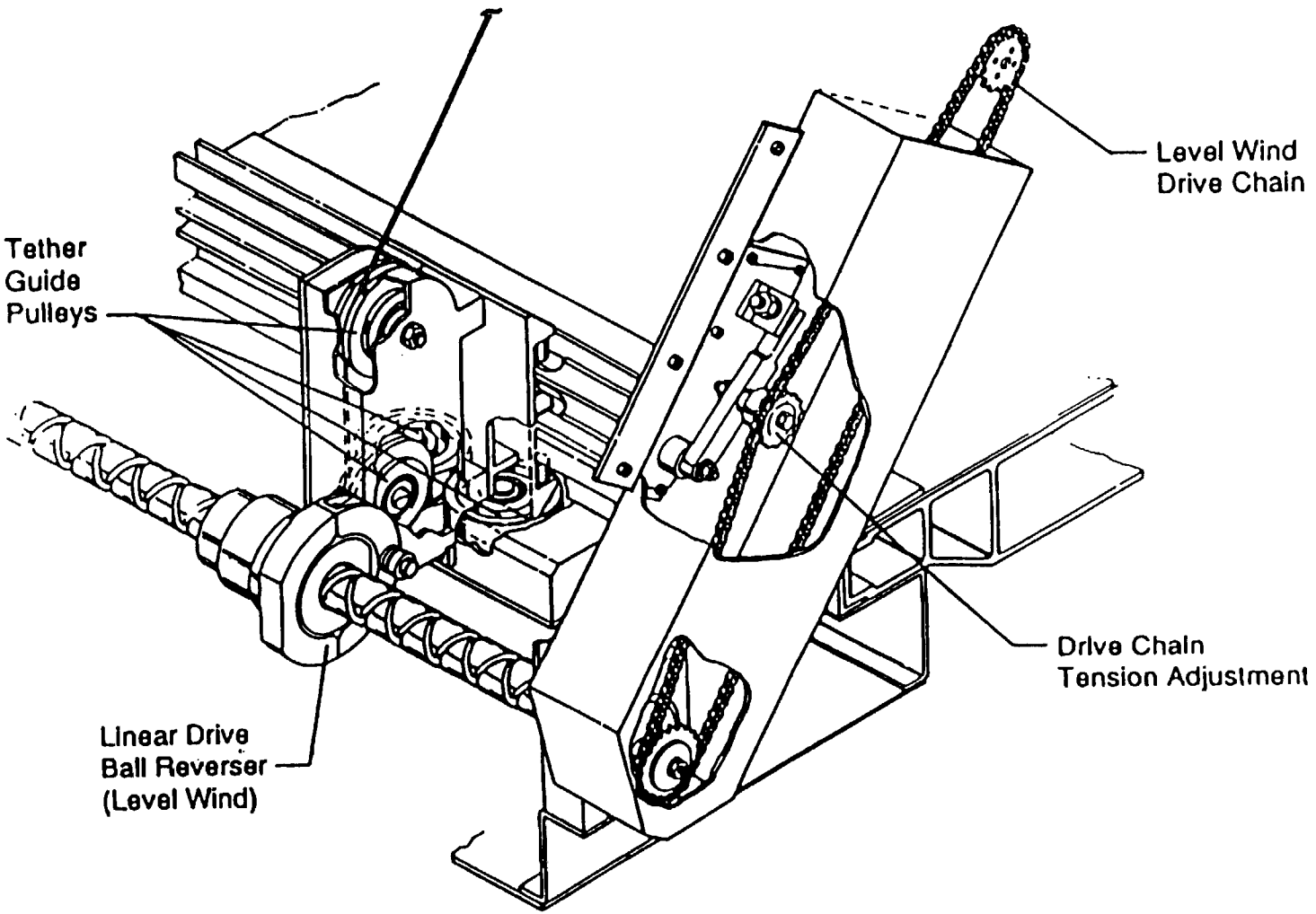

Figure 16. Level wind mechanism for tether reel.

TSS MISSION OBJECTIVES

— **DEMONSTRATE CAPABILITY TO DEPLOY A 525 KG (1100 LB) TETHERED SATELLITE TO A DISTANCE OF 20 KM (12 MILES) ABOVE THE SPACE SHUTTLE, ACQUIRE SCIENTIFIC AND OPERATIONAL DATA, AND RETURN THE SATELLITE TO THE SHUTTLE FOR REUSE ON LATER FLIGHTS.**

— **INVESTIGATE ELECTRICAL AND MECHANICAL BEHAVIOR OF THE COMBINED SATELLITE, TETHER, AND ORBITER SYSTEM.**
- TETHER CURRENT AND VOLTAGE MEASUREMENTS
- SATELLITE AND ORBITER CHARGING STUDIES
- SYSTEM DYNAMIC RESPONSE MEASUREMENTS

— **INVESTIGATE CHARACTERISTICS OF PLASMA WAVES GENERATED BY THE TSS.**
- IN-SITU PROBES OF LOCAL WAVE PHENOMENA
- GROUND-BASED OBSERVATIONS OF VLF AND ELF WAVES

— **CONDUCT STUDIES THAT UTILIZE THE UNIQUE ASPECTS OF THE TSS AS A REMOTE OBSERVING STATION.**
- MAGNETIC EFFECTS OF UPPER ATMOSPHERIC CURRENT SYSTEMS
- MEASUREMENTS OF SATELLITE WAKE EFFECTS
- OBSERVATIONS OF ELECTRON BEAM GENERATED E-M RADIATION

— **TETHERED OPTICAL PHENOMENA INVESTIGATION.**
- SURFACE FLUORESCENCE OF ELECTRONS
- DISCHARGE EFFECTS
- ELECTRON BEAM PHENOMENA

Figure 17. TSS-1 science overview—mission objectives.

Specifically, the electrical and mechanical behavior of the combined satellite, tether, and orbiter system were to be investigated. Because the orbiter and satellite are connected by the tether, they become one orbiting system. From an operational standpoint while the satellite is deployed, the orbiter cannot operate in its standard reference frame, but must work in the system reference frame. Of interest is the satellite and orbiter charging phenomenon as well as tether current and voltage measurements. Understanding the system dynamic response, especially of the tether and satellite dynamics, is key for future tether applications. Verification of these dynamic characteristics can only be accomplished on orbit, because ground test of a long cable (tether) in a vacuum and zero-g is not possible. Other objectives were to investigate characteristics of plasma waves generated by the TSS, to conduct studies that utilize the unique aspects of the TSS as a remote observing station, and to investigate tether optical phenomena.

Figures 18 and 19 are a more detailed listing of the science objectives, some of which were implemented by instruments in the shuttle cargo bay and satellite. Figure 20 is a pictorial representation of the satellite, tether, and orbiter system showing current flow, beams, etc., including satellite spin and the geomagnetic field lines.

This is a short overview of the science objectives. More details can be obtained from the project office and the scientists involved in the mission.

D. Mission Profile

The mission profile is approximately 30-h long and is broken into five distinct phases. Phase I is the deployment which is planned to last 5.3 h. Phase II is to be 10.5-h long for science experiments with the tether fully deployed at 20 km. In phase III, the tether is retrieved down to 2.4 km during a 6.75-h time period. The tether is planned to stay at 2.4 km for 5 h for damping dynamics, preparation for final retrieve, and maybe more science (phase IV). Phase V is the final retrieval and satellite docking. The mission priorities of the mission phases are shown on figure 21. The highest priority was deployment. Priority two was the science during phase II. All other phases (including retrieval of the satellite) were of priority three. Other activities present during the mission are also shown on the chart. They include such things as when the satellite was to be spinning and what instruments were on. The other items associated with skiprope control will be discussed later.

The next section will discuss the dynamic phenomena associated with a satellite tethered from the space shuttle vehicle.

III. DYNAMIC PHENOMENA OF A SATELLITE TETHERED FROM THE SPACE SHUTTLE

Developing a simulation (model) for a satellite deployed on a tether from an orbiting vehicle, platform, or station is a very complex problem. Not only is the system in orbit, basically in a vacuum, in zero-g, and under gravity gradient and magnetic forces, but it has the time-varying dynamics of a long, flexible, variable length tether, the orbiter, and the satellite. The system also has to deal with the deployer mechanism and docking. This modeling task required that a description be written for the environments, natural and induced, which includes gravity gradient, the Earth's magnetic field, current-flow-induced magnetic fields, solar pressure, and thermal. Further, the satellite and its control system had to be modeled along with the tether characteristics and the orbiter characteristics.

- SETS / WILL STIMULATE AND MEASURE CHANGES IN THE SYSTEM'S ELECTRICAL PROPERTIES USING AN ELECTRON GENERATOR AND SEVERAL MONITORS.

- CORE / **CORE EQUIPMENT,** IS A SUPPORT FACILITY FOR THE SATELLITE AND ORBITER BASED SCIENCE INVESTIGATIONS. ELECTRON GENERATORS PROVIDE CURRENT FLOW. TETHER CURRENT MEASUREMENTS, AND SATELLITE GYROS' WILL HELP CHARACTERIZE CURRENT FLOW AND TETHER DYNAMICS.

- SPREE / **SHUTTLE POTENTIAL AND RETURN ELECTRON EXPERIMENT,** WILL DETERMINE THE ORBITER'S ELECTRICAL POTENTIAL IN RELATION TO THE PLASMA SURROUNDING IT AND THE EFFECT OF RETURN CURRENTS.

- RETE / **RESEARCH OF ELECTRODYNAMIC TETHER EFFECTS,** WILL EXPLORE PHYSICAL PROCESSES IN THE SPACE CHARGE REGION SURROUNDING THE SATELLITE, WHICH DETERMINE PARTICLE COLLECTION AND HENCE CURRENT IN THE TETHER.

- TEMAG / **TETHER MAGNETIC FIELD EXPERIMENT FOR TSS EMISSIONS,** WILL INVESTIGATE THE MAGNETIC SIGNATURE OF THE TETHER CURRENT AND ITS CLOSURE THROUGH THE STRUCTURE OF THE SHEATH SURROUNDING

- ROPE / **RESEARCH ON ORBITAL PLASMA ELECTRODYNAMICS,** WILL MEASURE THE DISTRIBUTION AND BEHAVIOR OF CHARGED PARTICLES IN THE VICINITY OF THE TSS SATELLITE.

Figure 18. Cargo bay and satellite science.

- **EMET / INVESTIGATION OF EM EMISSIONS BY THE ELECTRODYNAMIC TETHER,** WILL ESTABLISH THE DETECTABILITY OF ULF AND ELF ELECTROMAGNETIC EMISSIONS.

- **TEID / THEORETICAL AND EXPERIMENTAL INVESTIGATION ON TSS DYNAMICS,** WILL CHARACTERIZE THE DYNAMIC NOISE OF THE TSS.

- **IMDN / INVESTIGATION AND MEASUREMENT OF DYNAMIC NOISE,** IN CONJUNCTION WITH TEID WILL CHARACTERIZE THE DYNAMIC NOISE ENVIRONMENT OF THE TSS.

- **TMST / THEORY AND MODELING IN SUPPORT OF TETHER,** WILL INVESTIGATE AND CHARACTERIZE THE ELECTRODYNAMIC COUPLING BETWEEN A MOVING CONDUCTOR (TSS) AND THE IONOSPHERE.

- **QESEE / OBSERVATIONS AT THE EARTH'S SURFACE OF EM EMISSIONS BY TSS,** IN COOPERATION WITH EMET, WILL CHARACTERIZE THE RECEPTION ON THE EARTH'S SURFACE OF ELECTROMAGNETIC VLF/ULF/ELF SIGNALS FROM AN ELECTRICALLY CONDUCTING MODULATED TETHER IN LOW EARTH ORBIT.

Figure 19. Theoretical science investigations.

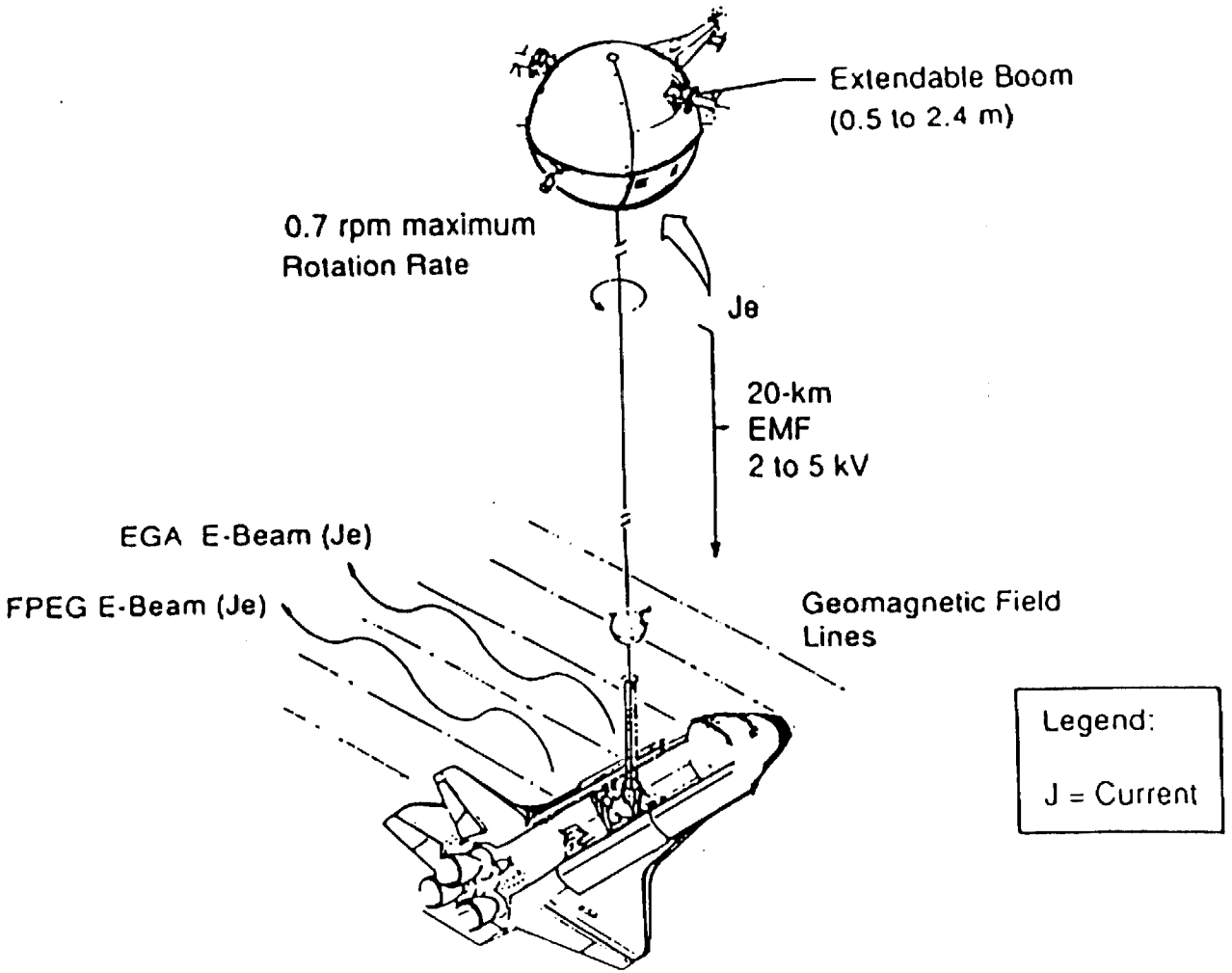

Figure 20. TSS-1 science overview—mission objectives.

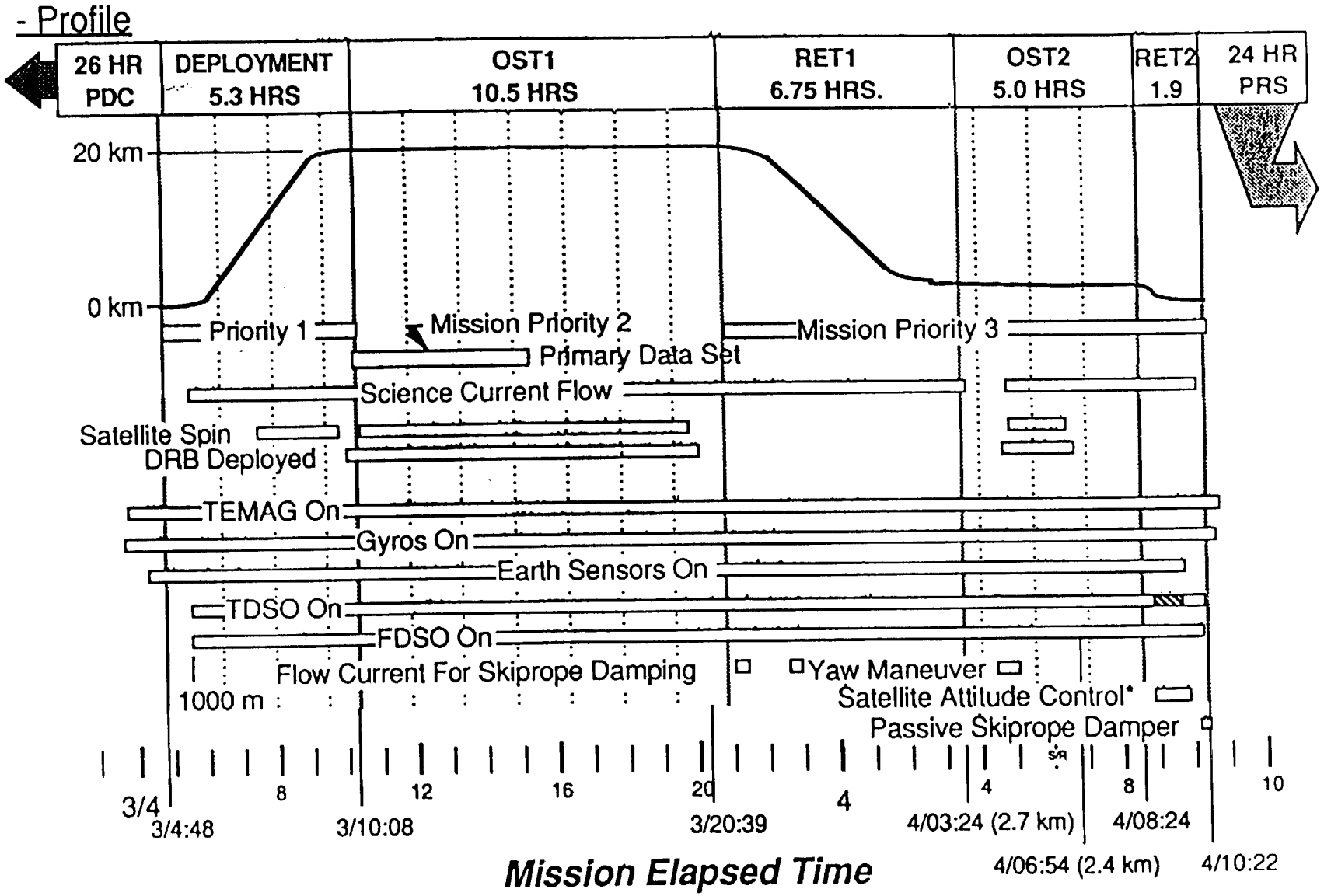

Notes:
* This Damps Skiprope

Figure 21. Timeline of mission activities.

This dynamic system is a closely coupled system between basic orbital mechanics, dynamics, control, mechanisms, and orbital environments. It is a system problem complicated by the zero-g environment which precludes complete ground verification. In addition, it is a system with low dynamic frequencies (long periods). The parts have the potential to interact and tune which creates various dynamic situations that must be understood. Depending on the particular phenomenon under study, various assumptions were made that simplified the problem, giving more efficient development of information. The following section discusses the basic model developed.

A. Basic Model

The satellite itself was modeled as a rigid body in translation and rotation with a constraint force introduced by the tether which is connected to the orbiter. This established a single system in orbit characterized as a classical orbital mechanics problem. Because the tether is attached by a yoke to the satellite, constraint exists in yaw in that any induced satellite spin in one direction has to be taken out by introducing equal amounts of opposite spin. The reaction jet control forces had to be modeled along with the control logic. The same is true of the orbiter and the tether deployment mechanism. Before looking at all the details, it is prudent to understand the orbital mechanics and dynamics of the system assuming a rigid tether.

1. General ("Dumbbell" Configuration). The TSS tethered to the space shuttle is, for all practical purposes, a "dumbbell" although the two masses are different. If the tether is assumed rigid, then the forces acting on the system are as shown on figure 22.

In this case, the upper mass experiences a larger centrifugal force than gravitational force, and the lower experiences a larger gravitational force than centrifugal. This results in a vertical orientation due to the force couple. This orientation is stable with equal masses or with unequal masses either above or below the center of gravity. Displacing the system from local vertical produces restoring forces at each mass which tend to return the fixed length system to the vertical orientation (fig. 23). Dynamically, the system will oscillate about this equilibrium position until damped. This mode is called libration.

Another point needs to be made. The masses are constrained by the tether to orbit with the same angular velocity as the center of gravity of the system. The orbital speed, period, and angular velocity depend on the orbital radius, and are independent of the tether system mass.[1] This tether system now rotates about its center of gravity once per orbit, because it stays in a vertical orientation. The angular speed of the two masses is the same. If they were cut loose, the upper mass would be slowed down, while achieving a higher altitude. At the same time, the lower mass would speed up while going to a lower altitude. All system forces are through the tether. Even though the system is stable, the forces from the magnetic field, solar pressure, and the aerodynamics cause the system to deflect and oscillate in the orbit plane as well as perpendicular to it (out-of-plane). Excessive oscillation (above 64°) must be controlled or the cable loses its tension (see later sections).

Next, the two masses rotate about their respective centers of mass where the restoring force is the tension in the cable. Additional restoring forces can be introduced using attitude control and control rate damping. This is called the pendulous mode (fig. 24).

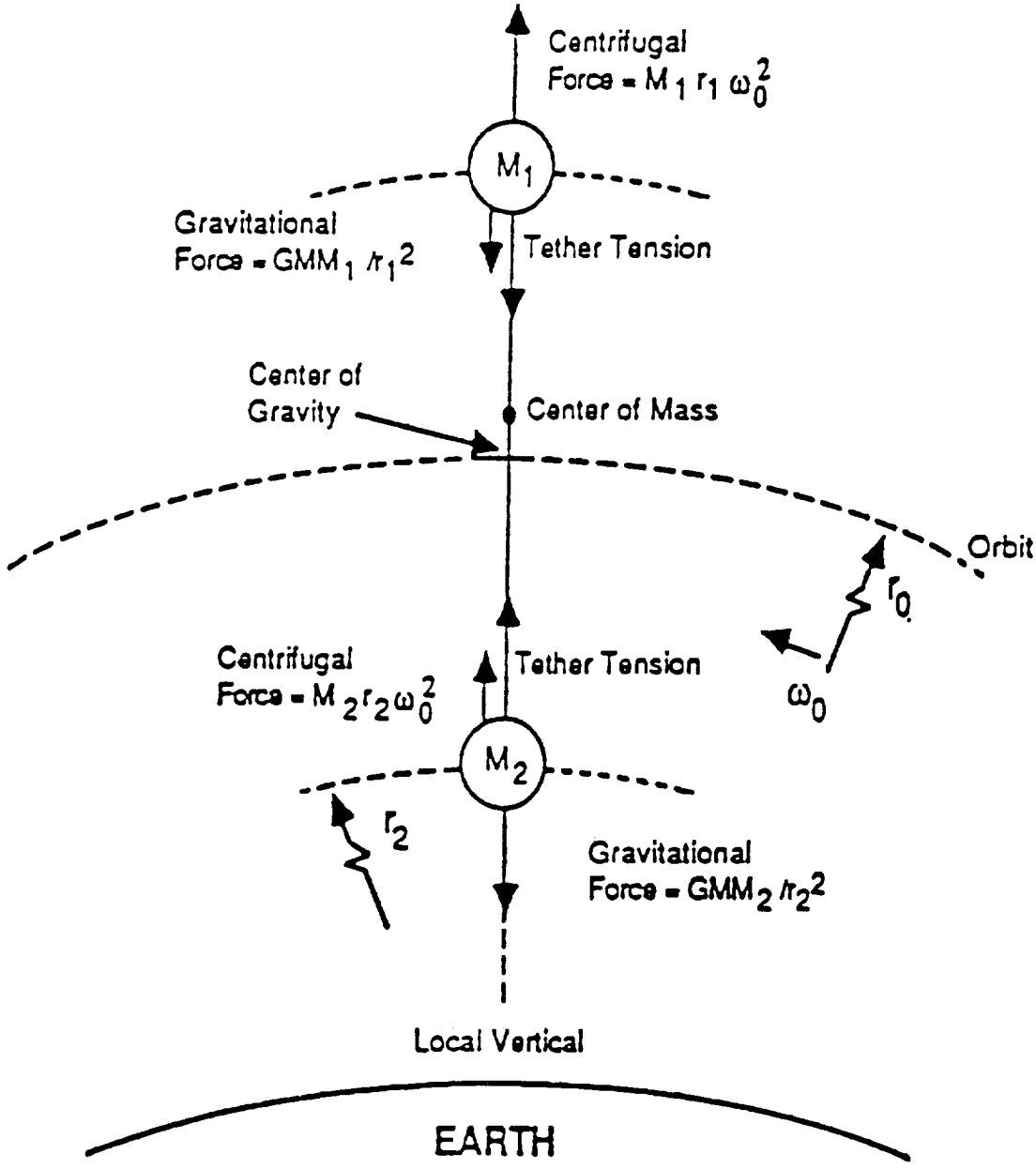

Figure 22. Forces on tethered satellites.

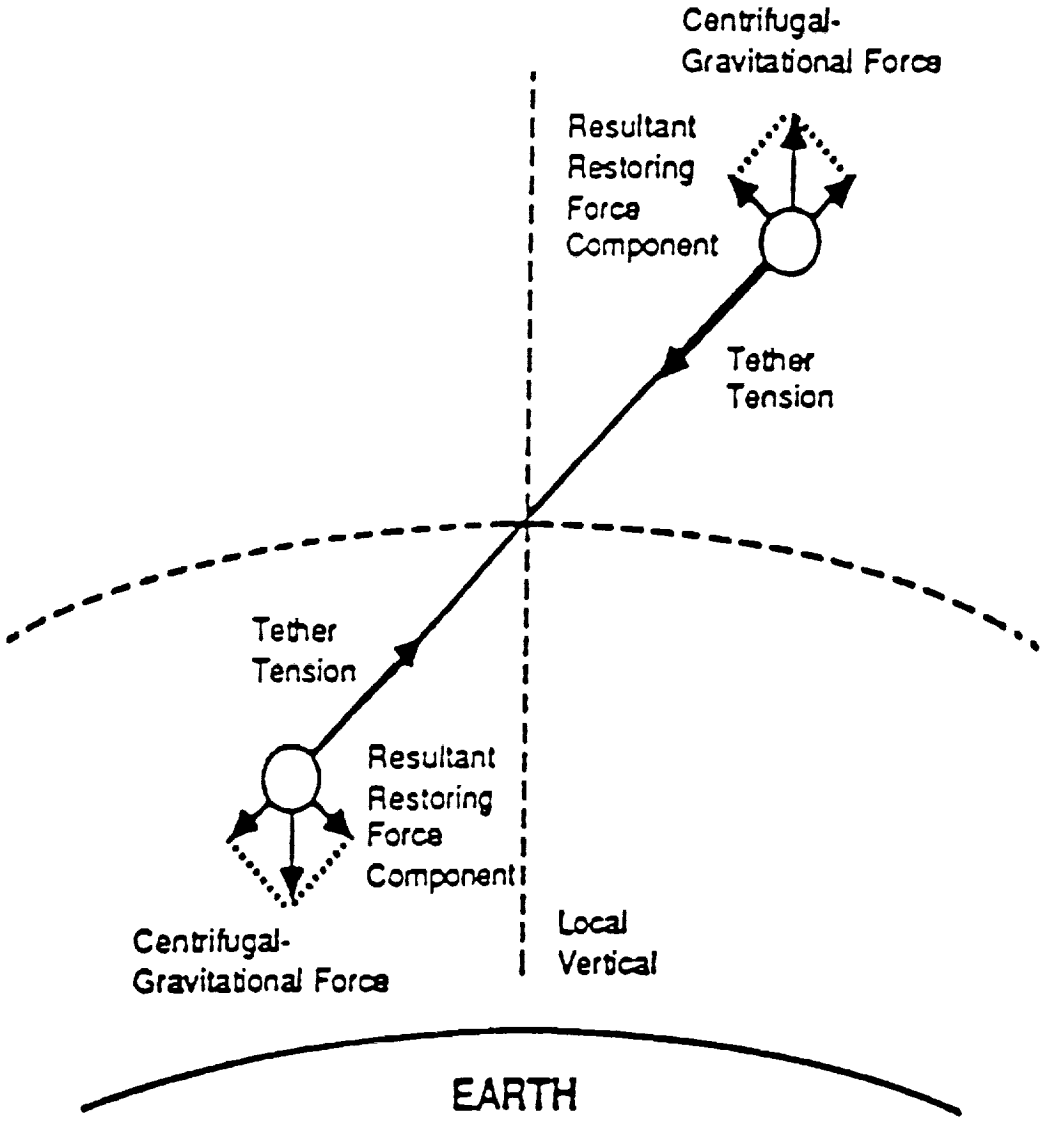

Figure 23. Restoring forces on tethered satellites.

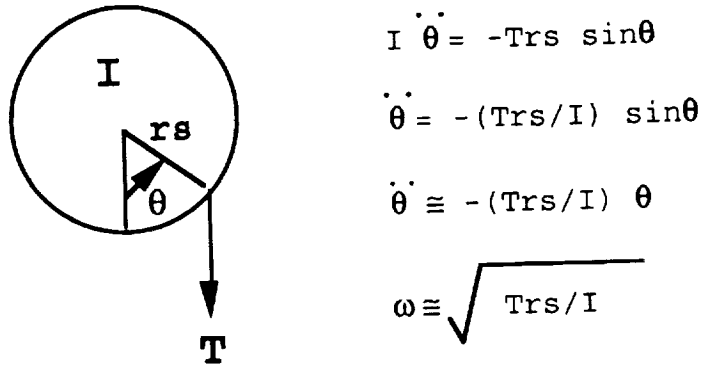

Figure 24. Pendulous mode.

Removing the assumption of tether rigidity opens up many additional modes that have to be modeled, understood, and controlled. The first of these assumes that the reel mechanism is locked and, therefore, the only additional force is due to the tether elasticity. In this case, the satellite bobs by stretching and contracting the tether (fig. 25).

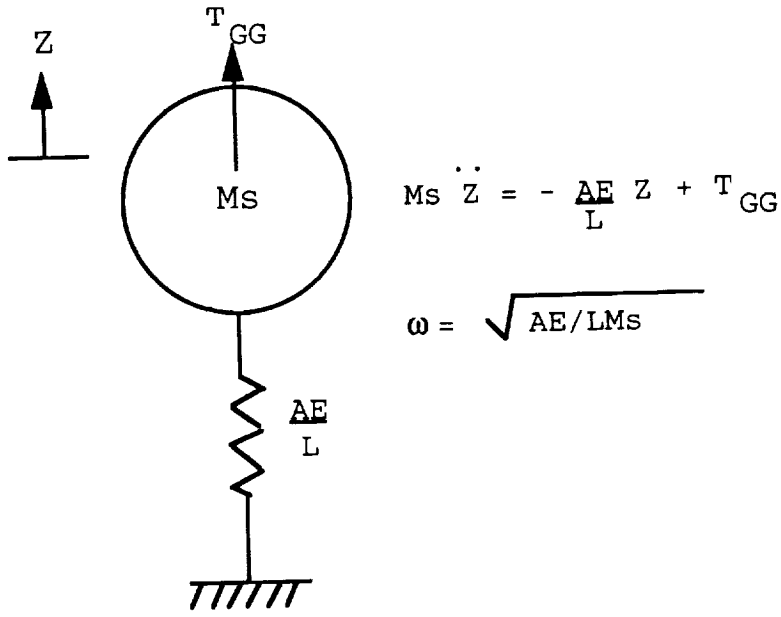

Figure 25. Bobbing mode (reel locked).

This simple model assumes the orbiter mass is much greater than the satellite. However, the bobbing mode still occurs if the masses are equal, in which case there would be two modes, one where the masses are in phase and one where they are out of phase.

If the reel is unlocked and is active in tether control, then the bobbing mode is more complex (fig. 26). The reel motor dynamics and control become an integral part of the equation including the motor and the reel inertia. This adds a variable tension force proportional to the reel in and out acceleration. Gravity gradient forces also play a role in the dynamics (a later section will deal with this control concept).

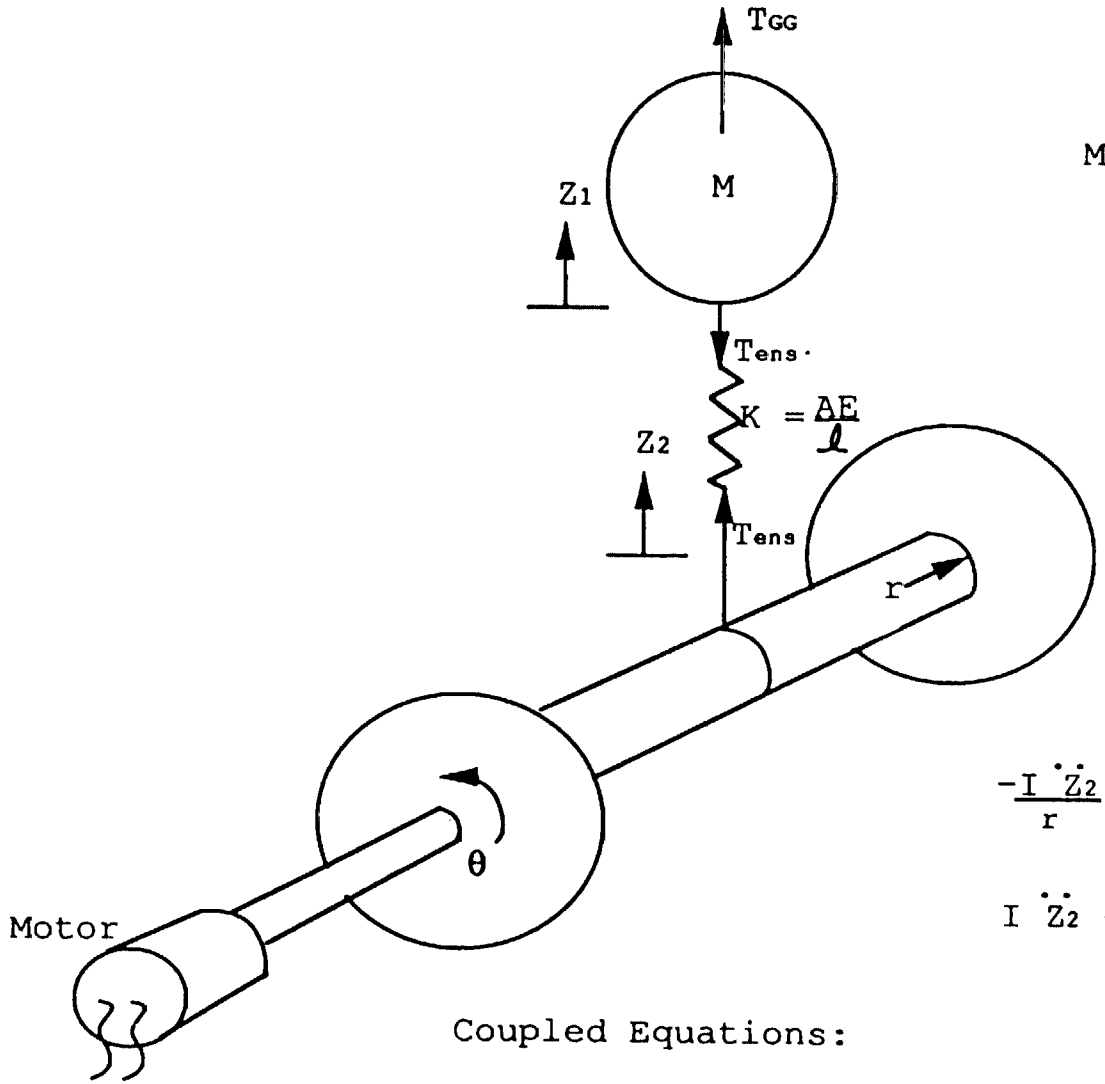

$$M\ddot{Z}_1 = T_{ens} + T_{GG} = \frac{AE}{\ell}(Z_2 - Z_1) + T_{GG}$$

$$I\ddot{\theta} = T_{ens} * r + M_{MOT}$$

$$\ddot{\theta} = -\ddot{Z}_2/r$$

$$M_{MOT} = \frac{K_T K_B}{r_{es}}\frac{\dot{Z}_2}{r}$$

$$-\frac{I\ddot{Z}_2}{r} = \frac{AE}{\ell} r (Z_2 - Z_1) + \frac{K_T K_B}{r_{es}}\frac{\dot{Z}_2}{r}$$

$$I\ddot{Z}_2 + \frac{K_T K_B}{r_{es}}\dot{Z}_2 + \frac{AE}{\ell} r^2 (Z_2 - Z_1) = 0$$

Coupled Equations:

$$M\ddot{Z}_1 + \frac{AE}{\ell} Z_1 - \frac{AE}{\ell} Z_2 = T_{GG}$$

$$-\frac{AE}{\ell} r^2 Z_1 + I\ddot{Z}_2 + \frac{K_T K_B}{r_{es}}\dot{Z}_2 + \frac{AE}{\ell} r^2 Z_2 = 0$$

Figure 26. Bobbing mode (reel active).

Additional modes potentially exist such as traveling waves and various couplings of the modes discussed. The modes that impact a mission must be characterized, modeled, and dealt with for mission success. Sensitivity analysis is a good approach to understanding these key areas.

2. Motion (Modal Curvature). In addition to the characteristics just described, the control forces from the orbiter, satellite, and deployer mechanism must also be modeled (see later sections) because they interact with the other dynamic situations discussed. The system becomes very dynamically complex due to the orbital mechanics and induced environments.

There are several ways to model this complex system. The first way is to use the energy approach which assumes normal lateral modes of the tether (modal synthesis). This approach makes very few assumptions and is more desirable; however, it is more complex and requires more simulation effort and, in general, more computer cost. This is particularly so when the tether length is varying. The second approach uses lumped masses for the tether, for instance 20, and is simple in concept and is computer efficient. The lumped mass (beads) uses many restrictive assumptions, particularly as the tether is reeled in or out and beads appear or disappear. The bead approach has been fairly accurate for long tether lengths, providing insight and simplifying computer simulations which increases computer efficiency. Both types of models, along with simplified reductions of these models, have been used to study the TSS-1 system characteristics and to develop control approaches. The energy approach is the baseline, determining when, where, and to what extent the more simple models can be used. Because the total systems model cannot be ground-verified, only discrete parts were verified and combined into the model. To protect against unknowns which are not ground-verifiable, sensitivity studies varying all the system parameters have been conducted to ensure success. Also, several different modeling approaches have to be used, compared, and understood.

B. Dynamic Characteristics

Solving the equations produces the characteristics of the system. Several distinct system modes exist (fig. 27). The first mode is the libration mode (fig. 28) where the satellite and orbiter oscillate about the center of gravity of the system. Actually, the orbiter oscillates also, but its amplitude is very small compared to the satellite due to the mass differences (factor of 200). The second mode is a bobbing mode where the elasticity in the tether (tensions plus materials) is the prime contributor. The third mode is between the satellite rotation and tether tension and is called the satellite pendulous mode. Next, several lateral string modes of the tether exist, and are typical modes of a string under tension and material elasticity. They are the classical modes of strings classified as first (fig. 29), second, third, etc. Also, traveling wave modes exist that travel along the tether at the speed of sound. Last, there exists the local yaw attitude and spin mode of the satellite and orbiter.

Figure 30 is a plot of some of these fundamental frequencies as a function of tether length in meters. The satellite pendulous modes pass through resonance with the bobbing model (longitudinal) then the various string modes as the tether is shortened. Figure 31 shows a blowup of these frequencies in the resonance condition. The greatest energy transfer occurs around a tether length of 430 m when the first lateral string mode is in resonance with the satellite pendulous mode. At this condition, without any damping, 1 m of skiprope can introduce approximately 6° of satellite pendulous motion. This means that some means must be available to control both the satellite motion and the skiprope, or satellite recovery is not possible.

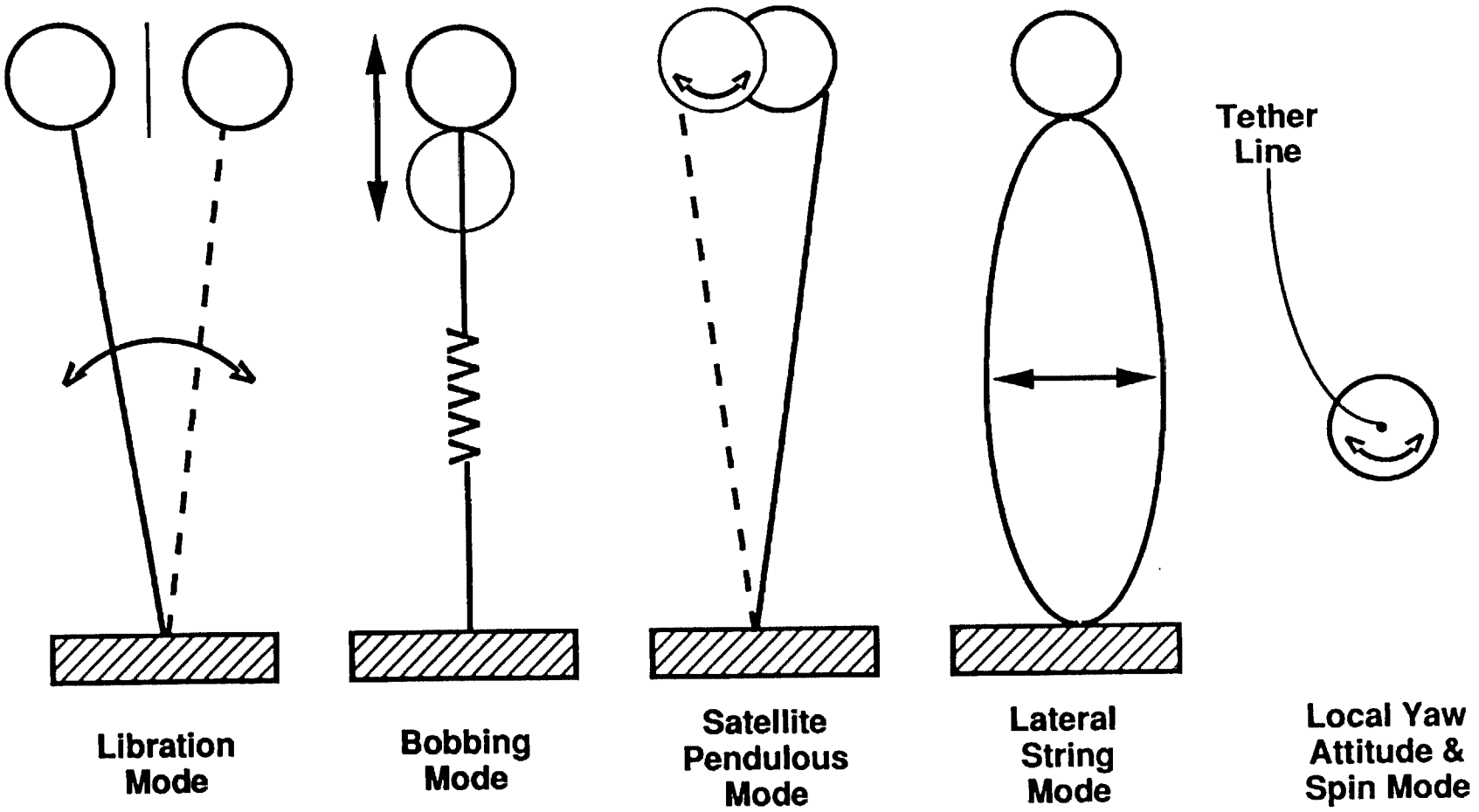

Figure 27. Vibration modes nomenclature.

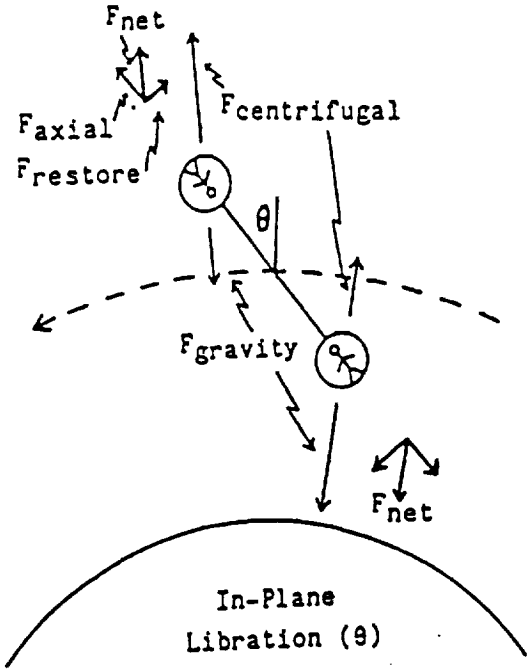

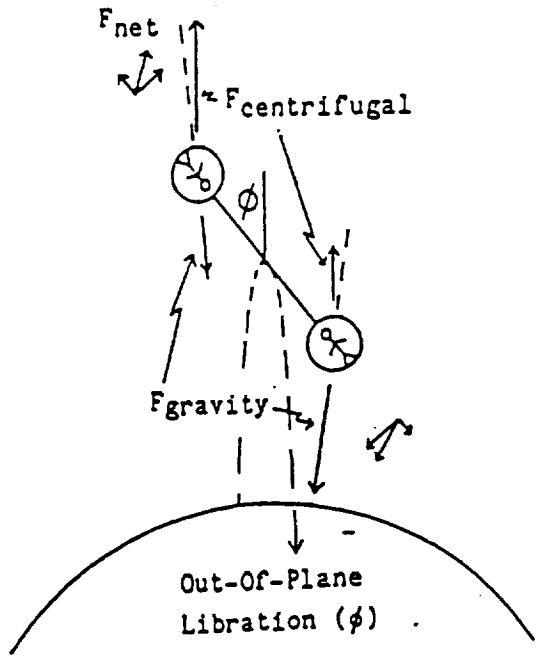

$\ddot{\theta} \approx -3n^2 \sin\theta \cos\theta = -1.5n^2 \sin(2\theta)$

$\dot{\theta} \approx \pm\sqrt{3}\, n\sqrt{\sin^2\theta_{max} - \sin^2\theta}$

$(\dot{\theta} \approx \pm\sqrt{3}\, n \sin\theta_{max}$ when $\theta = 0)$

$n_\theta \approx n\sqrt{3\cos\theta_{max}}$

$\ddot{\phi} \approx -4n^2 \sin\phi \cos\phi = -2n^2 \sin(2\phi)$

$\dot{\phi} \approx \pm 2n\sqrt{\sin^2\phi_{max} - \sin^2\phi}$

$(\dot{\phi} \approx \pm 2n \sin\phi_{max}$ when $\phi = 0)$

$n_\phi \approx 2n\sqrt{\cos\phi_{max}}$

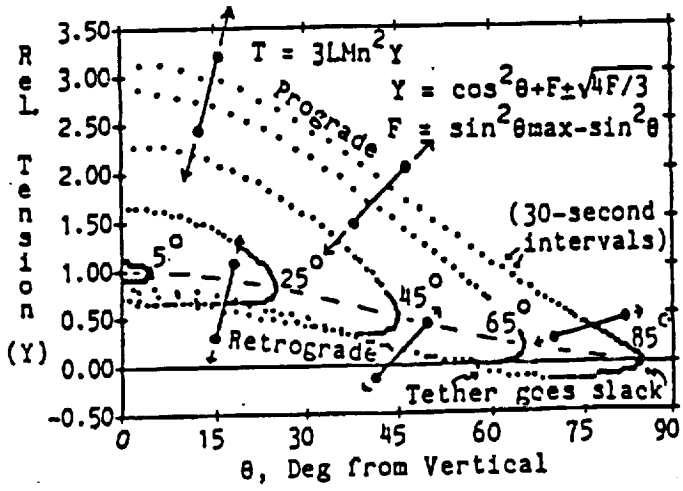

Tension Variations in Librating Dumbbells
(compared to tension in hanging dumbbells)

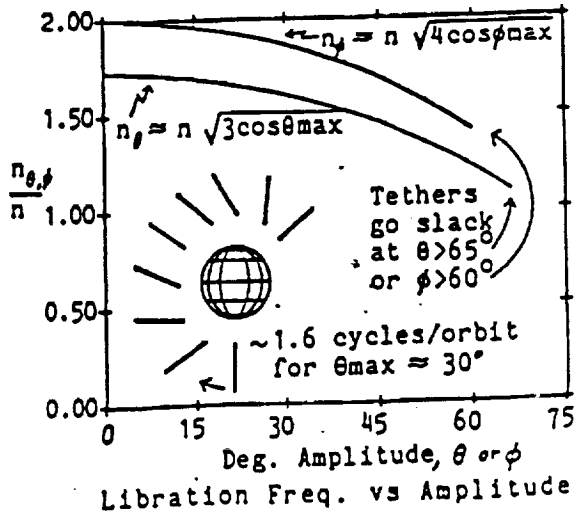

Libration Freq. vs Amplitude

Figure 28. Dumbbell libration in circular orbit.

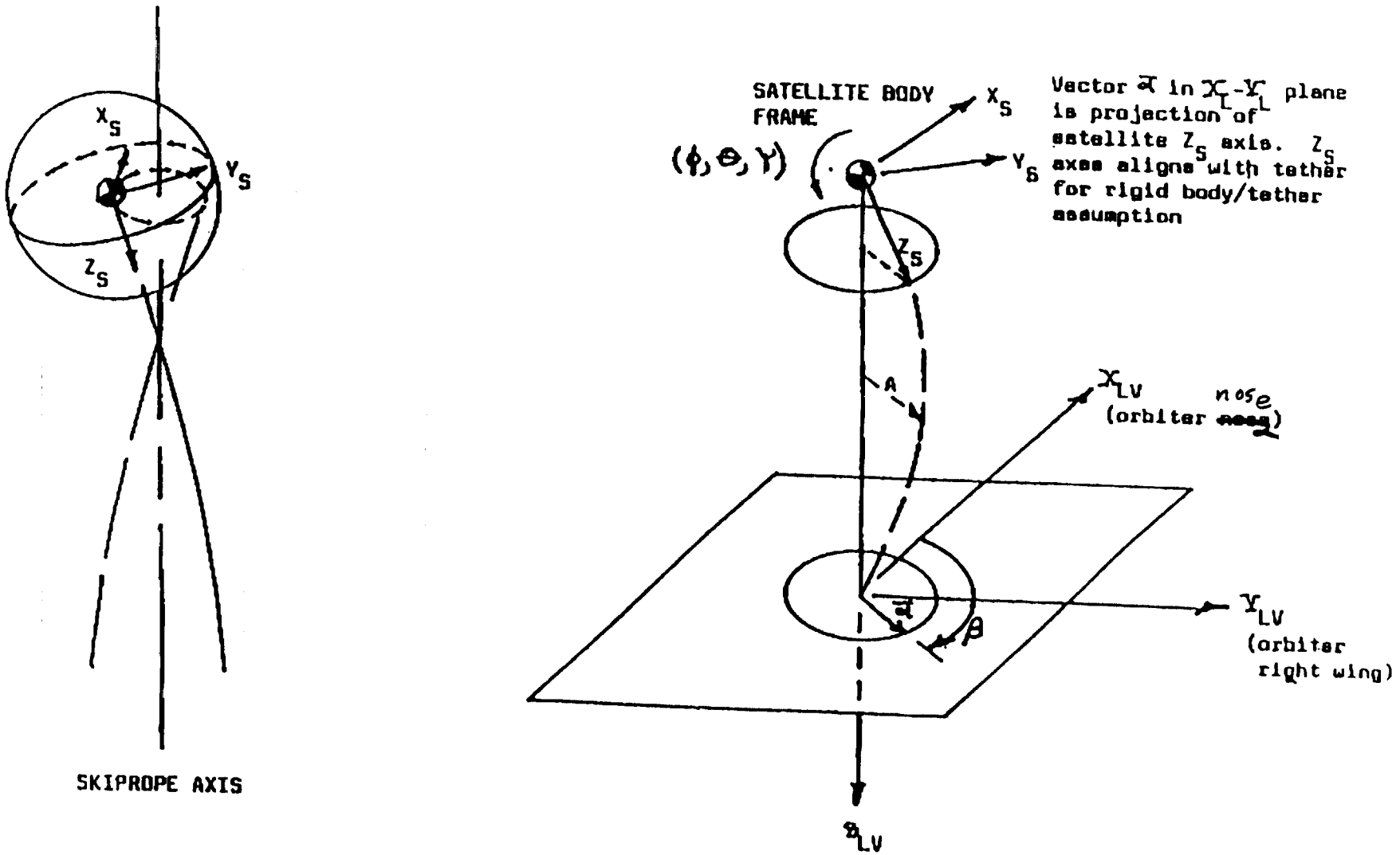

Figure 29. Skiprope observability geometry.

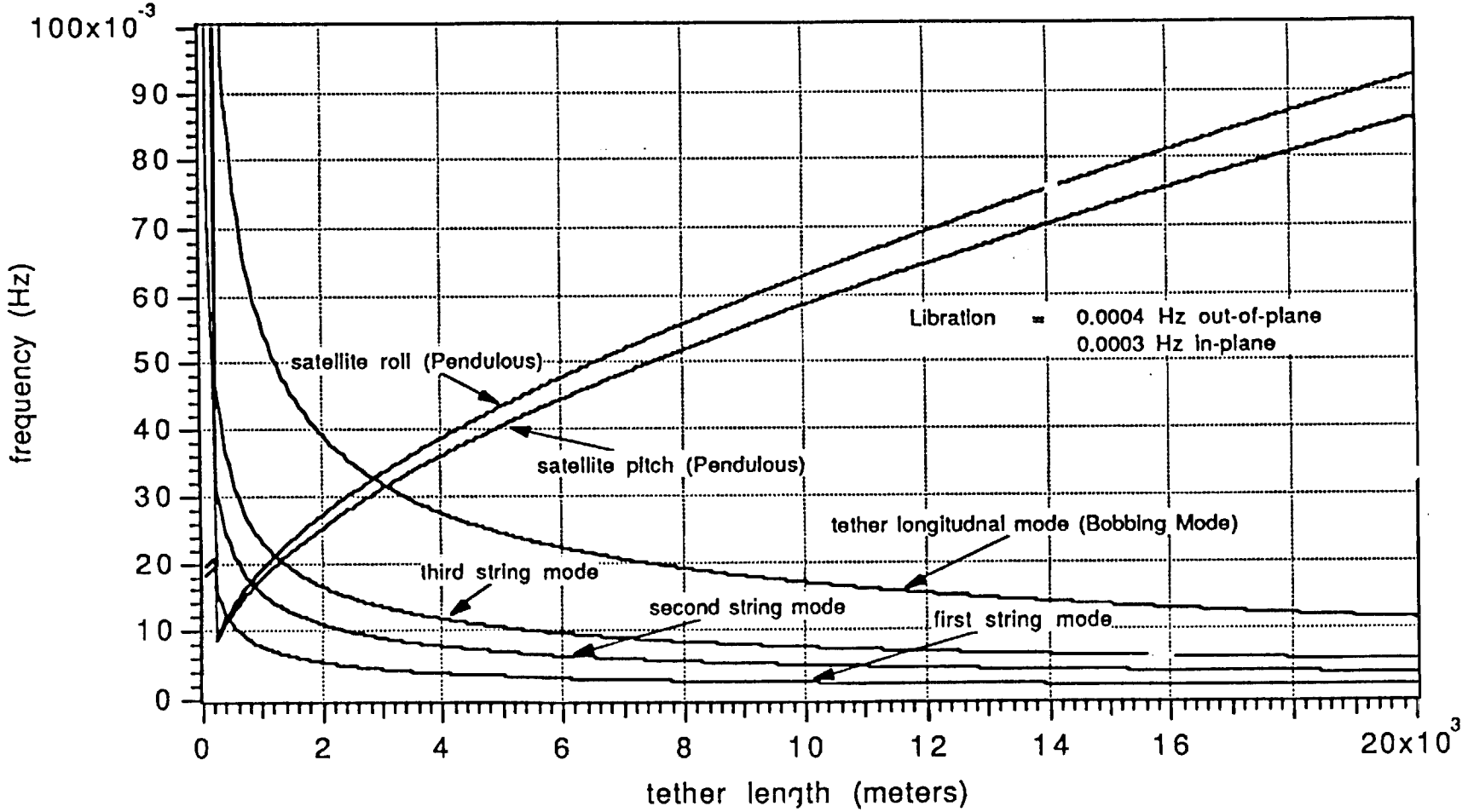

Figure 30. Resonant frequencies versus length for vibration modes.

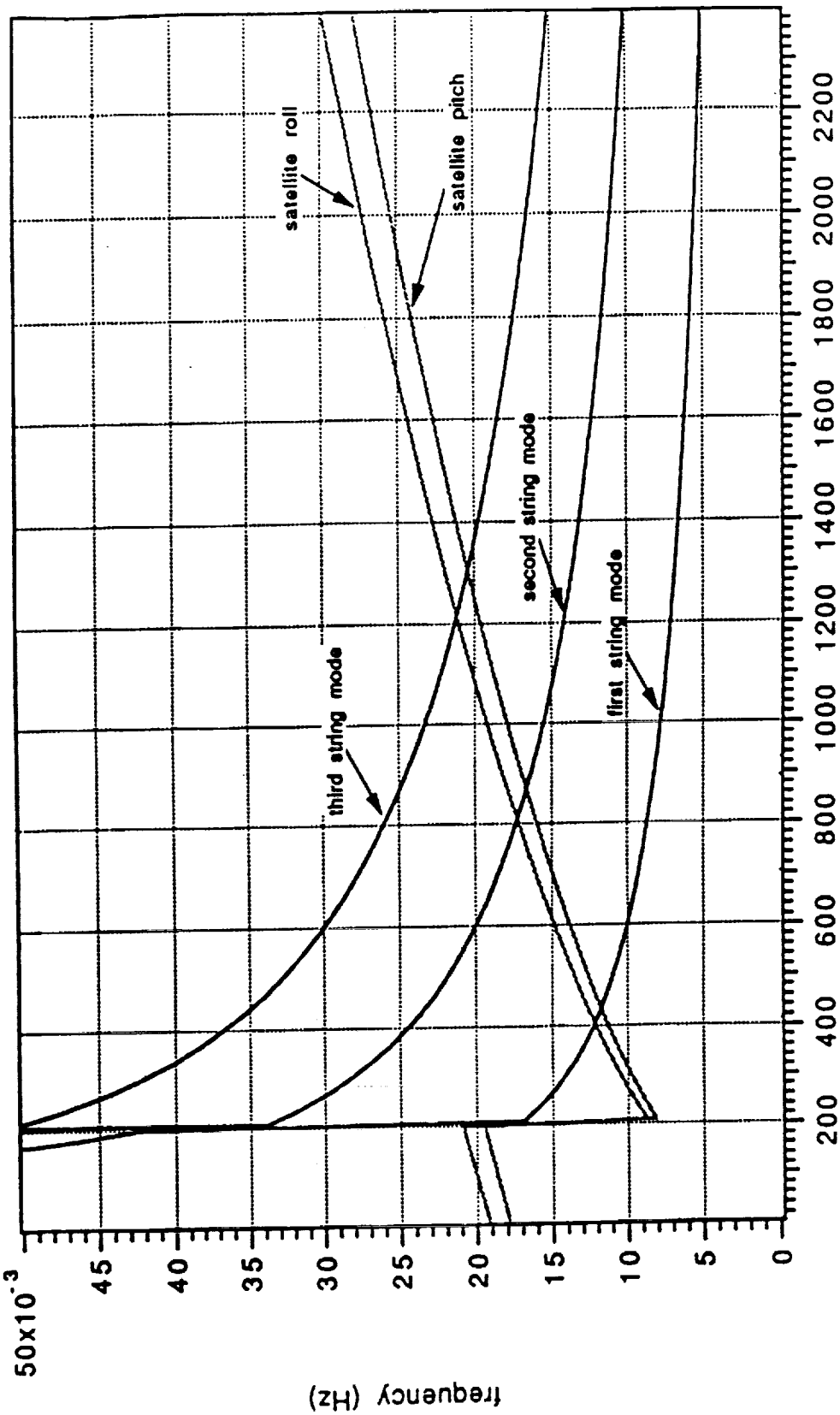

Figure 31. Resonance frequencies versus length for vibration modes.

C. Generalized Forces

The forces acting on the system must be described in more detail for this total system than those discussed previously. These forces are: gravity gradient, aerodynamic drag, electromagnetic, solar pressure, centrifugal, thermal gradient, debris impact, and control. They affect basic dynamics; for example, the electromagnetic force deflects the tether resulting in skiprope, the main thrust of this report. In addition to these forces, an understanding of deployment and retrieval forces needs to be acquired.

Aerodynamic drag can deflect the tether which may induce out-of-plane tether libration. The aerodynamics produce both a lift and drag force on the tether. This lift and drag can be formulated as a point force at the center of gravity or a distributed force. In general, only the point force is needed; however, in special cases, the distributed force may be needed. The drag point force is:

$$F_{drag} = 0.5 \int \rho C_D V_{rel}^2 \,(\text{width})\, \delta_r .$$

Gravity gradient and centrifugal forces can be graphically illustrated together. The gravity force is maximum at the end nearest the Earth, decreasing linearly with increasing distance from the Earth. The centrifugal force increases as the point moves along the tether from the lowest point. These two forces cancel out at the center of mass. At other locations, an object will experience a net force vertically away from the center of mass. This is called gravity gradient; however, part of this net force is due to the centrifugal force (fig. 32).

The electrodynamic force depends on whether the flow is into or out of the upper plasma conductor (satellite). If it flows in the tether and acts as a power (generator), the force is a decelerating force. Flow out produces a thrust (motor), and the force is a uniform accelerating force (fig. 33).

The control forces arise from the reaction jet control system of the satellite and orbiter and are a function of the control laws (see section D).

One other force is important to the problem being discussed; the deployment force that is created once the satellite is given an initial impulse away from the orbiter. The two end masses are in the same orbit, and, since the gravity gradient force is proportional to separation distance, after a certain distance from the orbiter, the combination of gravity and centrifugal forces is sufficient to overcome system losses (friction) and continue the separation. As was discussed earlier, because the two masses are constrained by the tether, the upper mass gains a higher kinetic energy per unit mass than the lower mass. The tether constraint is such that both the orbiter and satellite have the same angular velocity. During deployment, the lower mass will drag the upper mass until libration occurs. This results in momentum transfer through the tether from the upper to the lower mass as tether tension. The off-vertical attitude is caused by the coriolis term of the acceleration expression creating libration of the system as tether length is changed (fig. 34). The coriolis force is perpendicular to the Earth's radius for radial deployment/retrieval.

All these forces must now be expressed in terms of the system chosen to describe the characteristics of the tethered system. Those that have negligible effect on these characteristics can be deleted from the simulations.

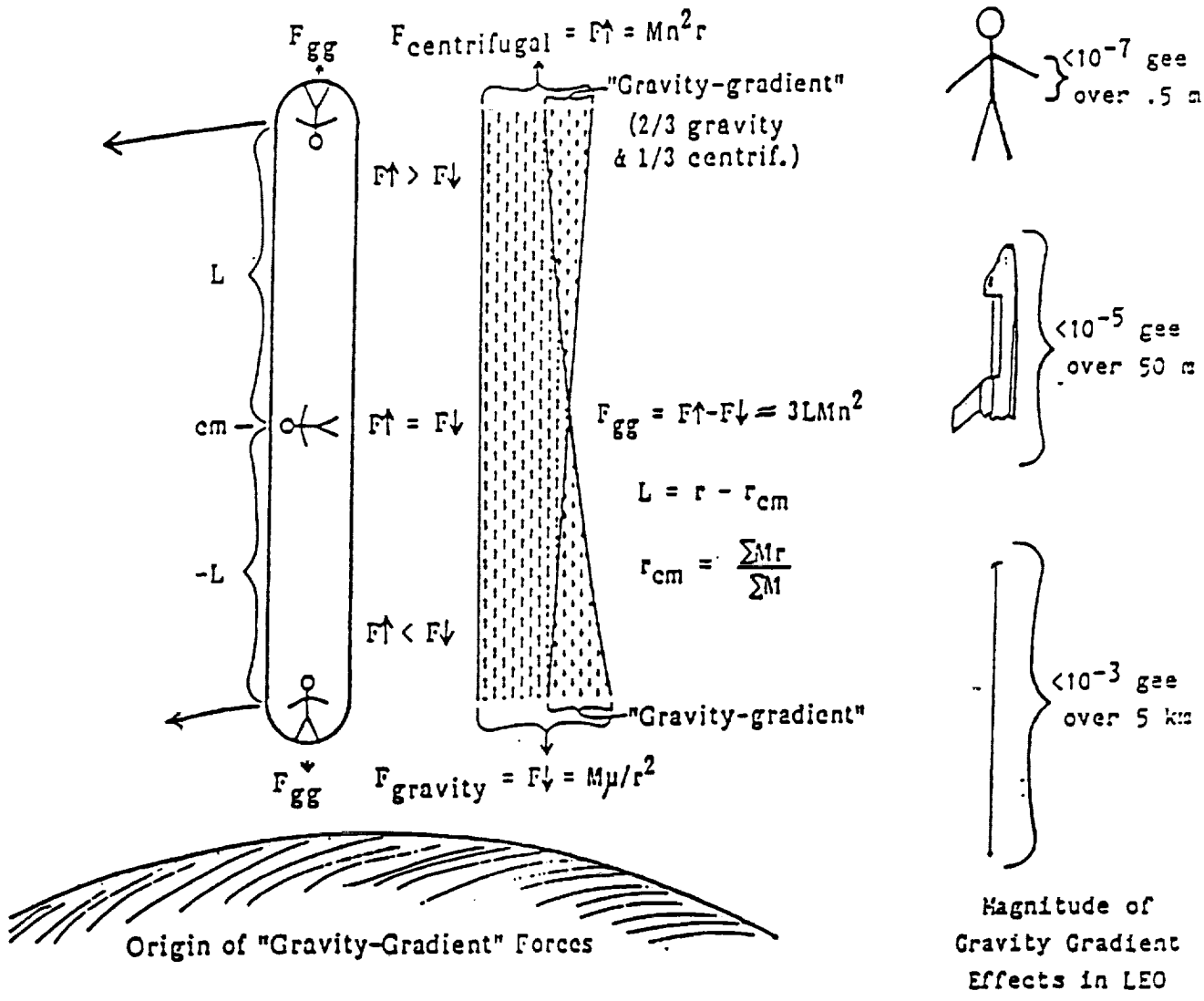

Figure 32. Gravity gradient/centrifugal force effects.

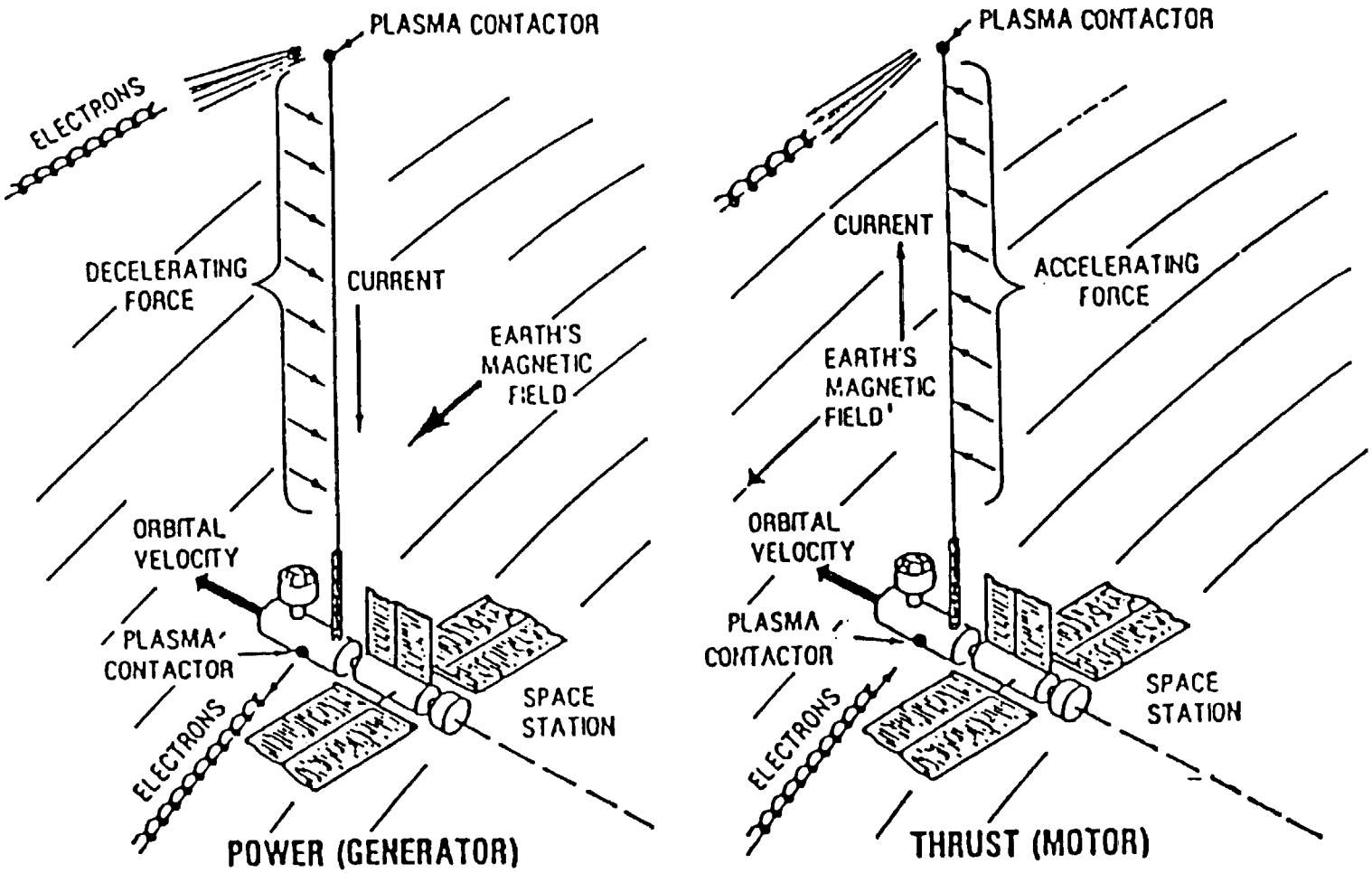

Figure 33. Electrodynamic tether principles.

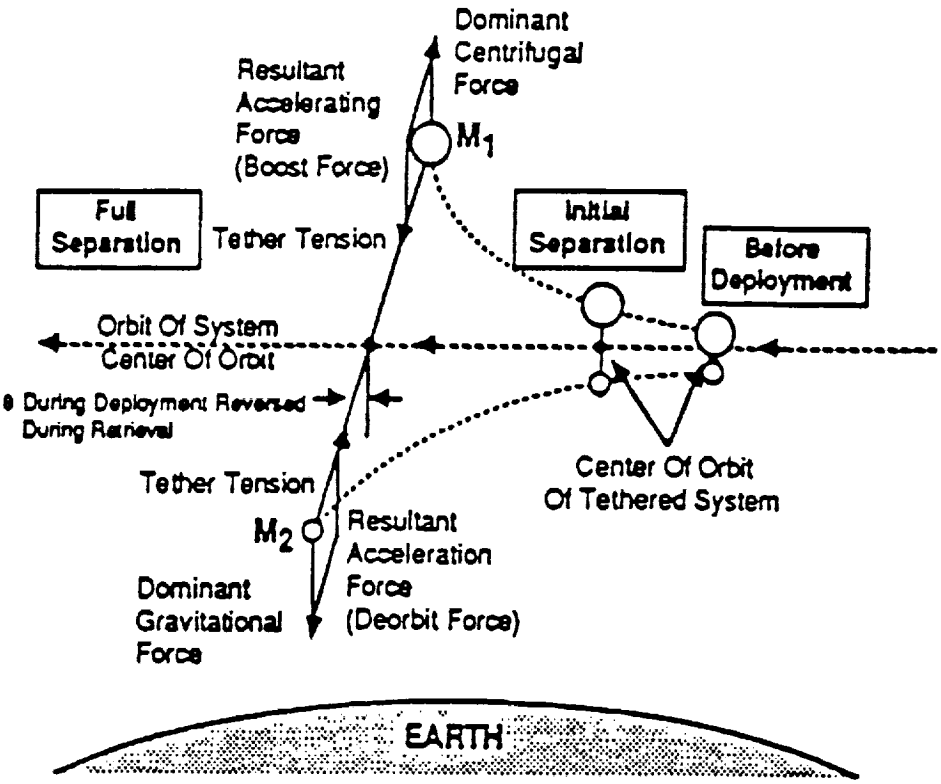

Figure 34. Dynamics during tethered deployment.

D. Control Systems

The last systems that have to be modeled are the control systems. These consist of the satellite, orbiter, and reel mechanism.

1. Satellite Control System. The satellite uses the attitude measurement and control system (fig. 35) to point or spin the satellite's yaw attitude (about the tether line) and to provide satellite attitude information to the orbiter crew and the ground. The satellite has four integrating rate gyros (one for each axis and one skewed) to provide real-time attitude data and two Earth sensors to update the attitude data. Four Sun sensors are used to measure the satellite's attitude, but are not used in the control loops. The satellite has 14 nitrogen gas jets: four jets provide tension augmentation (fail operational redundancy) when the natural tension is below two Newtons; four jets provide yaw attitude control; four jets provide pitch rate damping; and two jets provide roll rate damping. One valve controls the flow to two jets for tension augmentation, yaw control, and pitch rate damping. Another valve per jet is used to control roll rate damping. The pitch and roll rate damping jets do not produce pure torque; consequently, translation results which induces libration. If libration already exists, firing the proper thruster can reduce libration while reducing the attitude rate. If libration does not exist, alternately firing the opposite thruster will minimize the induced libration.

A closed-loop control system is used for the satellite's yaw attitude and to point, or spin, the satellite. While the satellite is spinning, the satellite's attitude information is not processed. The satellite spins during deploy and while on station. The electrodynamic experiments utilized the satellite spin to monitor tether current uniformity with satellite orientation. The satellite was designed to spin at 1.5°/s during deploy so that gyro saturation (which occurs at 2°/s) will not occur; otherwise, control could not be maintained using the gyro. On station, the design satellite spin rate is between 3.6°/s and 4.2°/s so that the skewed gyro will not be saturated. When the satellite

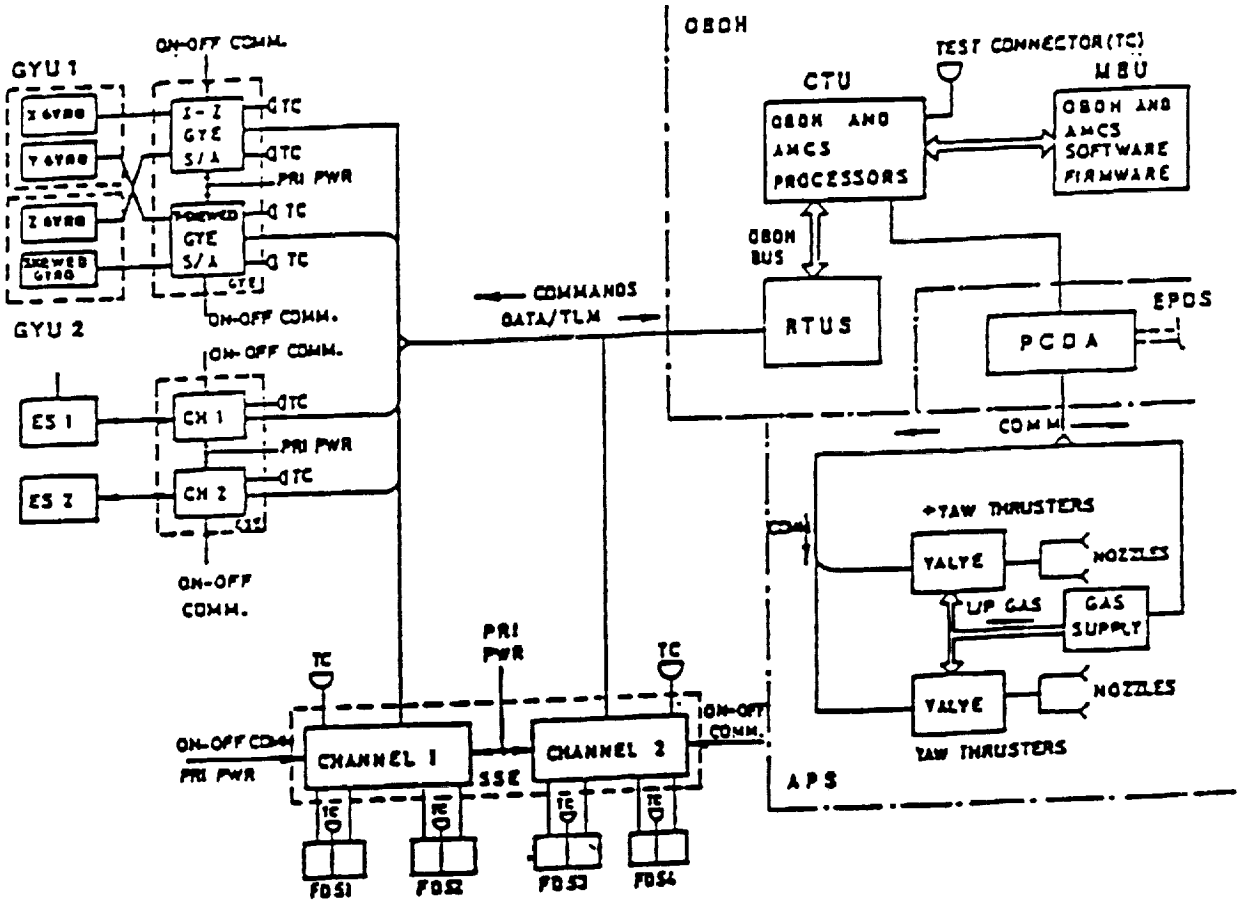

AMCS	Attitude Measurement and Control System
OBDH	Onboard Data Handler
APS	Auxiliary Propulsion System
EPDS	Electrical Power and Distribution System
TC	Thermal Control
GYU	Gyro unit
GYE	Gyro Electronics
ES	Earth Sensor
FDS	Fine Digital Sensor (Sun Sensor)
RTUS	Remote Terminal Unit Service
CTU	Central Terminal Unit
MTU	Memory Bank Unit
PCDA	Power Control Distribution Assembly
TLM	Telemetry

Figure 35. Satellite AMCS diagram.

changes from the spin mode to the attitude hold mode, it must go through the despin mode. This despins the satellite, orients the yaw axis, and initializes the attitude hold mode which allows the processing of attitude information for telemetry. The passive mode is used when deploying the satellite's antennas and for contingencies.

2. Orbiter On-Orbit Control System. The on-orbit control system uses six 25-lb thrusters for vernier attitude control and thirty-eight 870-lb thrusters for translation and attitude control. The orbiter provides libration control throughout the mission by performing orbiter translations. For tether lengths less than 6,000 m, the orbiter performs three-axis control. Beyond 6,000 m, the orbiter controls its yaw axis and damps its pitch and roll pendulous motion, while the tether force maintains orbiter pitch and roll attitude. The orbiter control system performs a yaw maneuver to damp skiprope which uses centrifugal force to reduce the energy in skiprope. Further information regarding the on-orbit control system can be obtained from reference 4.

3. Reel Mechanism Control. This system controls the reeling rates of the deploy and retrieve systems and, hence, the in-plane libration angle. The vernier motor at the top of the boom provides the force to overcome the friction in the mechanisms, while the reel motor regulates the retarding torques to provide the desired reeling rate. The logic for the retarding torque is shown in figure 36. The logic is resident in the data acquisition and control assembly (DACA) from which reel motor voltage commands are generated and to which encoder measurements of encoder length and length rate are received. Contingency controls are provided by direct command of motor pulse width by the crew. Their cues come from the encoder or radar length and length rate as well as tension which are displayed on the aft flight deck. This loop is illustrated in figure 37.

The computer logic contains profile computations which are based on controlling the in-plane libration angle. This logic generates the desired length and length rates which are compared to the measured values from the encoder. At reeling rates below 0.1 m/s, high gains are used to smooth reeling rates. This is done when $Kr > 0$. When $Kr = 0$, a meter of length error results in 0.5 V to the reel motor. Compensation is made for the back EMF in the reel motor by using the desired (commanded) reeling rate to produce a compensating control voltage.

E. Model Verification

The TSS project has used many different methods (equations, etc.) for describing their system characteristics. These have been used in design and verification, and will be key to skiprope control during operations. It became a key point that these simulations must be validated in order to ensure success of the mission. This has been accomplished through simulation comparisons and ground testing of both the tether and the mechanisms.

1. Simulation Comparisons. To ensure similarity of results between the various simulations, a set of 35 different mission cases was selected for analysis on each simulation. The results of this simulation comparison have been documented in reference 5. Adequate correlation between the various simulations existed, such that all models were declared adequate to perform the job assigned. Figure 38 shows the cases compared.

2. Tether Testing. The dynamics of the tether required testing to verify both the inherent structural damping, stiffness characteristics, and the modal phenomena. Understanding aerodynamic effects was also required in order to allow some atmospheric testing to save cost.

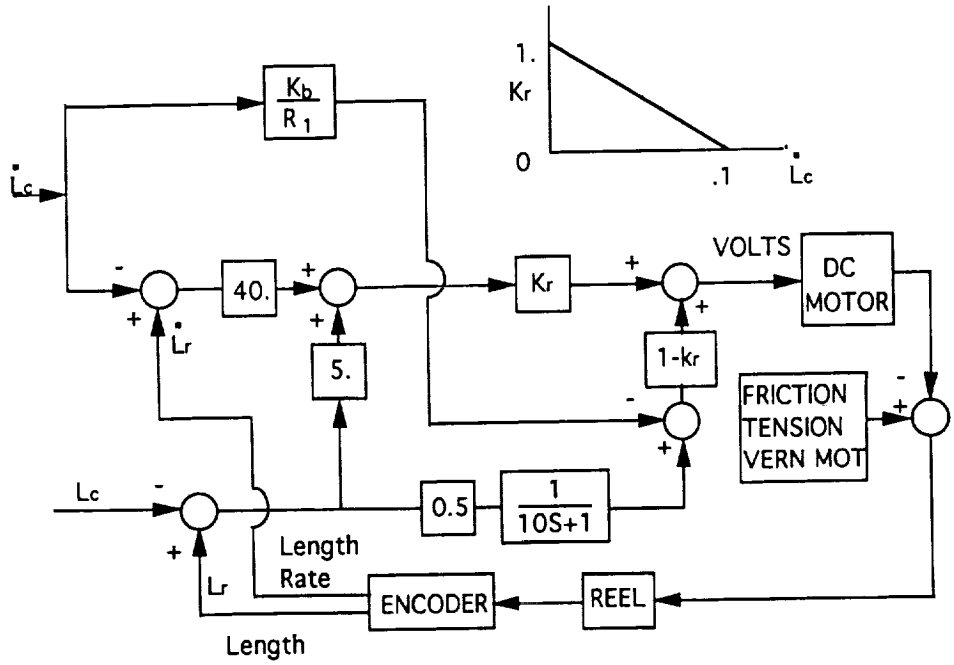

$\dot{L}_r$ - Spooled Length
L_c - Commanded Length
K_b - Back EMF Constant
K_r - Blend Gain

$\dot{L}_r$ -Spooled Length Rate
$\dot{L}_c$ -Commanded Length Rate
R_1 -Spool Radius
S - LaPlace Variable

Figure 36. Deployer control scheme.

Manual Control Mode
-Pulse widths typed in by crew into MCDS
-Crew uses nominal tables, radar, and MCC to determine inputs
-Radar provides estimate of libration angles

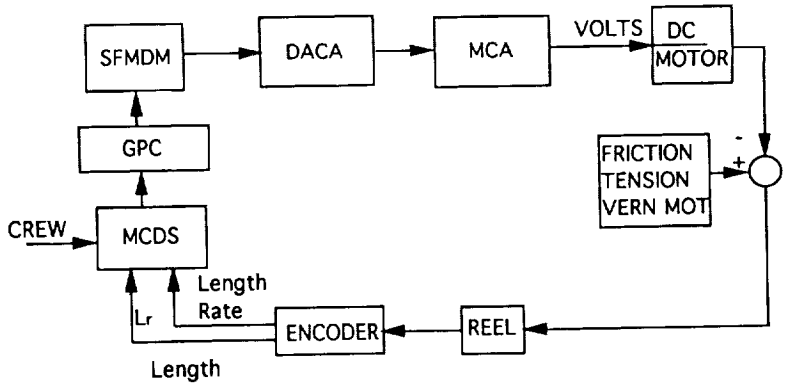

MCDS - Multifunction Command and Display System
GPC - General Purpose Computer
SFMDM - Smart, Flexible Multiplexer/DeMultiplexer
DACA - Data Acquisition & Control Assembly
MCA - Motor control assembly

Figure 37. Manual deployer control scheme.

Simulation Comparisons

- **An Effort Was Undertaken to Validate The Level 1 Simulations of JSC (STOCS) and MMAG (Model 3)**
- **35 Validation Cases Were Proposed**
  - **19 Environmental and Tether Model Cases**
  - **5 Subsystem Cases**
  - **11 System Cases**
- **All These Cases Have Been Run and Compared and Documented**

Figure 38. Model validation.

Initially, a series of tests was run on the tether to determine stiffness and damping characteristics. This was necessary due to the tether makeup shown in figure 9. In order to separate the structural damping from aerodynamic damping, tests of skiprope dynamics were run in both the vacuum chamber and in air using only short tether lengths because of facility limitations. The aerodynamics had effect and had to be accounted for in the atmospheric testing results. The test setup for one such damping test is shown in figure 39. The results of the test are shown in figure 40. Although the test lengths were too short to apply directly to TSS-1, the trend of the damping with length suggests that damping for operational lengths will be minimal. Consequently, most of the studies have been performed with no material damping simulated. This is considered to be a conservative approach.

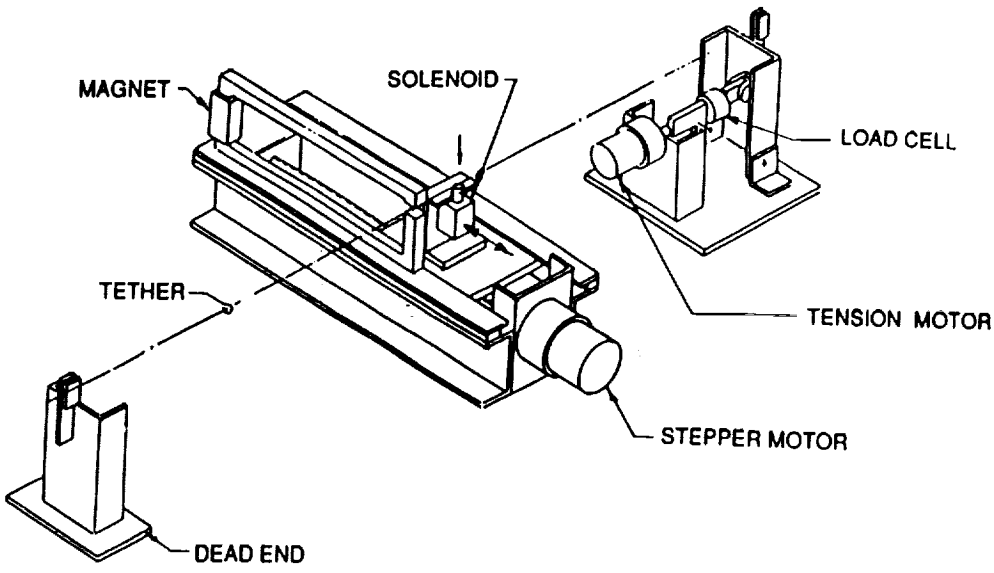

Figure 39. Twang test setup.

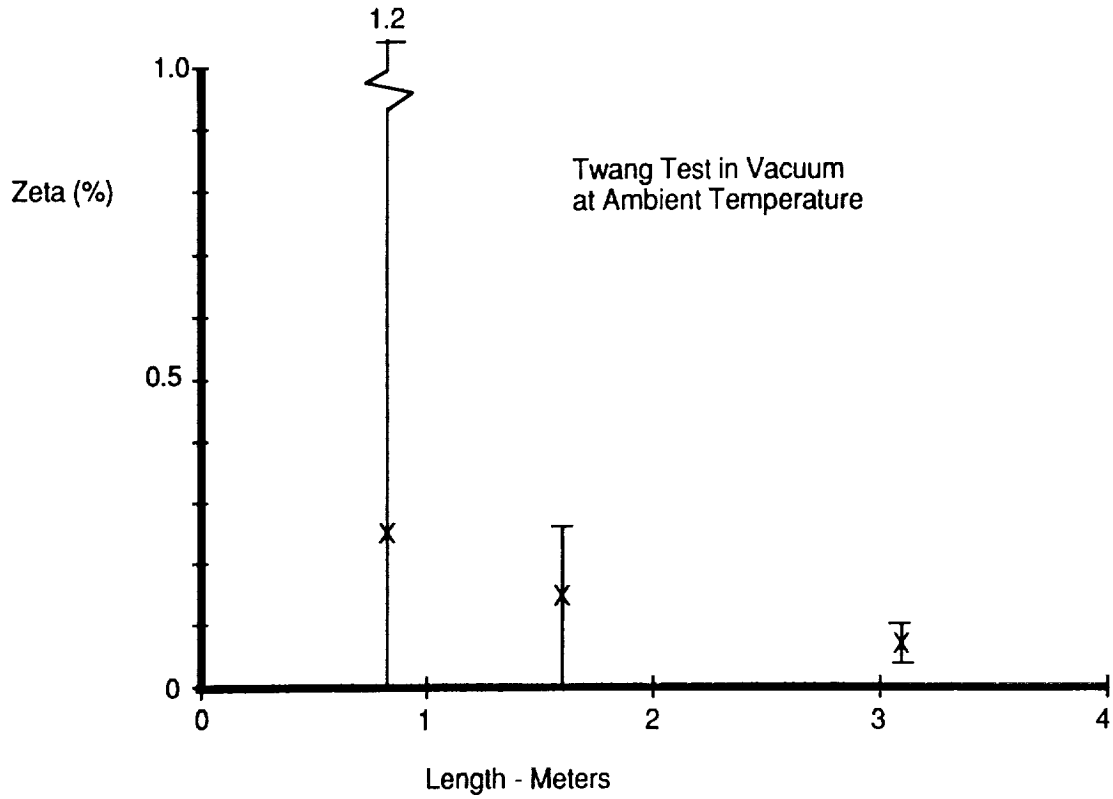

Figure 40. Material damping decreases with length.

The skiprope dynamic modeling approach had to be verified. Concern existed that the skiprope would introduce twist in the tether, creating various problems. Simulations assumed that no twist occurred, and what happened physically was energy transfer between string modes in the two perpendicular planes. Figure 41 illustrates this energy exchange phenomenon.

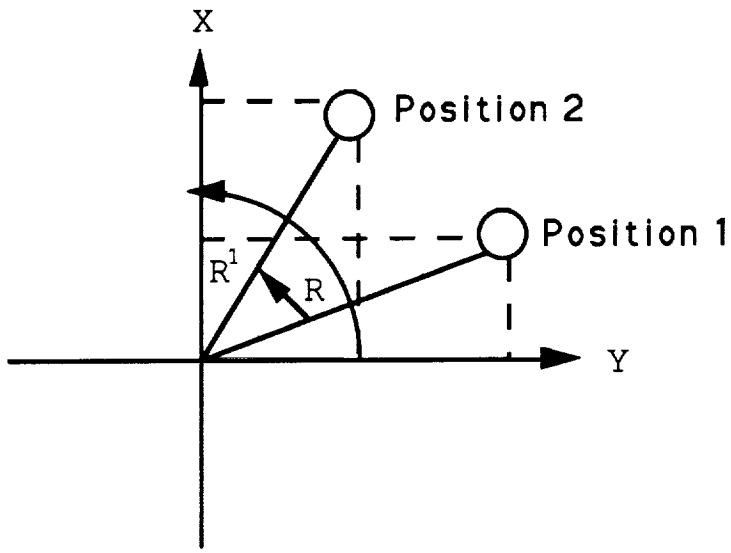

Figure 41. Skiprope phenomenon.

For each position of the tether in a circular skiprope motion ($R = R^1$), the deflection in the X and Y plane can be written as:

$$X(t) = \Sigma\eta_{x_\mu}(t)\gamma_\mu(Z)$$
$$Y(t) = \Sigma\eta_{y_\mu}(t)\omega_\mu(Z).$$

In moving from position 1 to position 2, the tether does not twist but merely transfers the energy from the Y plane to the X plane. Performing tests both in the atmosphere and in a vacuum demonstrated this to be the case. Motion pictures (video) were taken tracking points on the tether. There was never any tendency to twist, as any child knows from experience of holding the rope ends.

The last series of tests had to do with the deployer mechanisms themselves, because they are used in some manner to control the libration modes. These tests were run in both atmosphere and vacuum, including thermal effects. What could not be simulated was the zero-g effect.

IV. SKIPROPE CONTROL ELEMENTS/VERIFICATION

As the design evolved, it became apparent that skiprope had to be contained or a high risk that the satellite could not be recovered had to be accepted. There also existed some potential that excessive skiprope could be a safety problem due to entanglement with the orbiter. The crux of this paper, which follows, deals with the skiprope control elements and their verification for solving the skiprope problem.

A. Basic Problem Characteristics/Solution Approach

Recalling charts (figs. 27 through 31) and the dynamic frequencies of the system, the basic characteristics can be seen. Design of the mission was such that when the tethered satellite has completed deployment and is on station 1, science is conducted. As discussed previously, when current flows in the tether, regardless of the science mode under investigation, the electric field surrounding the tether interacts with the Earth's magnetic field to deflect the tether. As the system moves around the orbit, the science pulsing the current causes this deflection to become classical skiprope. Depending upon the conditions of the science conducted and when it is conducted, various amplitudes of skiprope can be excited. As the tether is reeled in from 20 km to 2.6 km (at the beginning of station 2), the induced skiprope remains. As the tether is reeled in from station 2, at approximately 500 m the first tether string mode resonance coalesces with the satellite's pendulous mode, transferring energy to this motion. If the satellite angular motion gets too large, docking and recovery of the satellite is impossible. In addition, the relative amplitude of the skiprope departure angle increases during retrieval, because angular momentum must be conserved. This coupling between satellite pendulous mode and the first lateral tether mode is the basic problem that must be solved in conjunction with containing the lateral string mode as the satellite is retrieved from 400 m.

These problems have led to the development of a multifaceted approach for containment of skiprope, producing successful satellite recovery, and the elimination of safety concerns involving the orbiter and crew. The basis of the approach is to determine how much skiprope amplitude can be handled from 600 m in and then provide a means of damping skiprope to this level prior to entering this period. The elements of this multifaceted approach are: (1) observing the skiprope amplitude and

phase using satellite control information (telemetry data); (2) orbiter yaw maneuvering during station 2 based on the observer data to reduce the skiprope amplitude below 20 m (the amplitude that can be handled during reel-in from 2.4 km); (3) attitude control of the satellite during the resonance period discussed; and (4) use of a passive tether damper to suppress skiprope as the satellite gets close to the orbiter. Figure 42 shows these basic schemes with acceptable gates for successful recovery of the satellite. In addition to these basic control mechanisms, a series of gates and priorities has been developed along with basic priorities that allows for cutting the tether and losing the satellite for safety reasons. The next sections will address, in detail, these various elements of skiprope control.

B. Observers (Time, Frequencies, and Visual)

As was stated previously, the capability of the observer to determine the skiprope amplitude and phase is one of the keys to handling the problem. The other keys are manual satellite attitude control (at least for TSS-1) and the use of a passive damper at the docking rings. First-, second-, and third-priority approaches have been developed with priorities two and three being active during operations as backup to priority one. These are: priority one is a time domain approach using Kalman filtering, priority two is a standard frequency domain approach, and priority three is visual by the crew using available cameras.

1. Time Domain Observer

a. Characteristics/Assumption. The time-domain observer is based on the assumption that there is a direct correlation between the satellite attitude data (telemetry) and the skiprope dynamics. The estimation is made based on a Kalman filtering technique and a nonlinear dynamic model of the tethered satellite system. Figure 43 gives the basic flow (characteristic) of the approach. The program contains a simulation of the skiprope and the satellite dynamics allowing the filter to project ahead based on past satellite data estimating the skiprope characteristics. This approach allows the observer to continue to predict skiprope even with telemetry data dropout. The frequency domain approach does not have this capability because it does not have predictive capability. Adjustment of the filter parameters and the degree of sophistication in the dynamic simulation allowed tuning of the approach to improve accuracy. For example, higher-ordered string modes, though not included for the TSS-1 mission, could be included in the nonlinear simulation to improve the accuracy of the prediction capability.

The basic characteristic of the time-domain filter is that it can operate with the satellite during:

- Deploying, retrieving, or on station
- Spinning, in yaw hold, or passive
- Flowing tether current or not.

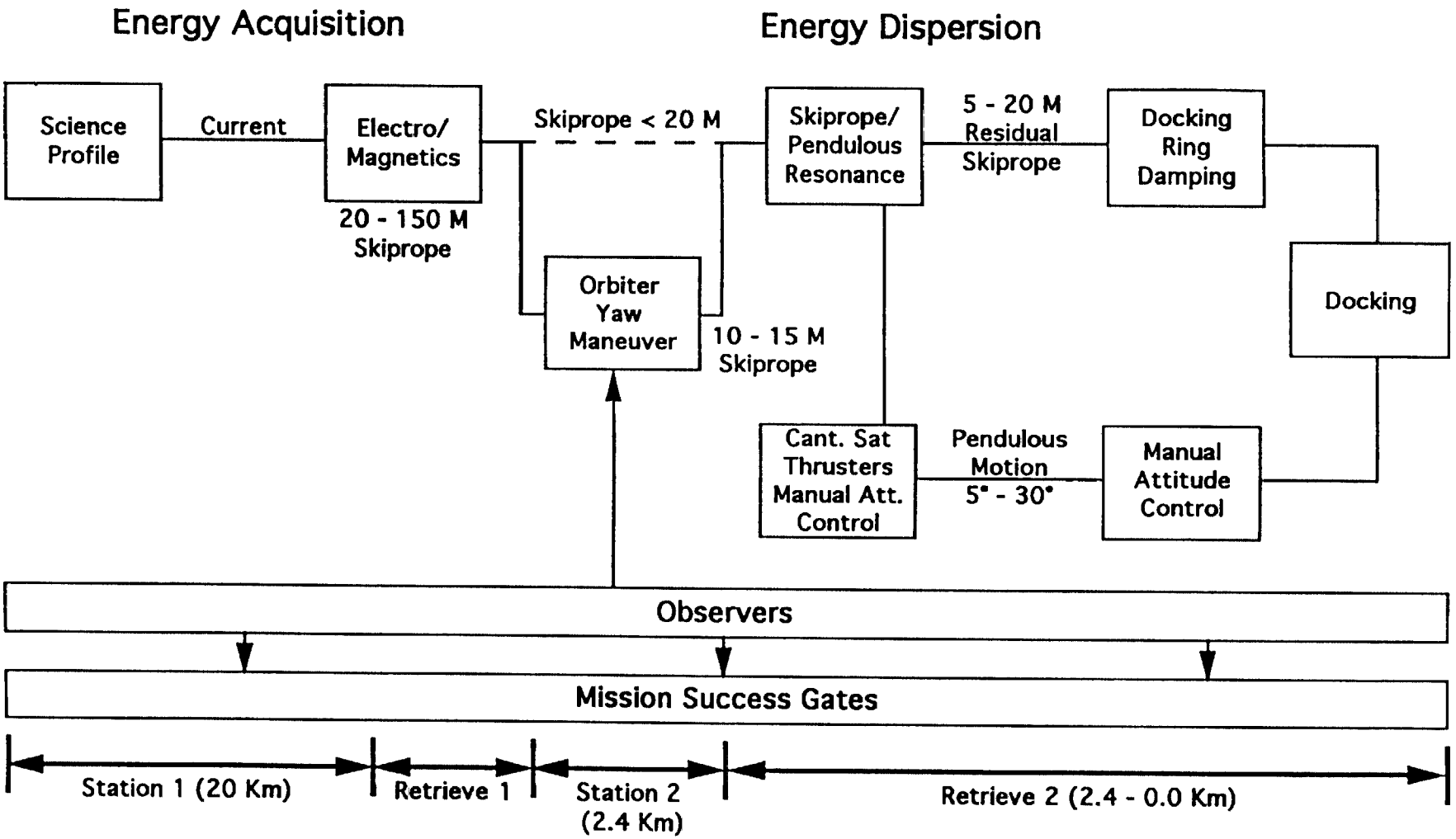

Figure 42. Skiprope containment flow diagram.

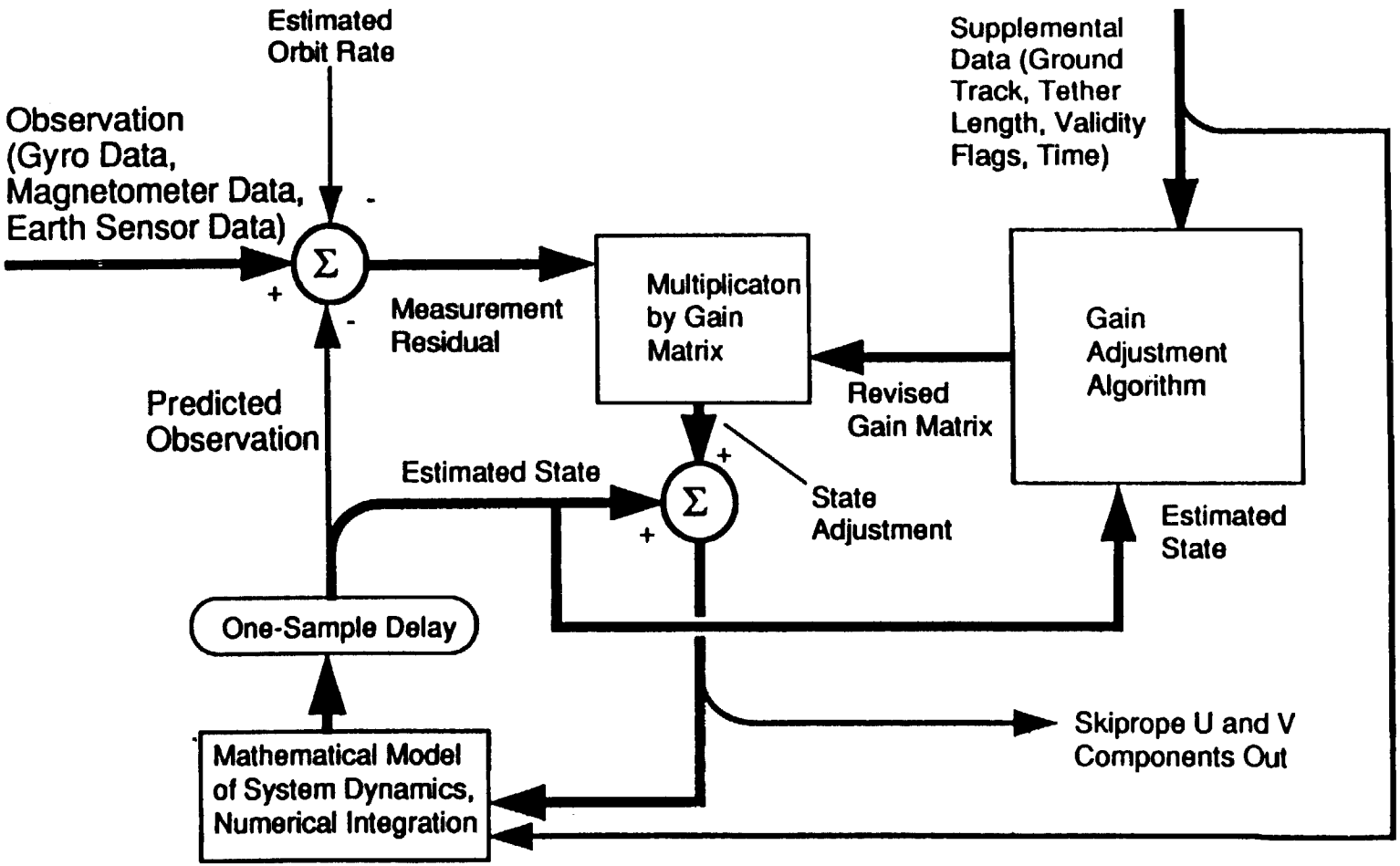

Figure 43. Simplified time-domain skiprope observer (TDSO) block diagram.

As mentioned previously, it can operate with some failed sensors and can handle limited telemetry dropouts. It is applicable for all tether lengths greater than 1,000 m and provides real-time display of tether motion. It estimates:

- Skiprope amplitude phase and direction
- Libration angles
- Skiprope period
- Satellite attitude.

It dead-reckons during loss of signal. It has an accuracy between 5 and 15 m and provides a real-time estimate of its own accuracy.

The current time-domain estimator is based on the following assumptions:

- Skiprope motion is predominantly first-mode
- No large tension oscillations
- System mathematical model is adequate
- Telemetry data used are available real-time.

The time-domain filter was developed and verified using a series of simulation results which used the models described in section III B. Data noise and various failure modes (telemetry) were used. These cases include:

- Deploy
- On station (1 and 2)
- Retrieval from station (1 and 2)
- During maneuvers
- With and without current flow, satellite spin.

Figures 44 and 45 describe the cases used.

The case YAWA station 2, starting with a skiprope amplitude of 50 m, is shown on figures 46 and 47. The actual case is compared to the filters estimation. Notice that the greatest prediction error occurs during the yaw maneuver. As soon as the yaw maneuver is over, the high prediction accuracy is present. Figure 46 is the U-axis plot, while figure 47 is the V-axis plot. In addition to these cases, sensitivity studies were run for:

ST1A: Station 1, Current Flow, Satellite Spinning at 4.2°/sec, Booms Extended

ST1B: Station 1, Current Flow, Satellite In Yaw Hold, Booms Retracted

ST1C: Station 1, No Current Flow, Satellite Spinning at 4.2°/sec, Booms Extended

ST2A: Station 2, Slow Retrieval, Current Flow, Satellite In Yaw Hold, Booms Retracted

ST2B: Station 2, Slow Retrieval, No Current Flow, Satellite In Yaw Hold, Booms Retracted, Yaw Maneuver Performed

ST2C: Station 2, Current Flow, Satellite Spinning at 4.2°/sec, Booms Extended

ST2D: Station 2, Current Flow, Satellite In Yaw Hold, Booms Retracted

YAWA: Station 2, Slow Retrieval, No Current Flow, Satellite In Yaw Hold, Booms Retracted, 50 m Skiprope, Yaw Maneuver Performed (5 Orbiter Revolutions)

YAWB: Station 2, Slow Retrieval, No Current Flow, Satellite In Yaw Hold, Booms Retracted, 50 m Skiprope, JSC Yaw Maneuver Performed (3 Orbiter Revolutions, 30 Minute Wait, 2 Orbiter Revolutions)

Figure 44. TDSO simulation test cases.

RET1A: Retrieval 1, Current Flow, Satellite In Yaw Hold, Booms Retracted (Mission Time of 19 Hours)

RET1B: Retrieval 1, Current Flow, Satellite In Yaw Hold, Booms Retracted (Mission Time of 21 Hours)

RET1C: Retrieval 1, Current Flow, Satellite In Yaw Hold, Booms Retracted (Mission Time of 23 Hours)

RET2A: Retrieval 2 at 2.35 km, No Current Flow, Satellite In Yaw Hold, Booms Retracted

RET2B: Retrieval 2 at 1.5 km, No Current Flow, Satellite In Yaw Hold, Booms Retracted

DEPA: Deployment at 1 km, Current Flow, Satellite In Yaw Hold, Booms Retracted

DEPB: Deployment at 10 km, Current Flow, Satellite Spinning at 1.5°/sec, Booms Retracted

Figure 45. TDSO simulation test cases.

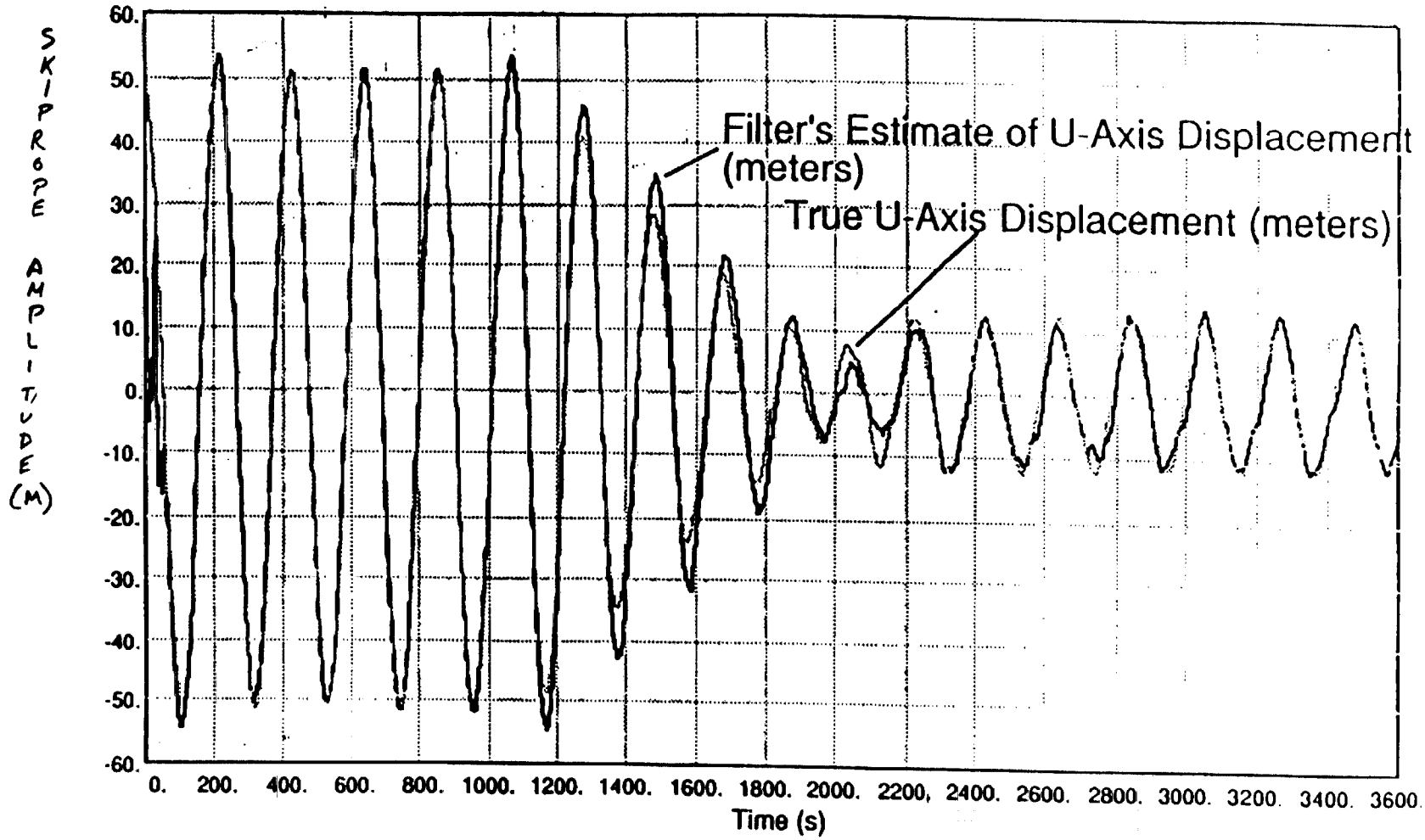

Figure 46. TDSO YAWA test case results.

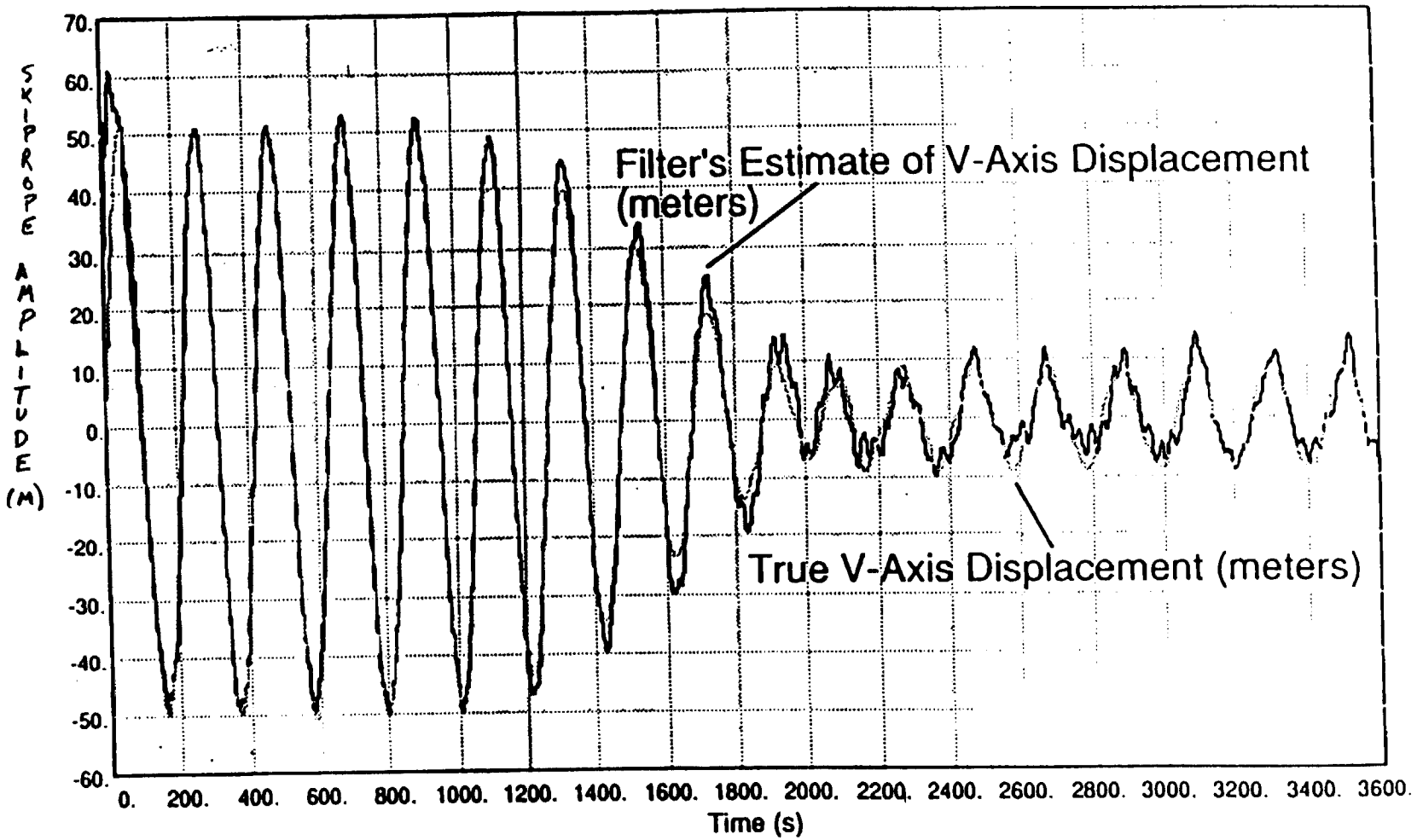

Figure 47. TDSO YAWA test case results.

- Modeling sensitivity

- Disturbances in higher translational modes

- Tension-mode disturbances.

Also, the filter was run in end-to-end simulations with high-fidelity dynamics simulated. The accuracy was typically 5 to 15 m, with the large errors occurring where predictions were not critical (dependent on high-mode content). There was low sensitivity to modeling errors, and the filter can cope with expected levels of tension oscillation. The filter was also effective in timing damping maneuvers (orbiter yaw).

Flight operations software was developed for the preprocessor of the telemetry data along with the filter software. Figures 43 and 48 show this total loop of the preprocessor and the time-domain filter. Portions of this same preprocessor could be used with the frequency domain filter; however, this was not the case for the TSS-1 implementation as completely independent implementation was chosen. This system was first programmed for the Mac II computer so that it would be accessible to several engineers to understand and stress the system. After this was accomplished, the software was converted to the MassComp computer at JSC that was used in operations. Several check cases were run on the operations computer (MassComp) and compared to the cases run on the Mac II system.

b. Certification. Upon completion of the development program, the filter went through formal certification. This was accomplished using documented requirements, test plans, and procedures. Thorough unit testing was accomplished, verifying all requirements. The software was then put under configuration control. All testing was witnessed by Quality Assurance (QA) and the Defense Projects Reliability Office (DPRO) and met all formal sign-off requirements, including a formal review board.

c. Examples. Many cases of the dynamic skiprope have been run using various conditions to serve as tests for the filter accuracy. These cases were used as inputs to the filter and served as the standard. These cases included telemetry dropout as well as different maneuvers and science profiles. Figures 49 through 54 are some of these cases plotted in the time domain. Satellite motions and skiprope motion are plotted.

d. Operations. During operations, the output of the filter will be observed by operations personnel in real time. From these data, they will determine the magnitude and phase required for the yaw maneuver. These data will also be recorded for use in understanding the skiprope phenomenon for later missions.

Training of the ground observer crew was accomplished through operations training at the Houston (JSC) operations center. Primary and backup personnel were trained for the mission.

In addition to determining the yaw maneuver characteristics to be uplinked to the crew, mission design calls for the filter output to be used as input for the safety gates developed to ensure crew safety at all times. The use of safety gates is the standard operating procedure for all shuttle flights. Two separate computers and programs exist for redundancy.

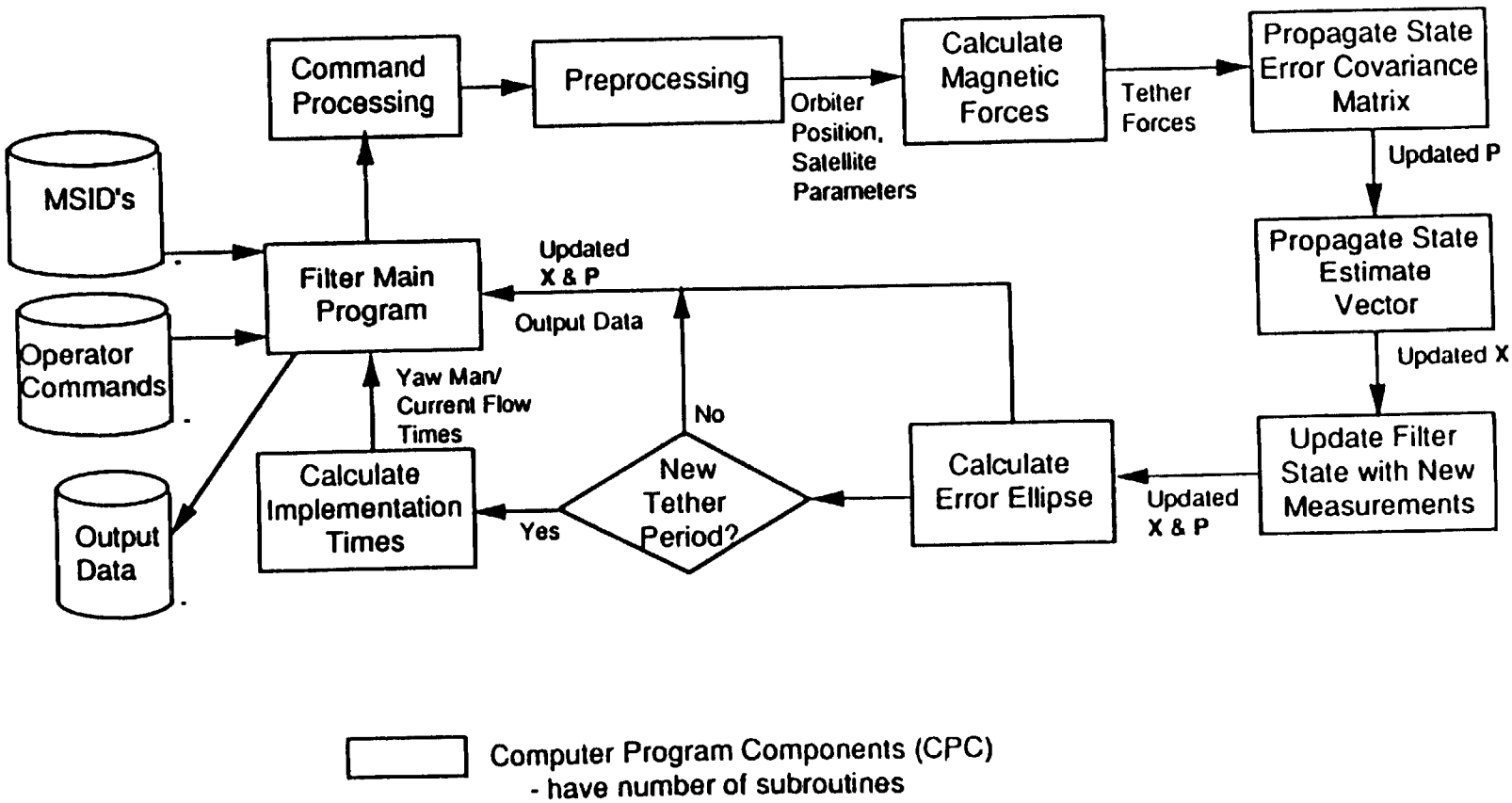

Figure 48. Time-domain skiprope observer software functional flow.

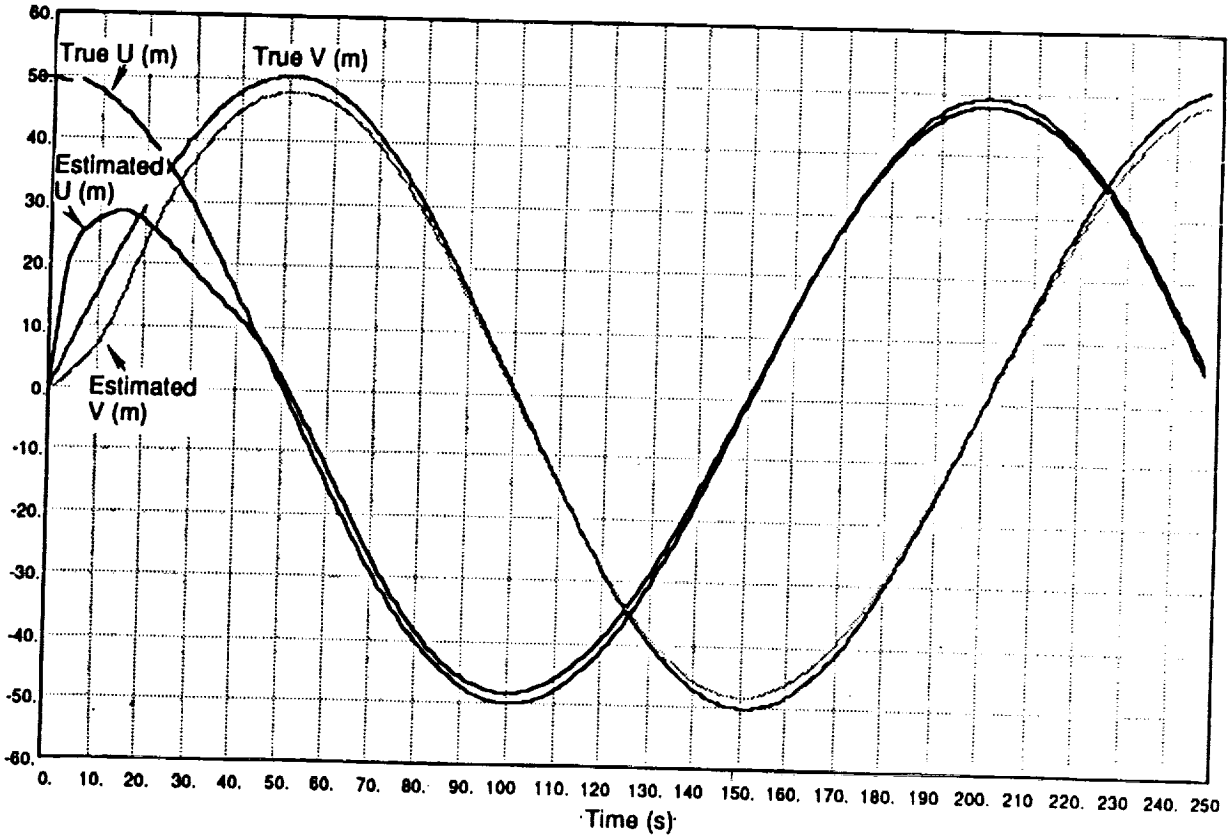

Figure 49. Typical results at 2,400 m, "noiseless" sensors, no current flow.

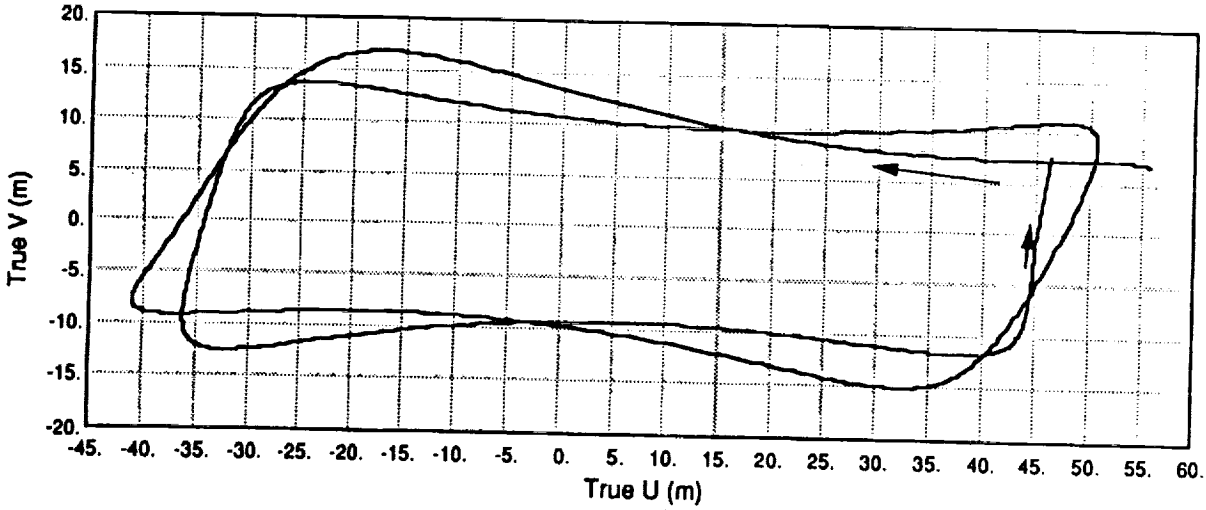

Figure 50. True motion pattern for retrieval case.

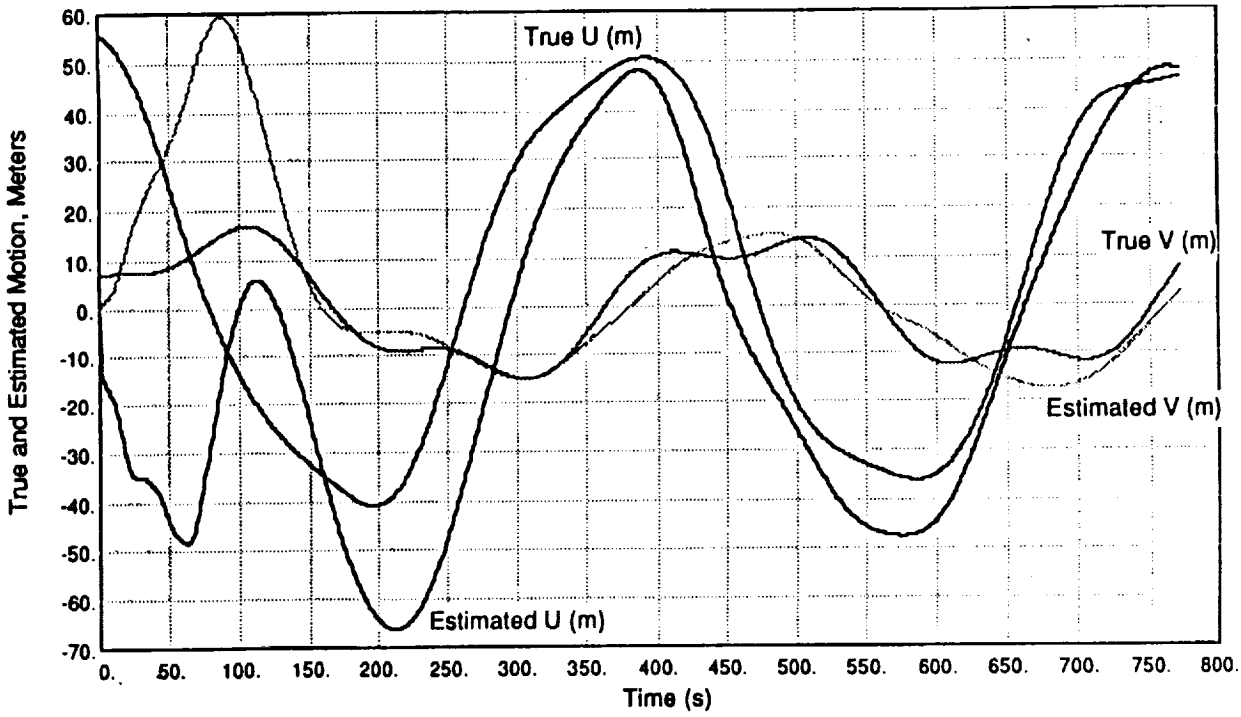

Figure 51. Filter U, V outputs compared to truth for noiseless retrieval case.

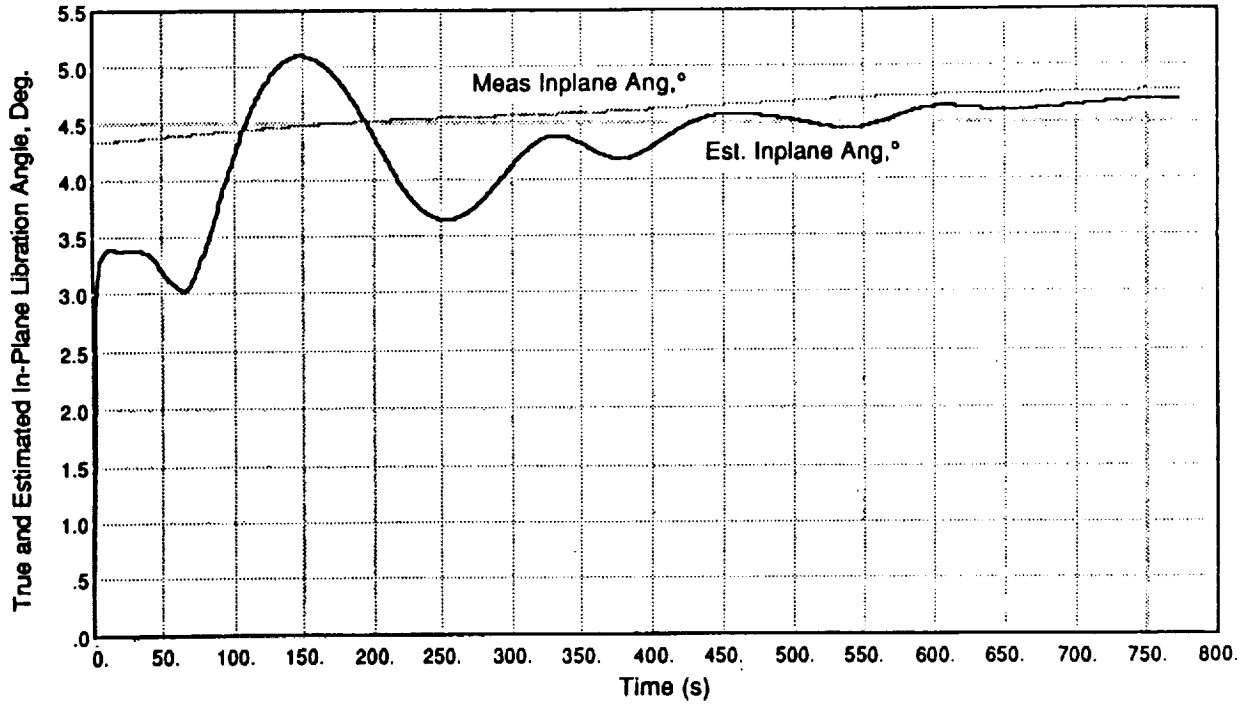

Figure 52. In-plane libration estimates by TDSO.

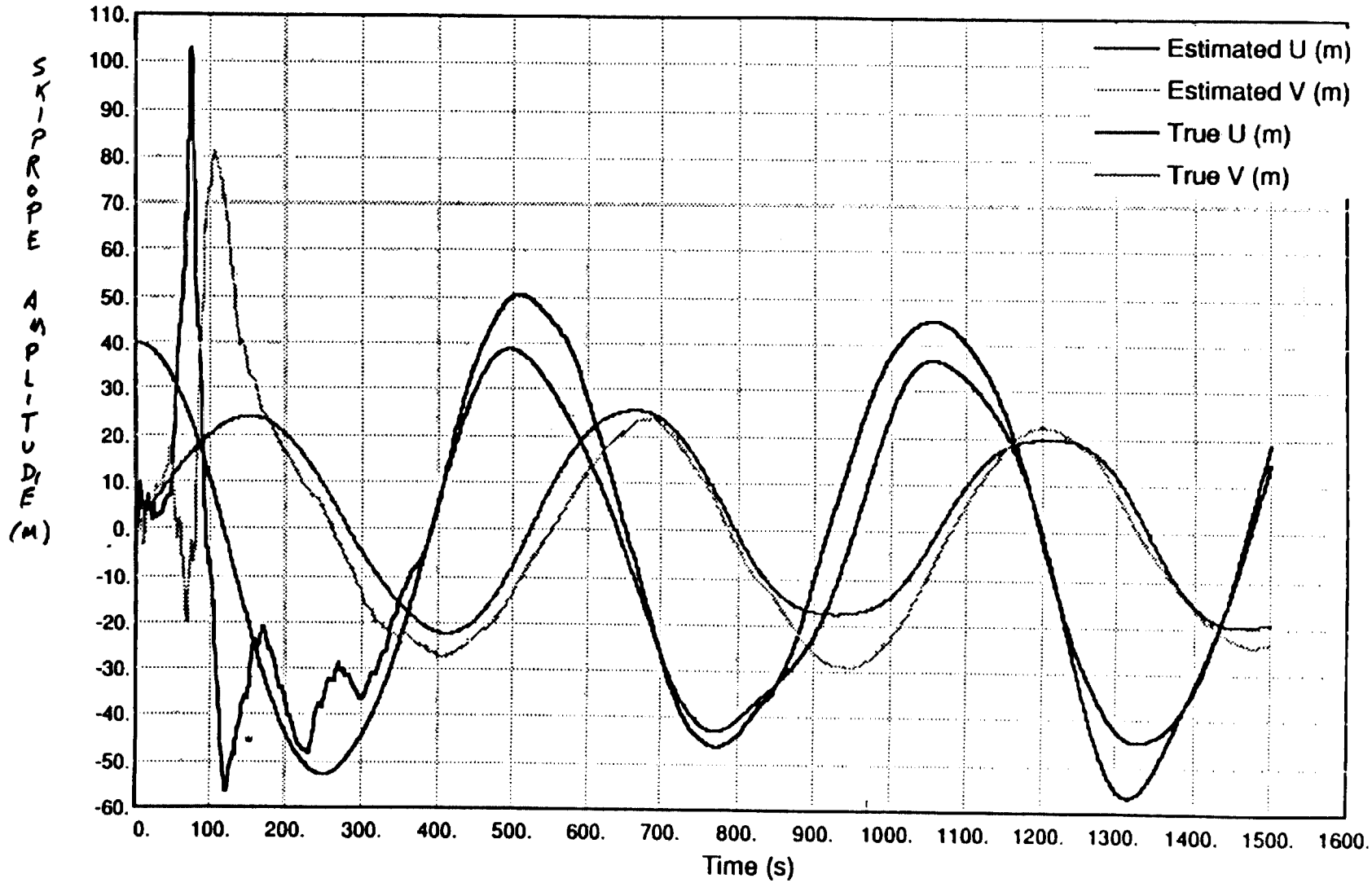

Figure 53. Filter output, station 1, noisy quantized sensor data.

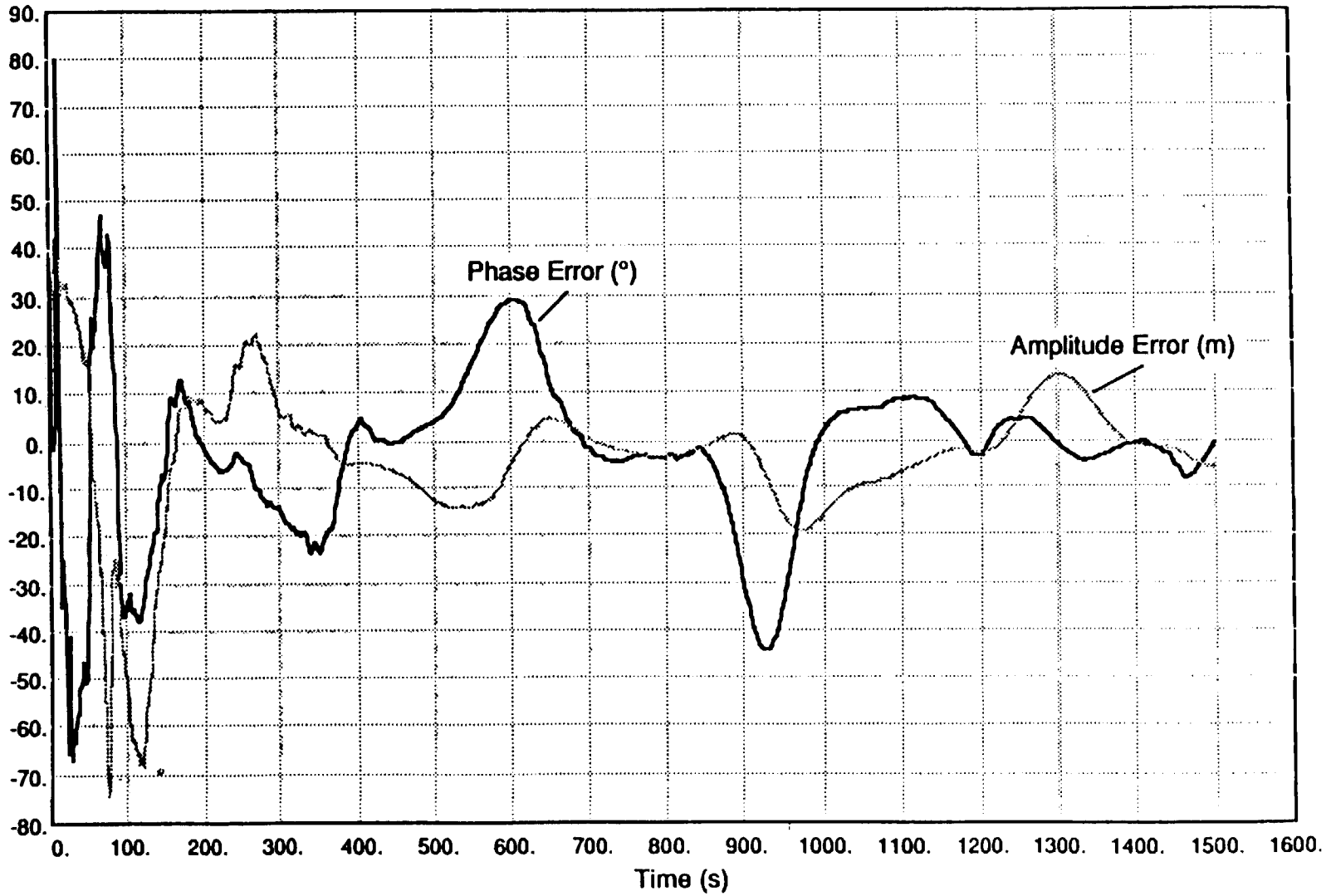

Figure 54. Errors at station 1, noisy quantized sensor data.

2. Frequency Domain Skiprope Observer (FDSO). The frequency domain observer had the same purpose as the time domain observer. It was used to backup the time domain filter and was to be run in parallel during flight operations. The frequency domain estimator is based on a Fourier transformation of the satellite telemetry data. Data are recorded continually in time by keeping a constant time increment and sliding a 30-min data window along, thus capturing the data in a 30-min buffer. The stored data set is then analyzed by Fourier transform for discrete frequency, amplitude, and phase. Figure 55 is a block diagram of this process.

The same check cases have been used for the frequency observer as were used for the time observer. Tables 1 and 2 are the results of these check cases. Adequate results were obtained for understanding the skiprope phenomenon, and, for orbiter yaw, a maneuver command was obtained. More recent studies (not incorporated for TSS-1 (STS-46)) have enhanced this filter's capability to predict nonconstant amplitude and also phase during spinning.

The frequency domain observer went though the same certification as the time domain and was witnessed by software QA. The accuracy was typically between 5 and 15 m.

The assumptions made in developing this observer were:

- Tether motion in phase with gyro rates
- Motion proportional to gyro rates of opposite axes
- Proportionality factor a function of tether length
- Motion nearly periodic
- Motion at approximately predicted frequency
- Precession, if any, is slow.

The test cases with synthetic telemetry from simulation were run for:

- Station 1 and 2
- With and without satellite spinning
- Varied motion amplitude
- Circular and elliptical motion
- Mock gyro test signals.

Operations aspects are the same as described for the time domain observer.

3. Visual. For shorter tether lengths (at or below 2.4 km), the skiprope motion can be observed by the flight crew by eyesight or by the use of an on-board camera. This is a contingency mode that the flight crew has trained for in case telemetry is lost. To date, it has shown to be effective in prescribing the yaw maneuver characteristics.

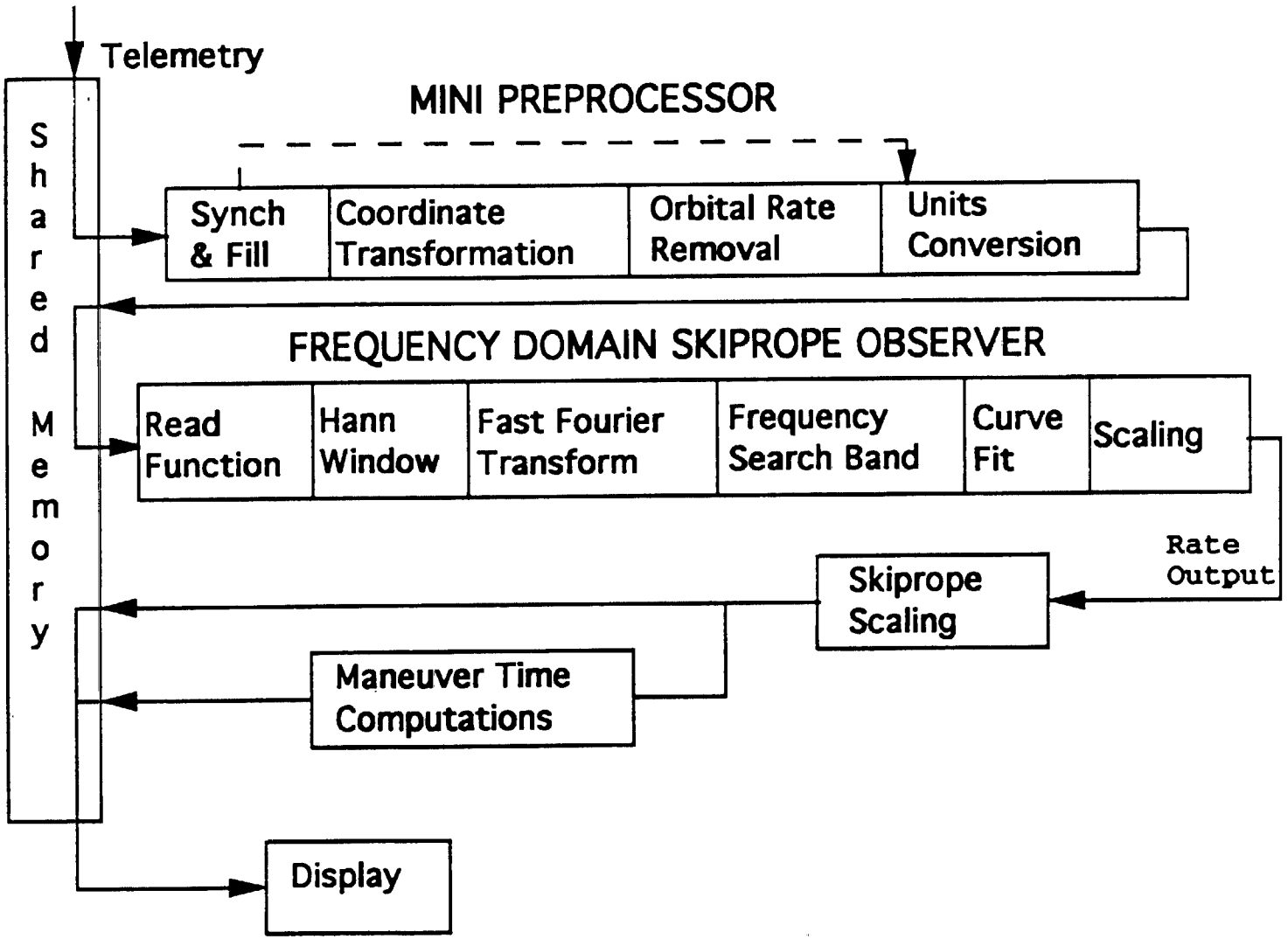

Figure 55. Frequency domain skiprope observer (FDSO) block diagram.

Table 1. FDSO simulation results.

Case	Length	Status	Truth		MSFC Filter		RMS EMP Err (Percent)	RMS Phase Err (°)	
			U	V	U	V			
1	2.4 k	No spin	20	20	20.35	20.10	7.65 / 6.05	9.9 / 3.96	MSFC/UNO
2	2.4 k	No spin	60	60	60.23	59.93	4.72 / 4.97	9.55 / 4.31	
3	2.4 k	No spin	80	40	61.51	61.23	29.5 / 34.42	21.9 / 22.11	Nonstationary
4	20 k	No spin	80	40	83.62	42.04	10.3 / 9.2	8.1 / 6.5	
5	20 k	No spin	80	80	83.45	84.08	5.71 / 5.80	6.06 / 4.70	
6	20 k	Spin	32	16	31.25	15.8			
7	20 k	Spin	60	30	60.00	30.26			

Table 2. FDSO results using model 3 data (September 25, 1991, MMAG memo).

Case	Length (km)	Time Slice Seconds (ΔT=1)	Model 3 (2) Meters U	Model 3 (2) Meters V	FDSO (1) Meters U	FDSO (1) Meters V	Comments
DEPB	9.65–14.9	1–2,000	12.5	5	16	4	T = 2,700, spin 1.5D/S, current on
ST1A	20	1–2,000	30	15	26	12	T = 2,700; spin 4.2D/S; current on
ST1B	20	1–2,000	50	20	57	17	T = 2,700; current on
ST1C	20	1–2,700	25	22	33	11	T = 2,700; spin 4.2D/S; no current
RET1A	17.6–15.3	1–2,700	33	10	34	9	T = 2,700; current on
RET1B	11.3–8	1–1,500	35	5	40	5	T = 2,700; current on
ST2A	2.72–2.63	1–850	12	26	10.5	23	T = 2,700; slow retrieval (SR); current
		900–1,800	18	22	19	19	on
		1,800–2,700	26	15	24.5	12.5	
ST2B	25.5–26.5	1–750	23	15	25	16	T = 3,600; SR, yaw maneuver; no current. Burn time off by 20 WRT MMAG.
		2,500–3,500	10	12	7	10	third harmonic after maneuver.
ST2C	2.4	1–900	30	18	40	26	T = 2,700; spin 4.2; current on
		1,500–2,700	25	12	25	20	
ST2D	2.4	1–750	30	20	25	22	T = 2,700; current on;
		100–1,650	15	32	15	27	third harmonic is large
		2,000–2,700	28	12	25	16	
RET2A	2.36–0.67	1–749	22	22	22	25	T = 2,700; no current
		750–1,500	20	20	23	28	
		1,400–2,000	25	25	27	28	
YAWA	2.71–2.59	1–749	50	50	52	52	T = 3,600; no current; TBURN = 1,118 (MMAG) = 1,120 (FDSO)
		2,250–3,000	10	8	12	8	Residual
YAWB	2.71–2.52	100–750	50	50	52	52	T = 5,400; no current; TBURN = 1,118 (MMAG) TBURN = 1,120 (FDSO); two maneuver case
		2,000–3,500	20	18	19	16	For second burn
		4,200–4,800	5	5	4	6	Residual

C. Orbiter Yaw Maneuver

As was discussed previously, the orbiter yaw maneuver is designed to be used on station 2 (2.4 km) to reduce the skiprope amplitude to a level that is manageable during final retrieval and docking; less than 20 m of skiprope. Figure 56 shows the yaw maneuver technique to dampen the skiprope. The yaw maneuver is managed via observers (ground ops) who send up the amplitude and timing for the maneuver. Simulations have been run to show the effectiveness of the maneuver using both a continuous maneuver and two separate maneuvers. Table 3 shows two simulation cases. Figure 57 shows how well the skiprope amplitude is reduced using the two separate yaw maneuvers. In order to accomplish this damping of the skiprope:

- The orbiter rotations must lag the skiprope motion by 90°
- The orbiter rate must equal the skiprope rate
- The skiprope amplitude and the offset of the deployer boom from the orbiter center of gravity dictate how many orbiter rotations to perform
- Errors in phase and frequency reduce yaw maneuver effectiveness.

Data that must be telemetered to the crew in order to perform the yaw maneuver are calculated by the skiprope observers:

- Time to start maneuver (skiprope phase)
- Orbiter yaw rate (skiprope rate)
- Number of orbiter rotations (skiprope amplitude).

Examples:

Figure 58 describes operational constraints on a case run to illustrate the effectiveness of the yaw maneuver. Figure 59 shows the orbiter yaw rate, figure 60 is a plot of the skiprope amplitude, and figure 61 is a plot of the skiprope angular momentum.

Figure 62 describes another simulation run. In this case, it is one maneuver. Figure 63 is the orbiter rate, figure 64 is the skiprope amplitude, and figure 65 is the angular momentum. Because the original skiprope was elliptical and 10 by 20 m, the overall amplitude was not reduced much; however, the angular momentum of the skiprope was reduced by 75 percent.

Many other cases have been run, all demonstrating the effectiveness of the yaw maneuver.

D. Satellite Attitude Control

The satellite has in-plane (pitch), out-of-plane (roll), and yaw thrusters. Originally, the thrusters were used as pure libration (in-plane and out-of-plane), and yaw control (fig. 3). In addition, there were in-line thrusters for tension augmentation during deployment and retrieval. As the program developed, and in particular the understanding of the systems dynamic (line modes/skiprope

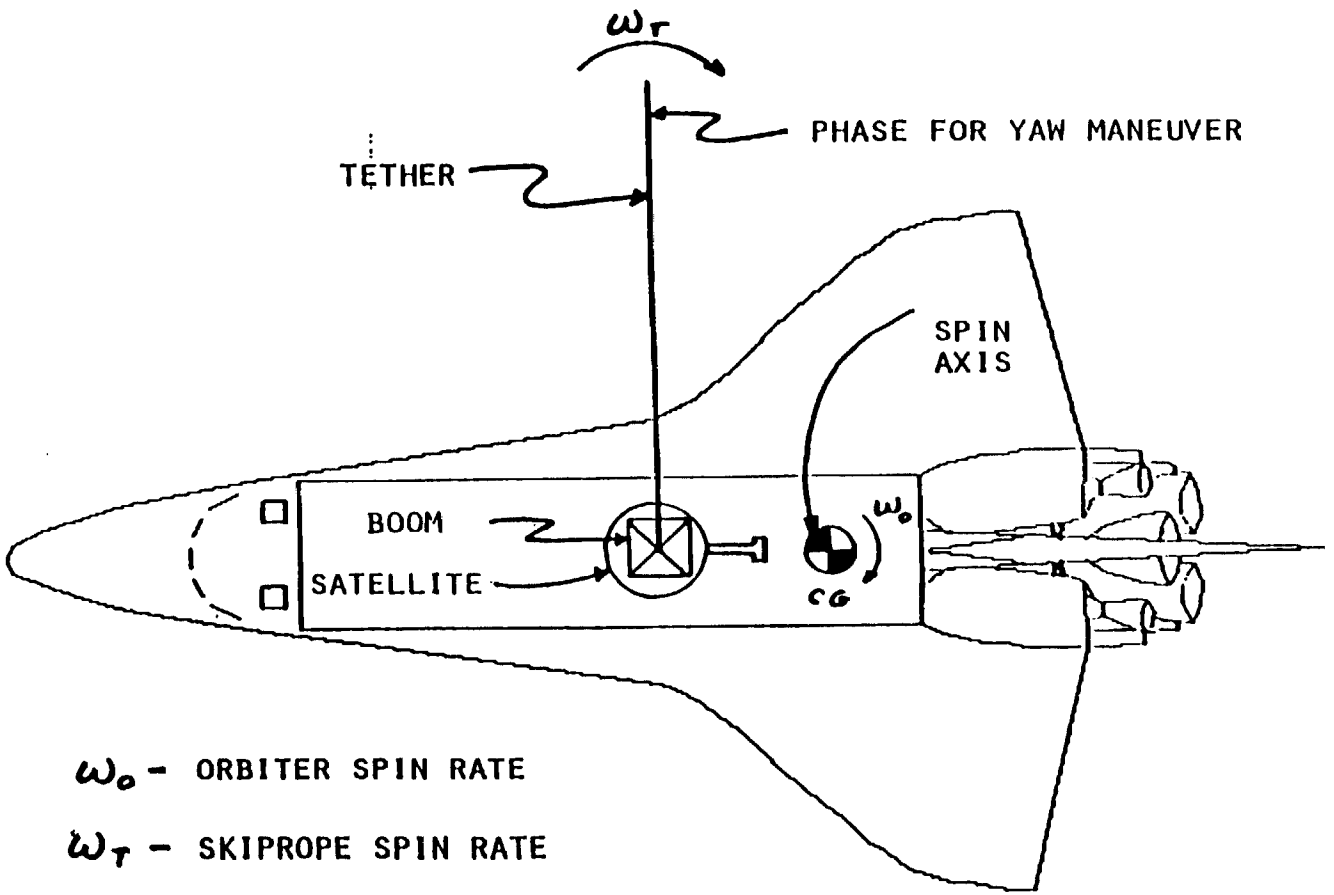

Figure 56. Yaw maneuver technique.

Table 3. Yaw maneuver simulation results.

Case	Yaw Maneuver	Initial Skiprope (m)	Final Skiprope (m)	Initial Angular Momentum (N-m-s)	Final Angular Momentum (N-m-s)	Number of Orbiter Rotations
1	1	50 by 50	22 by 17	850	125	3
1	2	22 by 17	8 by 3	125	0	1.5
2	1	25 by 10 5 m Third Mode	22 by 5 5 m Third Mode	100	40	0.7

- Gates to leave station 2
  - With satellite attitude control 20 m (133 N-m-s)
  - Without satellite attitude control 7 m (16 N-m-s).

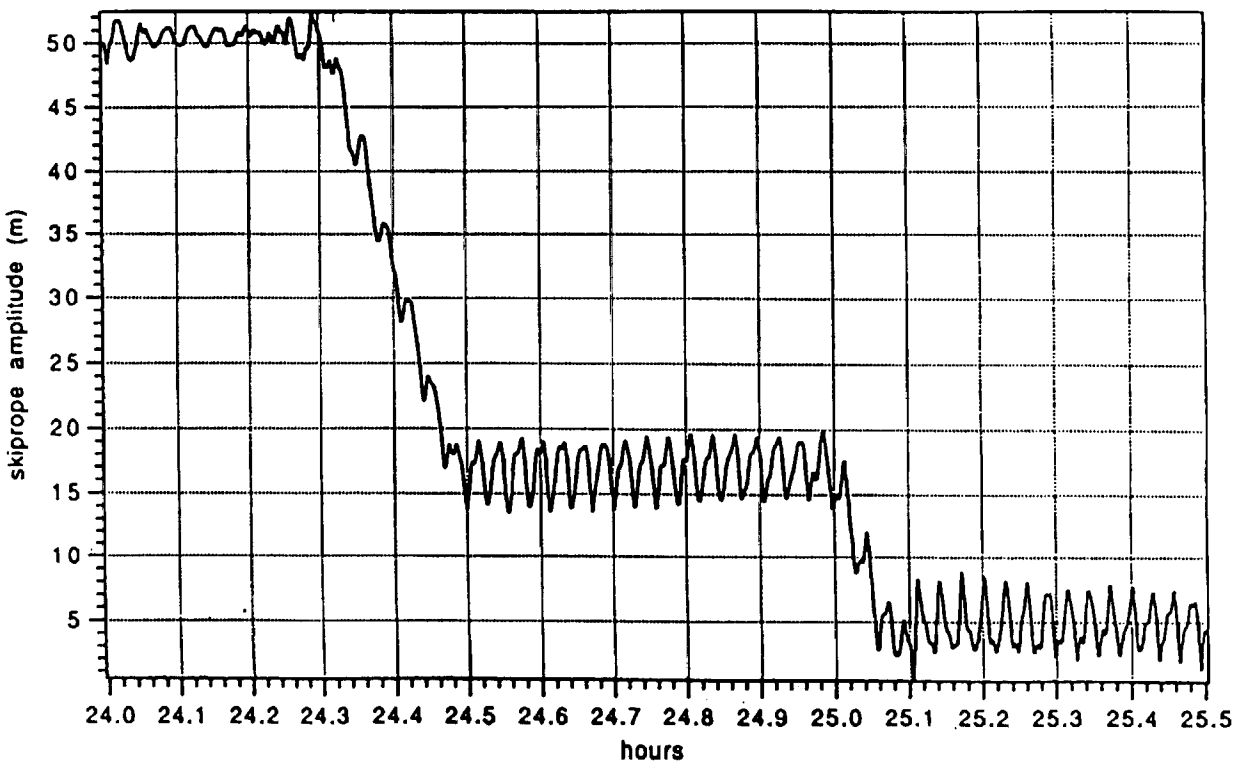

Figure 57. Yaw maneuver simulation (skiprope amplitude).

- **Initialized A 50 Meter Circular Skiprope.**
- **Simulation Run From A Mission Time Of 24.0 Hours To 25.5 Hours.**
- **Tether Length Varies From 2.7 KM To 2.542 KM.**
- **No More Than 3 Orbiter Rotations Performed Per Yaw Maneuver.**
- **2 Yaw Maneuver Performed.**
  - **First At 24.31 Hours With 3 Orbiter Rotations**
  - **Second At 24.99 Hours With 1.5 Orbiter Rotations**

Figure 58. Yaw maneuver simulation.

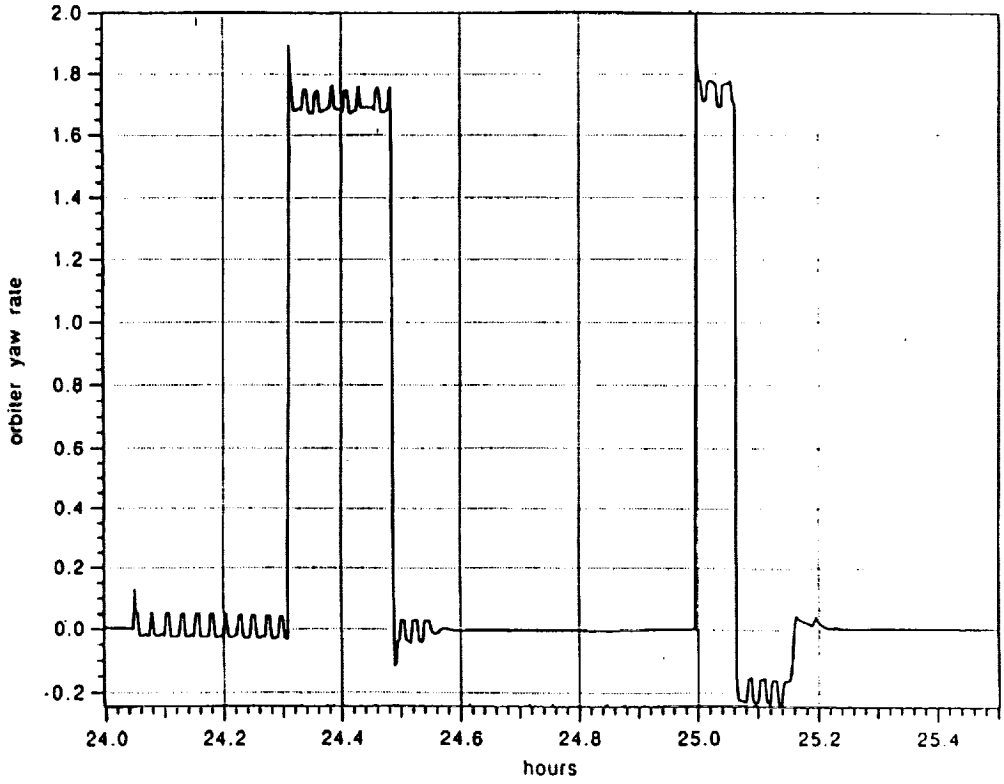

Figure 59. Yaw maneuver simulation (orbiter yaw rates).

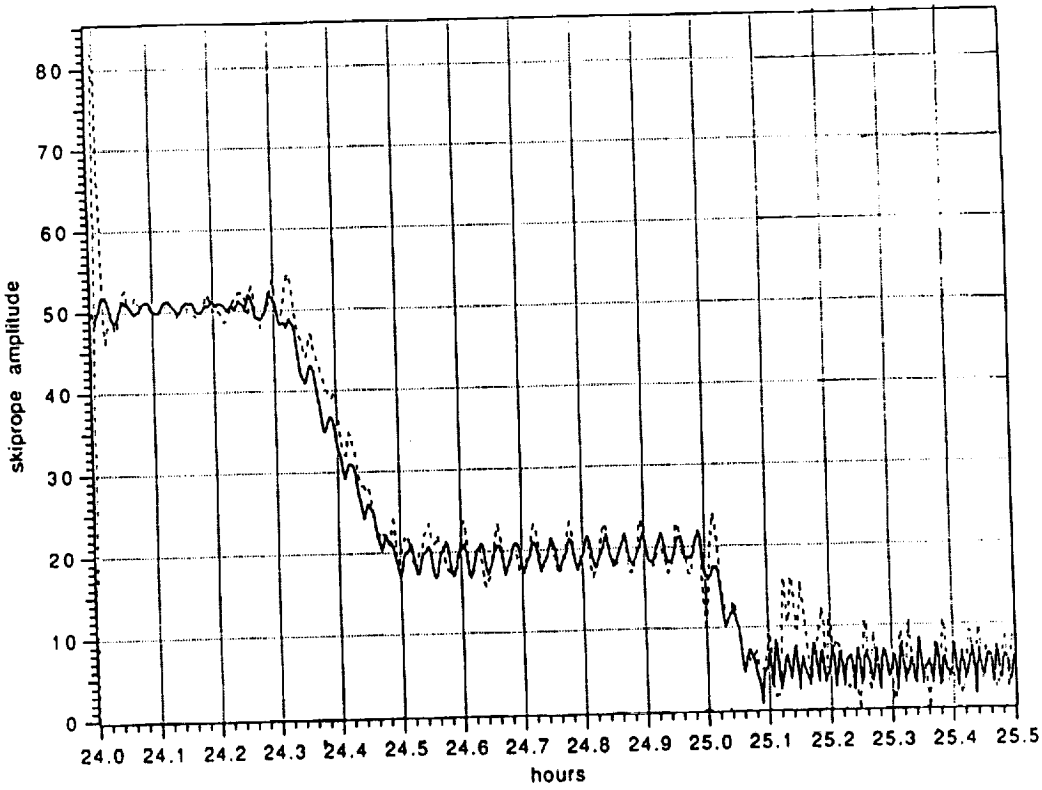

Figure 60. Yaw maneuver simulation (skiprope amplitude).

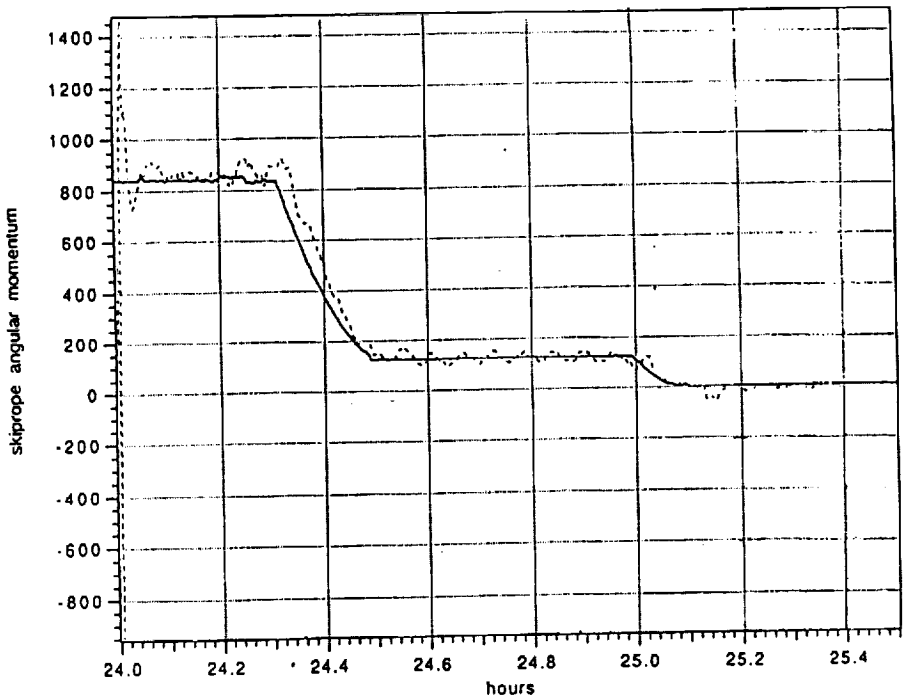

Figure 61. Yaw maneuver simulation (skiprope angular momentum).

- **Used Skiprope Initial Conditions Generated By Using The May 1991 Science Current Profile For The Nominal Mission.**
- **Started With A 25 By 10 Meter Elliptical Skiprope With Approximately 5 Meters Of Third Mode Amplitude.**
- **Simulation Run From A Mission Time Of 25.5 Hours To 26.5 Hours.**
- **Tether Length Varies From 2.542 KM To 2.431 KM.**
- **Yaw Maneuver Performed At 25.83 Hours With 0.7 Orbiter Rotations**

Figure 62. Yaw maneuver simulation.

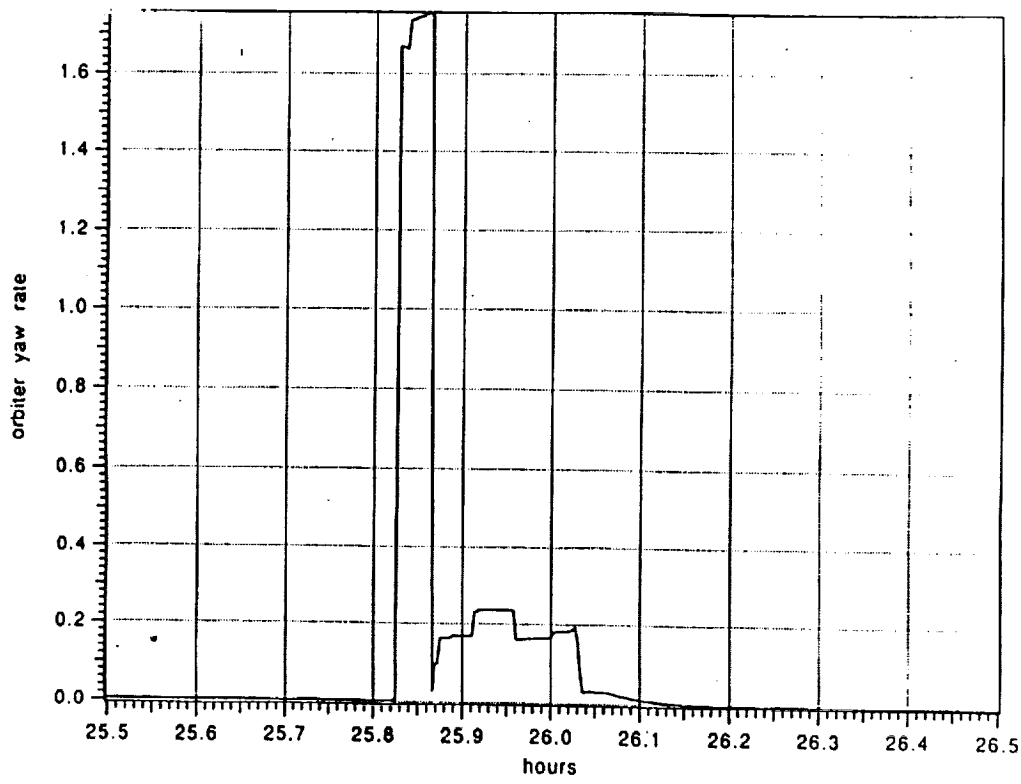

Figure 63. Yaw maneuver simulation.

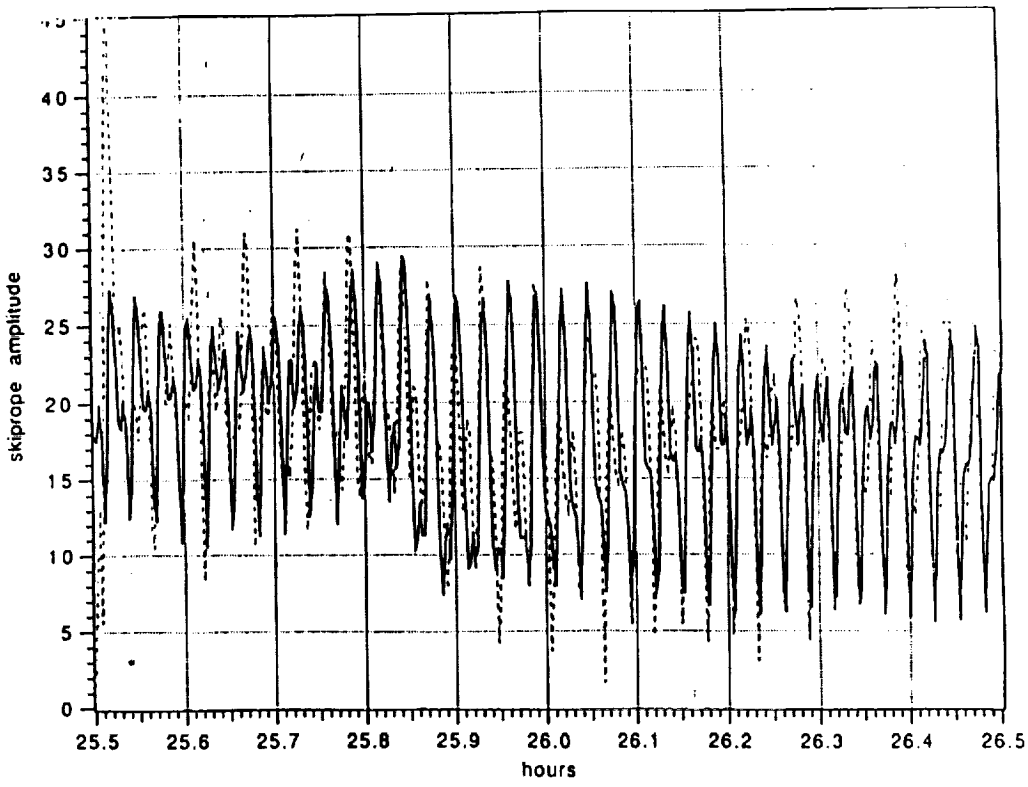

Figure 64. Yaw maneuver simulation.

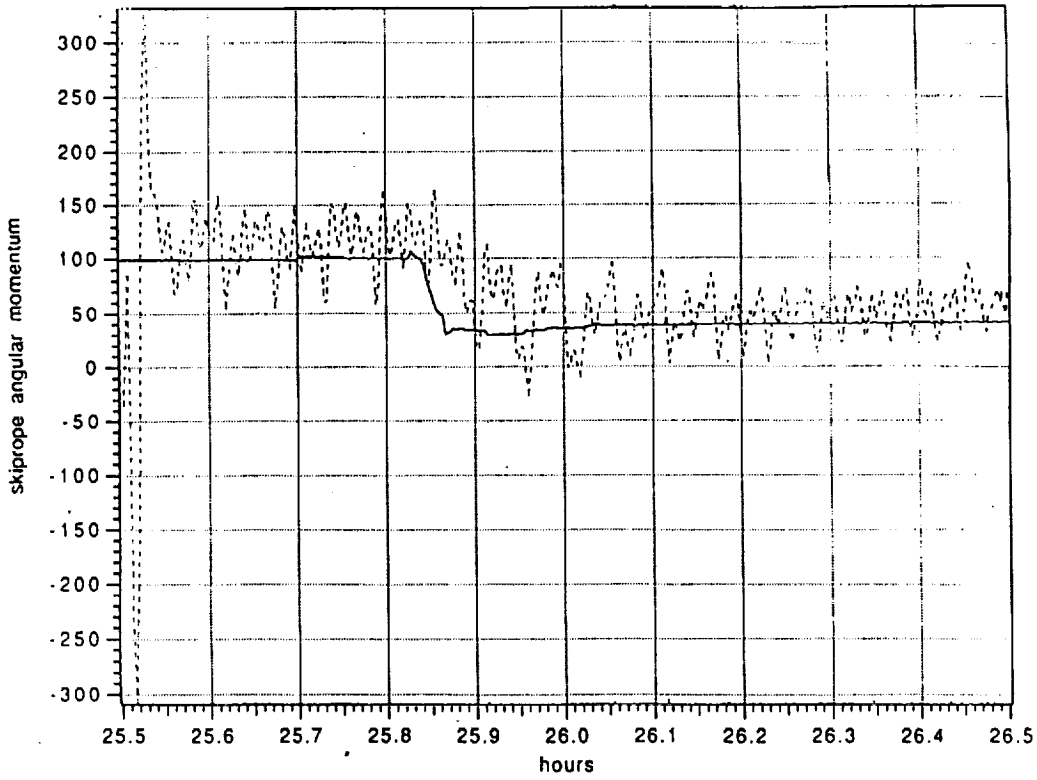

Figure 65. Yaw maneuver simulation (skiprope angular momentum).

and satellite attitude frequencies), the need for satellite attitude control developed. In order to achieve this attitude control by firing the thrusters without totally redesigning the APS system, the out-of-plane thrusters and the in-plane thrusters were both canted (20° and 30°, respectively), thus producing moments for control (fig. 66) as well as a remaining, but now unwanted, translational component. To offset the effects of the translational components, control firings must involve thrusters on opposite sides in relatively equal amounts.

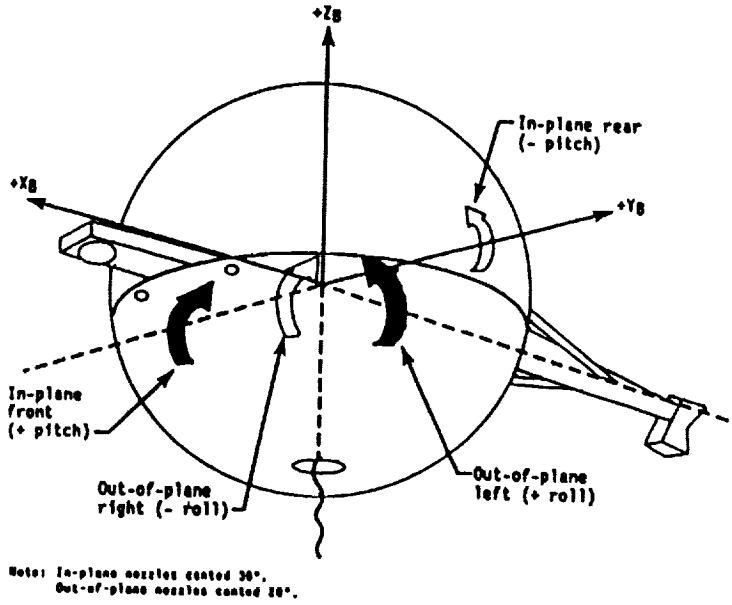

Figure 66. Satellite auxiliary propulsion system.

The need for attitude control developed when it was understood that, at approximately 430 m, a coalescence of the skiprope and the satellite attitude frequency (pendulous) occurs with significant transfer of energy. During this coalescence, the satellite attitude can be excited (6° satellite attitude for each meter of skiprope). Without satellite attitude control, skiprope motion greater than 7 m will drive the satellite attitude beyond recovery limits. Canting the thrusters allows this attitude control.

During tether operations, the orbiter receives and displays the satellite attitude data (fig. 67). Using these data, two options are available for satellite attitude control: (1) the crew can command attitude control by reading the displays and firing the thrusters, and (2) the payload control supervisor (PCS) orbiter computer system can receive the signals and command the thruster firings. This is a psuedo-closed-loop approach relieving heavy man-in-the-loop activity. Both of these options are based on satellite attitude rates. It has been demonstrated that 20 m of skiprope is manageable using either of these approaches. Because of the labor intensity of the man-in-the-loop option, the PCS approach was chosen as the prime. The man-in-the-loop was chosen as the backup.

Numerous off-line cases have been run to verify the approach. Table 4 shows the results of two of these cases, while figures 68 through 73 show the responses plotted versus length.

The PCS satellite control had been baselined to be active from 1,200 m to 180 m. In the off-line simulations cases run, satellite angular deviations were small and docking occured. Results from preflight shuttle mission simulator (SMS) simulations with high-fidelity PCS software simulations did not support the performance of the PCS, so that its usage as prime for TSS-1 was very questionable. Manually controlling satellite attitude in the SMS was still acceptable.

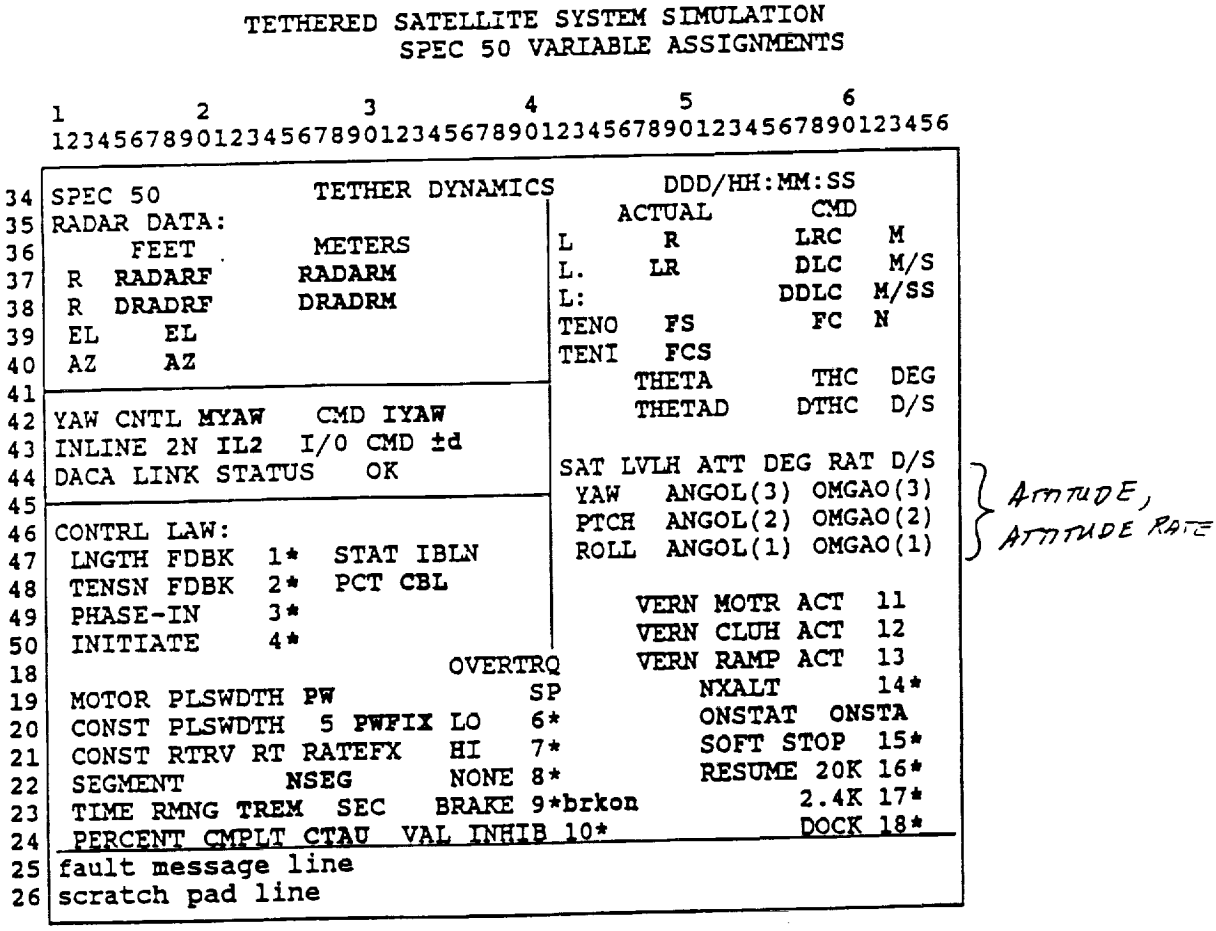

Figure 67. Multifunction CRT display system for tether dynamics.

Table 4. Satellite attitude control simulation.

Case	Skiprope at Station 2 (m)	Maximum Satellite Pitch	Maximum Satellite Roll	Maximum Satellite Pitch Rate	Maximum Satellite Roll Rate	Docking Angles* at 20 m
1	20 by 20	25°	23°	1.8°/s	2.5°/s	$\alpha = 8.0°$ $\beta = 9.0°$
2	30 by 30	60°	59°	3.0°/s	7.0°/s	$\alpha = 12.0°$ $\beta = 16.7°$

- Docking angle limits
  - Alpha < 10°
  - Beta < 10°

*See page 85 for alpha (α) and beta (β) definitions.

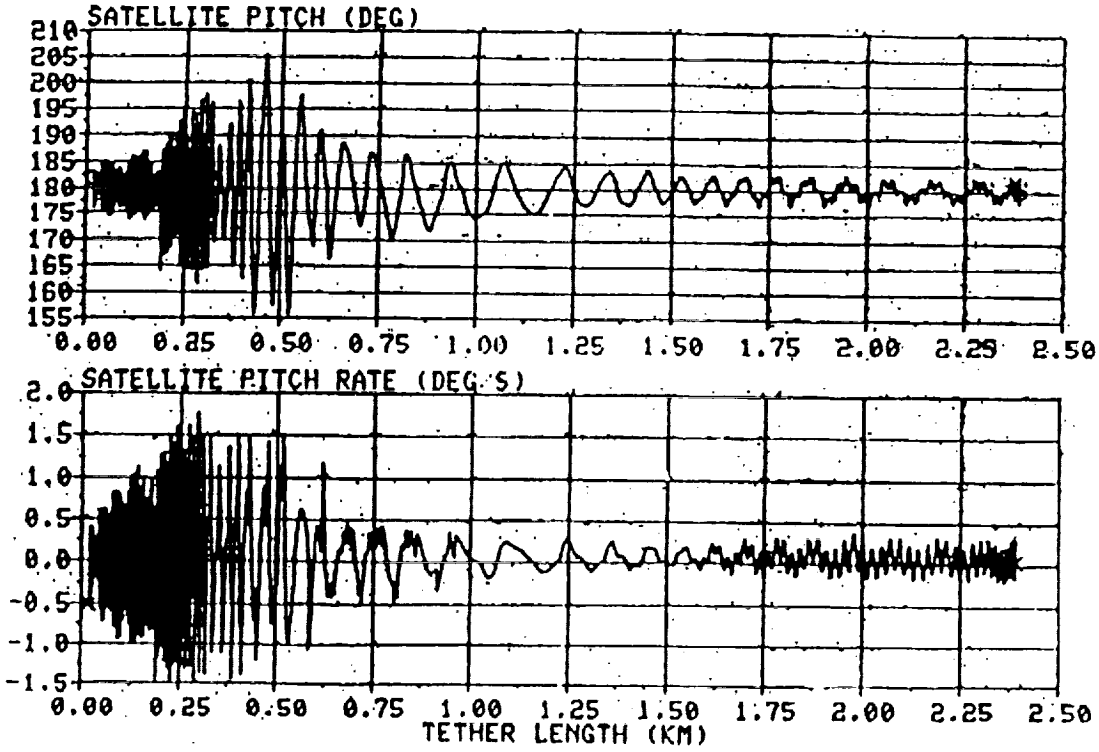

Figure 68. Satellite attitude control simulation (pitch and pitch rate).

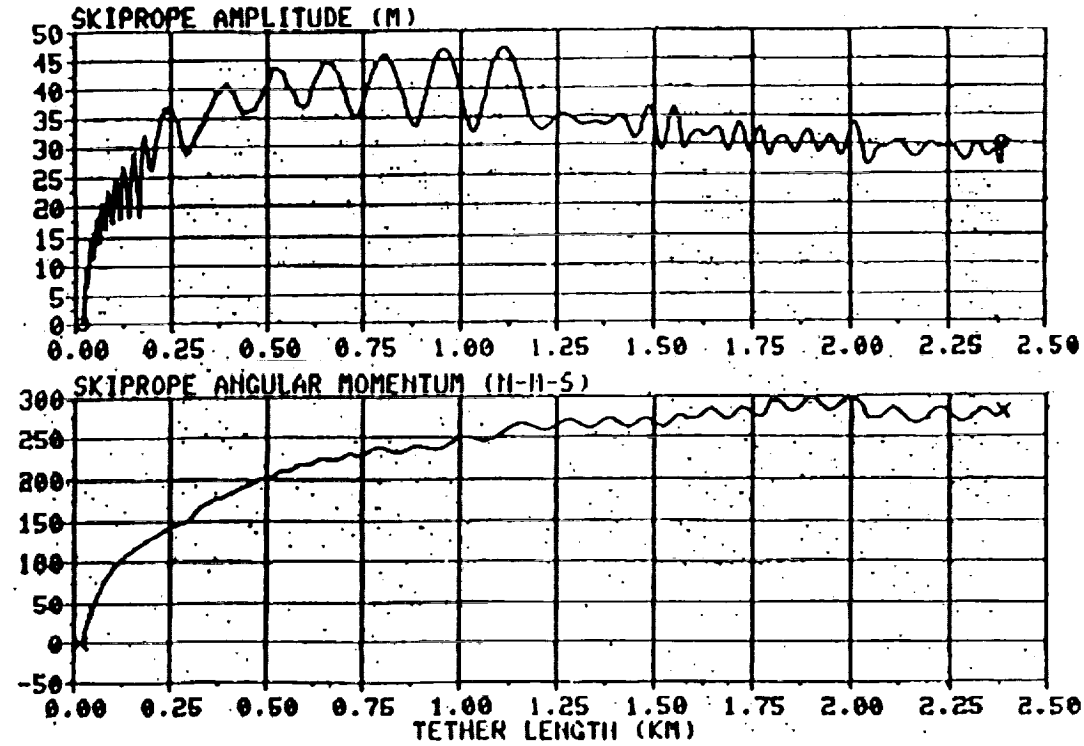

Figure 69. Satellite attitude control simulation (skiprope amplitude and angular momentum).

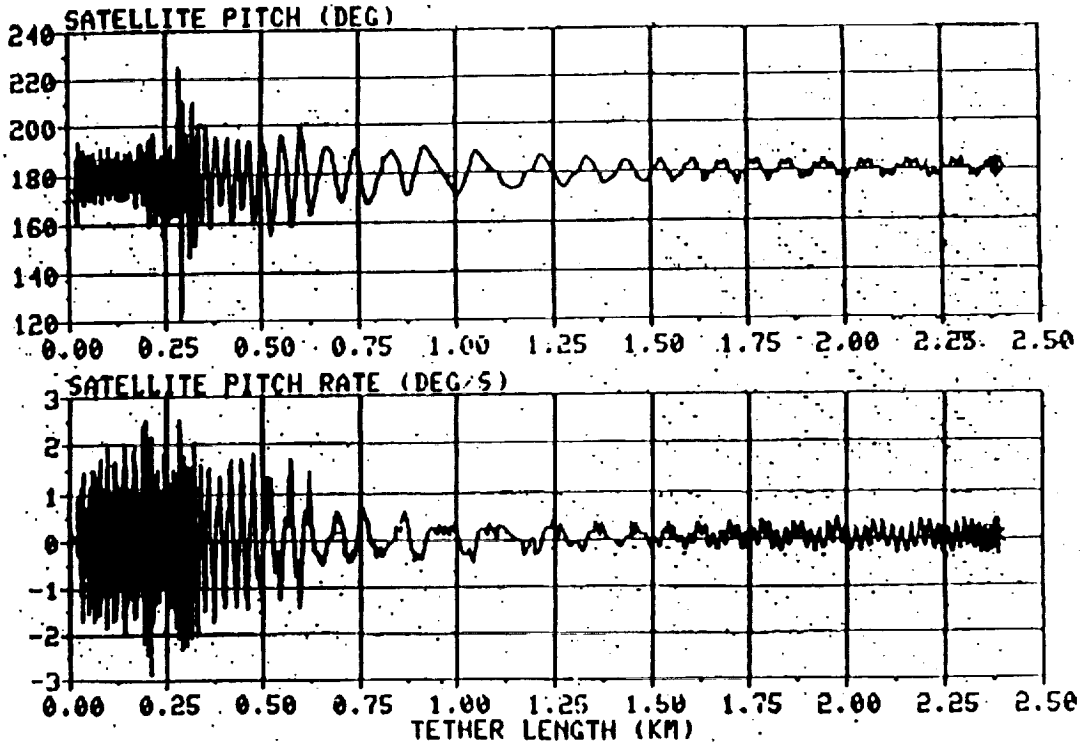

Figure 70. Satellite attitude control simulation (pitch and pitch rate).

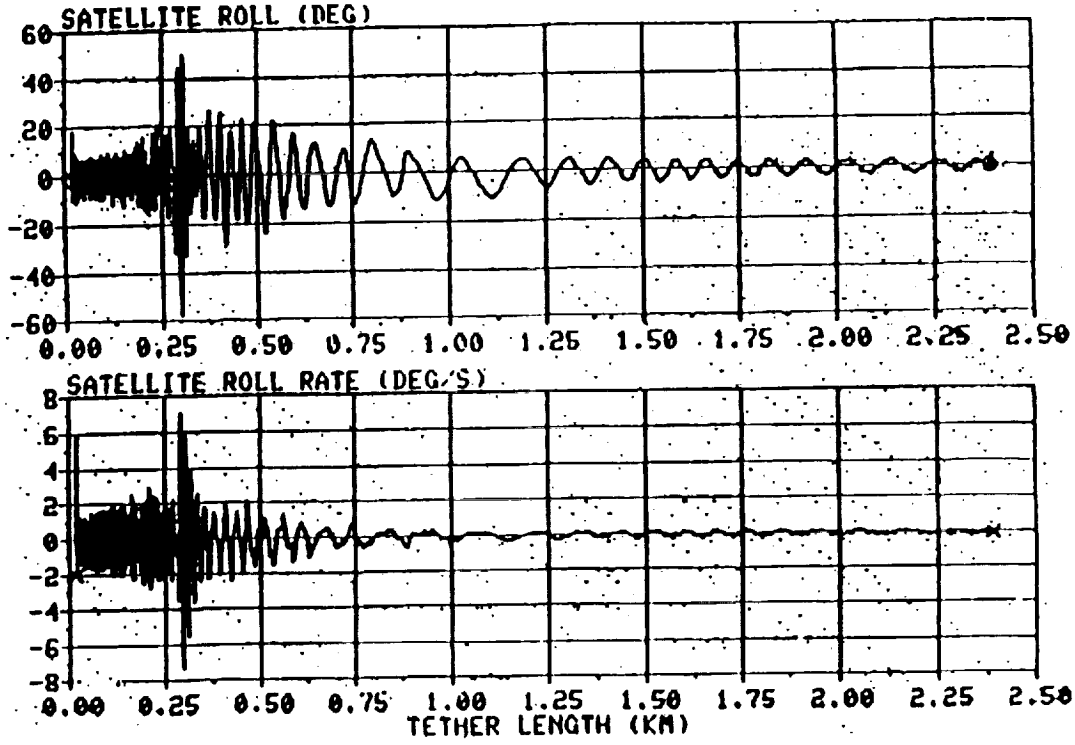

Figure 71. Satellite attitude control simulation (roll and roll rate).

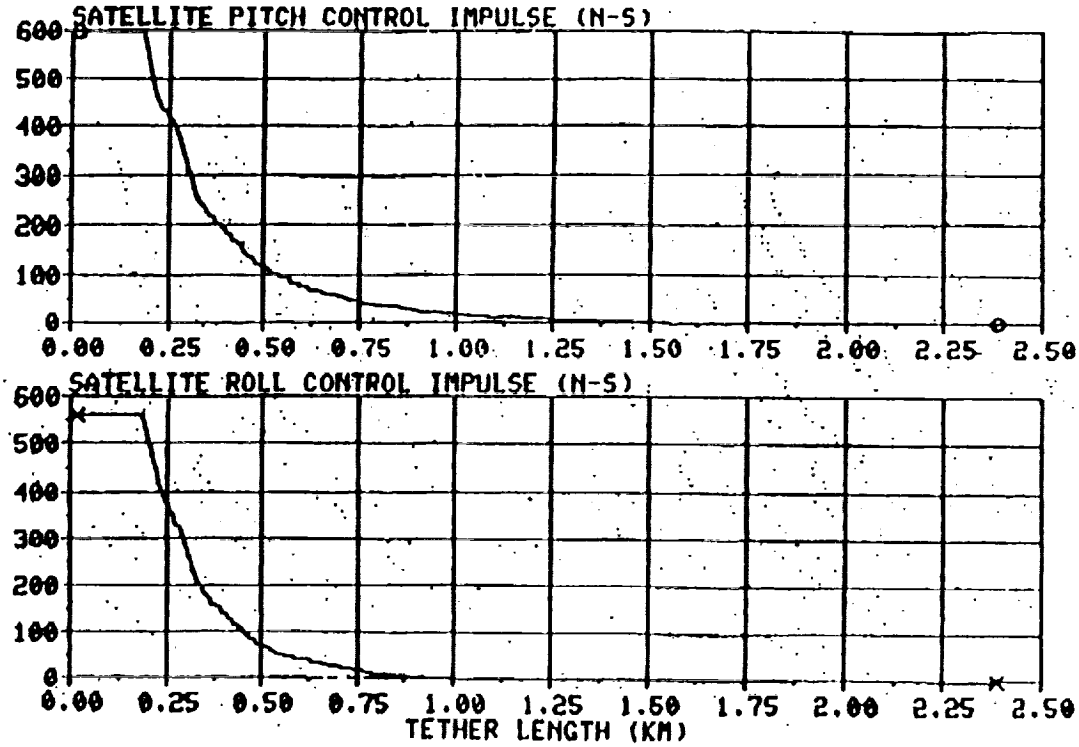

Figure 72. Satellite attitude control simulation (pitch and roll control impulse).

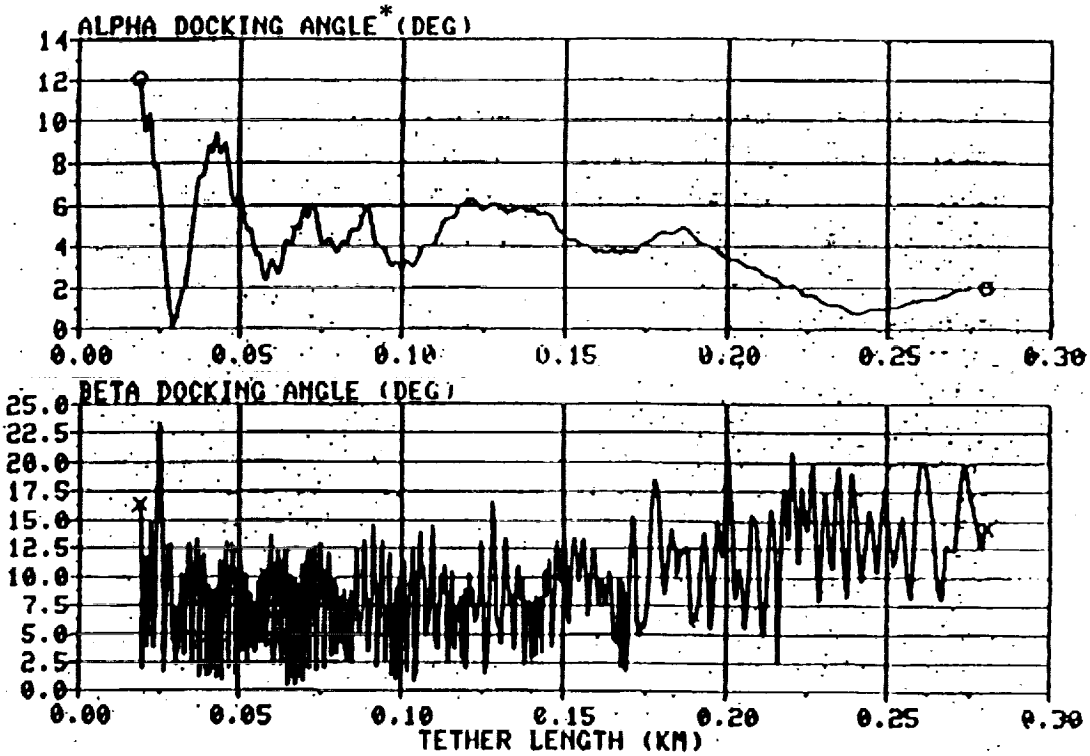

* See bottom of page 85 for alpha and beta definitions.

Figure 73. Satellite attitude control simulation (docking angles).

E. Docking Ring Damper

As was stated previously, not only must the satellite attitude be actively controlled but, because angular momentum is conserved, and, hence, the relative skiprope amplitude increases as the tether is retracted, a passive skiprope damper must be utilized. Passively damping the tether is not simple in that too much damping force introduced will only create a new end point (fixed point or node point) and become ineffective. Designing and verifying a tether damper for short tether lengths was, therefore, a major challenge.

Figures 74 through 76 are schematics of the damper used in the docking ring to provide damping. The system consists of a triangular yoke and ferrule connected to three individual negator motors attached to the docking ring. The negator motors are a constant spring (load) system that rolls in and out as the tether moves the yoke. Figure 77 shows the basic characteristics of the negator motor. Because these motors have to be a damper system and must perform in a vacuum at low temperatures, it was necessary to fully understand and model their characteristics so that an analytical prediction could be made of their effectiveness in damping skiprope as the satellite was retrieved. As a result, extensive engineering tests were conducted to prove the concept and establish data characteristics. The test results were correlated with simulations of the tests, and models reflecting the correlation were developed for use in time-domain mission skiprope simulations. In addition, the hardware went through the standard qualification/acceptance tests in thermal vacuum conditions.

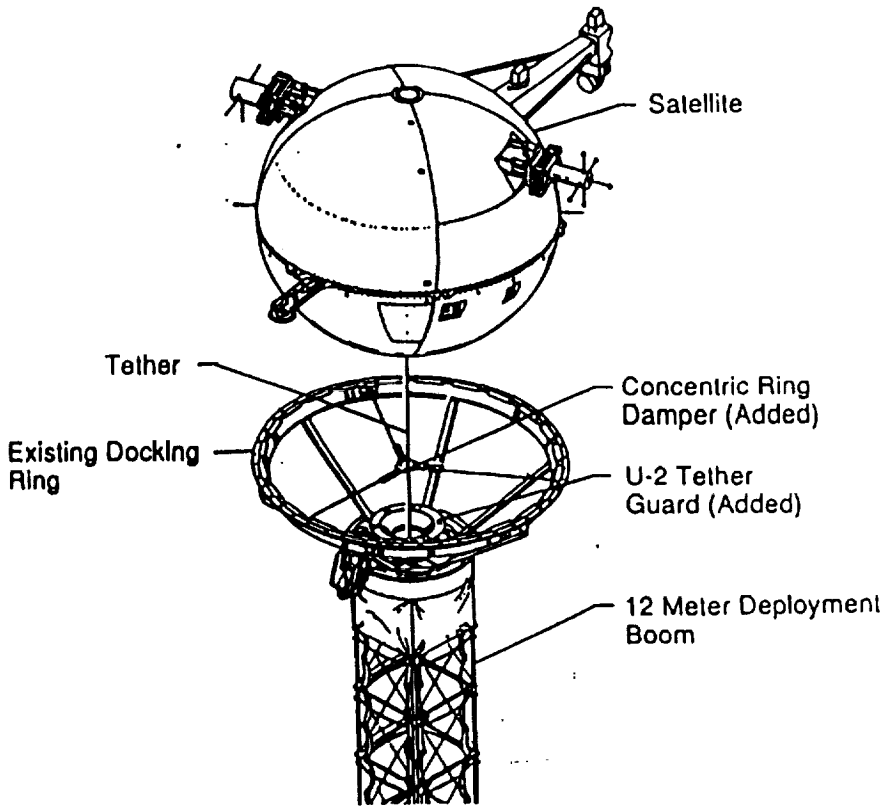

Figure 74. Skiprope docking ring damper.

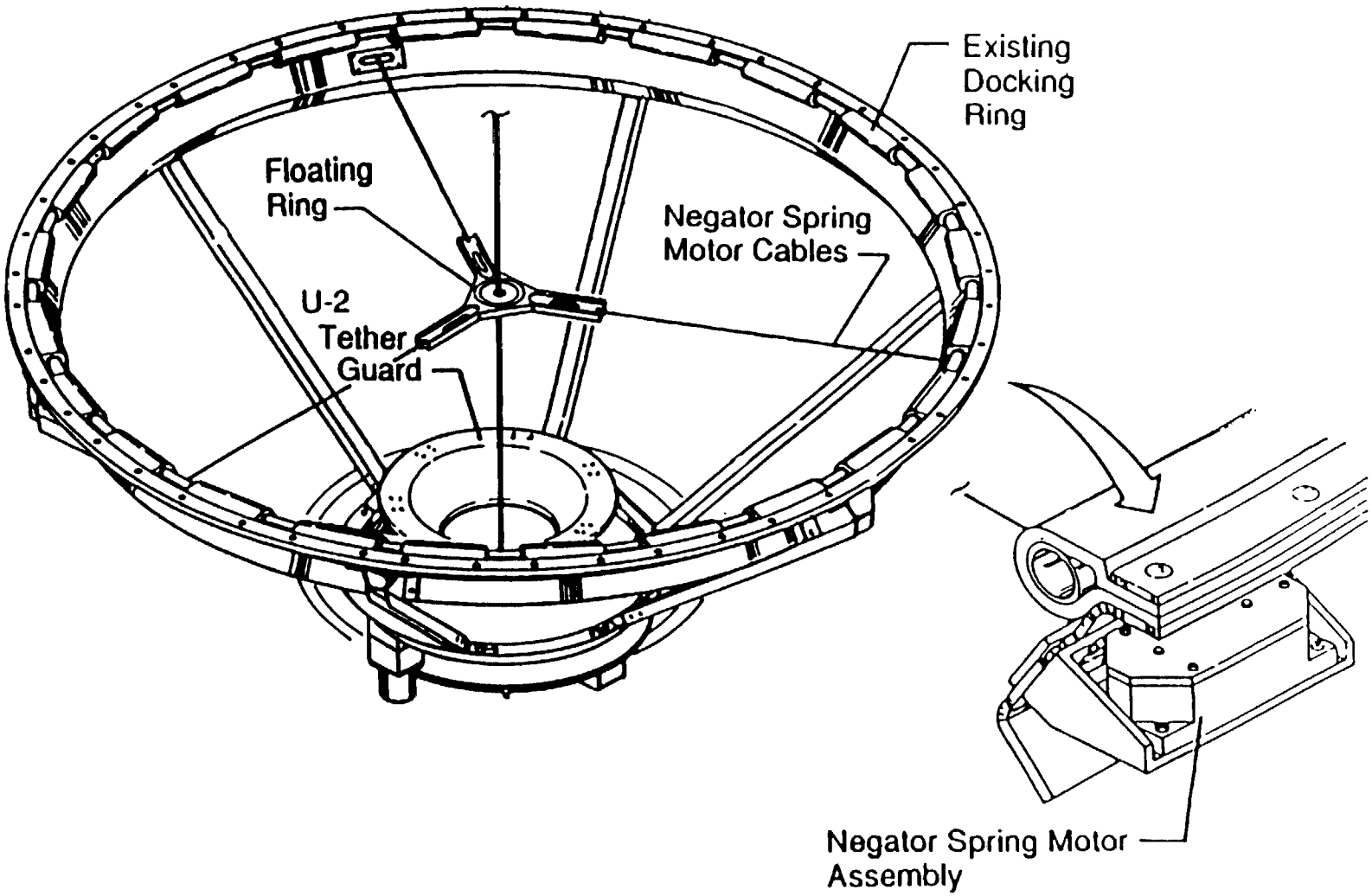

Figure 75. Skiprope docking ring damper.

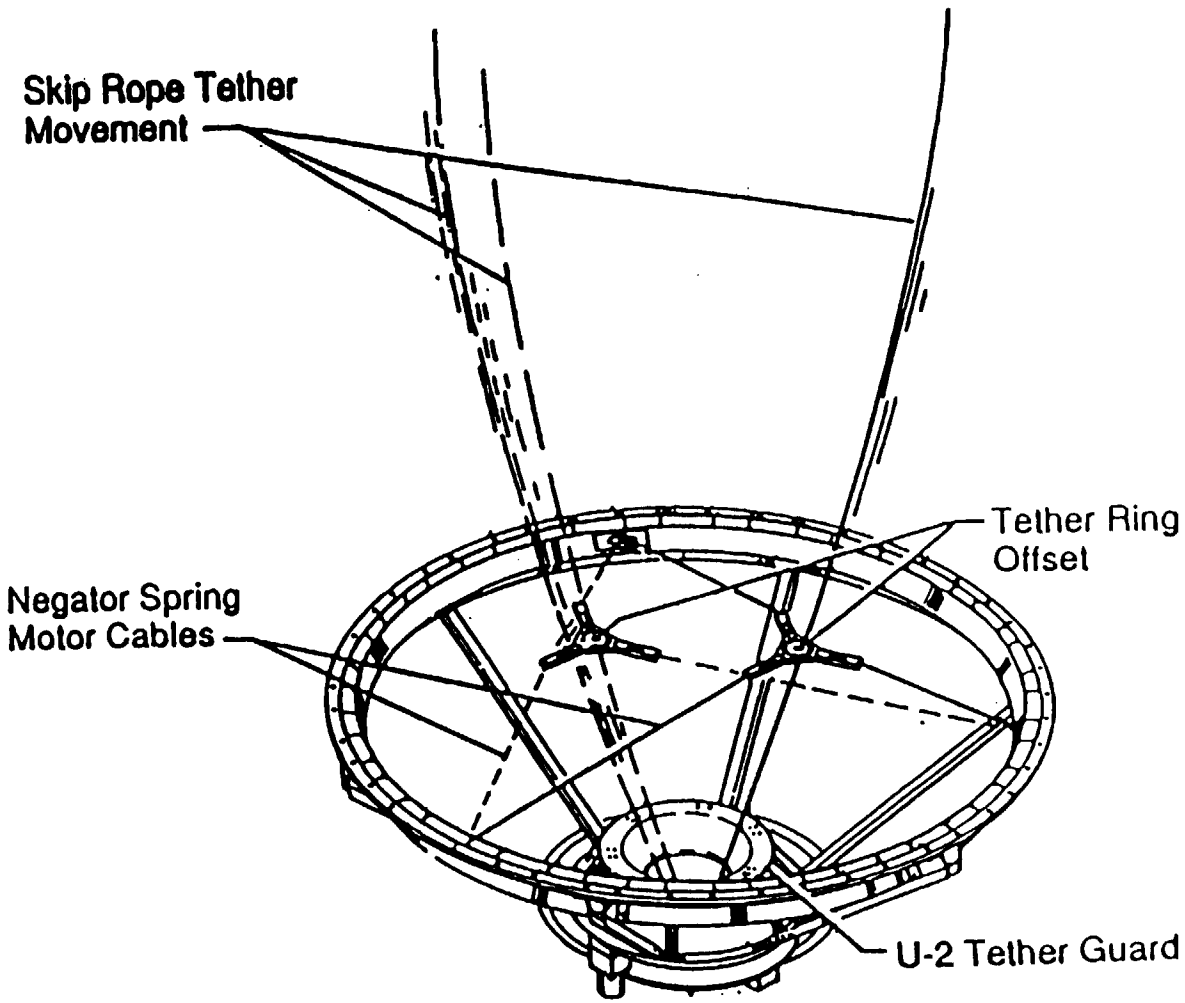

Figure 76. Skiprope docking ring damper.

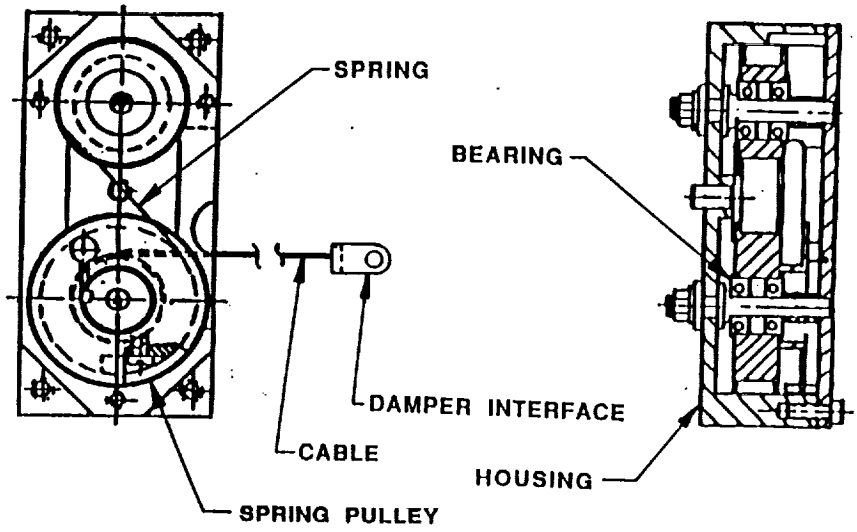

Figure 77. Negator spring motor assembly.

One set of tests was to determine the damping characteristics of the docking ring damper. This was conducted using the three negator motors and the yoke with a tether attached to the bugle and a bob mass with a light on the free end. Using a camera at a distance of 64 ft, the motion of the bob was tracked from an excited circular motion in free decay (fig. 78).

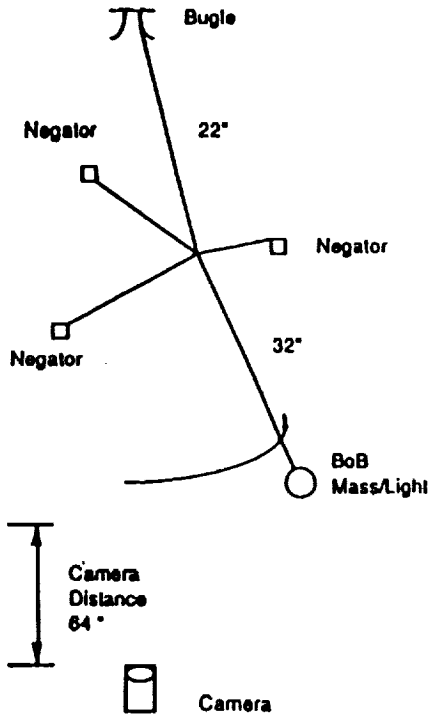

Figure 78. Circular pendulum test setup.

An analytical model was formulated of this test setup, including the force of gravity, the initial impulse, and the negator motors. The analytical model of this damping system includes terms of equivalent viscous damping for viscous, hysteresis, and coulomb friction damping. Typical values used in the simulations and a more detailed description of the tests performed to quantize these equivalent coefficients are found in reference 7.

Figures 79 and 80 are typical plots of test results compared to the analytical models. Very good results have been achieved in developing a model to match the test data.

Because the negator motors are temperature and vacuum sensitive, tests had to be run to simulate various conditions. Tests were run for temperatures of +100 °C, 25 °C, and −120 °C. The expected on-orbit operational temperatures should be near, but not exceed, the -120 °C case.

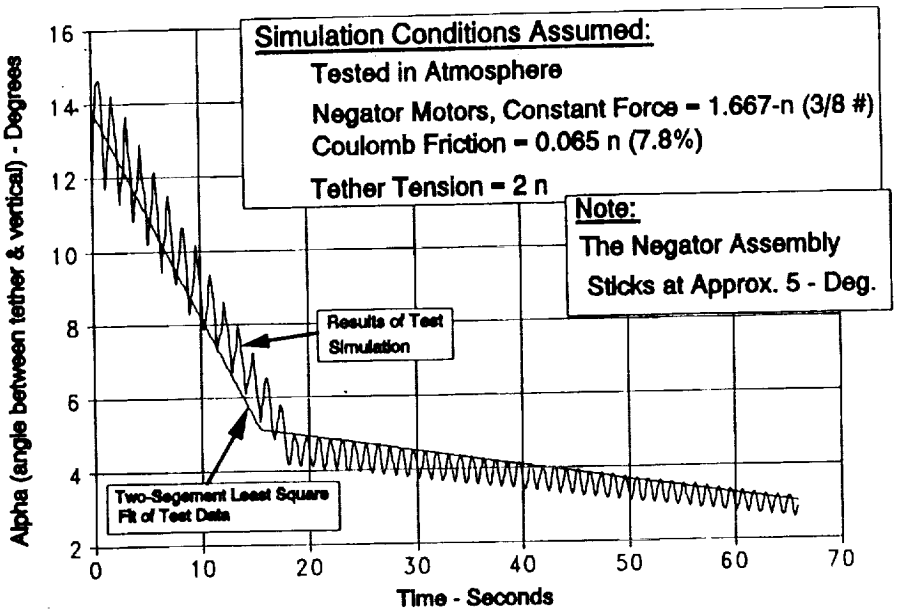

Figure 79. TSS skiprope damper, comparison of test data with simulation response.

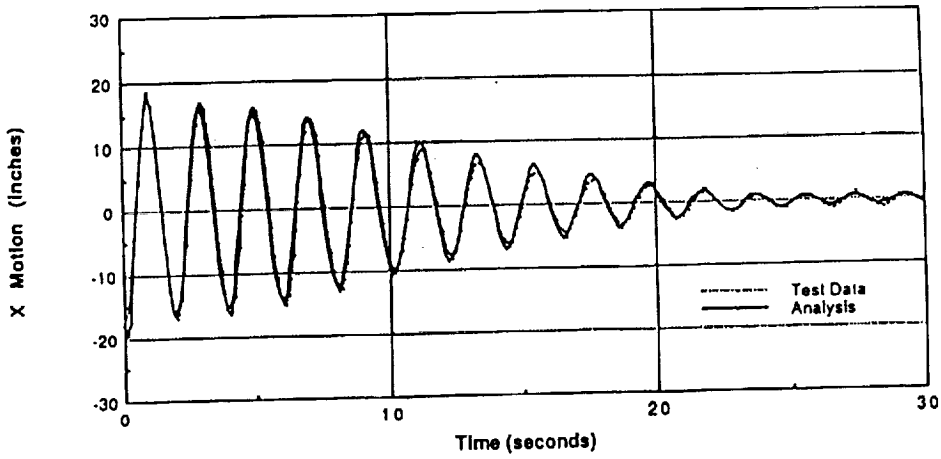

Figure 80. Skiprope damper circular pendulum test data (comparison with analysis).

Taking the test-derived (correlated) analytical model and incorporating it in the time domain, a skiprope dynamic simulation was run starting at a tether length of 100-m and 20-m skiprope, then retrieving it to 10 m. Figure 81 shows the results for the three different temperatures simulated. In all cases, the skiprope was damped to less than 1-m amplitude. The −125 °C case damped much quicker than the +100 °C and 25 °C cases. Later, this damping model was used in end-to-end simulations of the TSS-1 mission to show ability for satellite recovery.

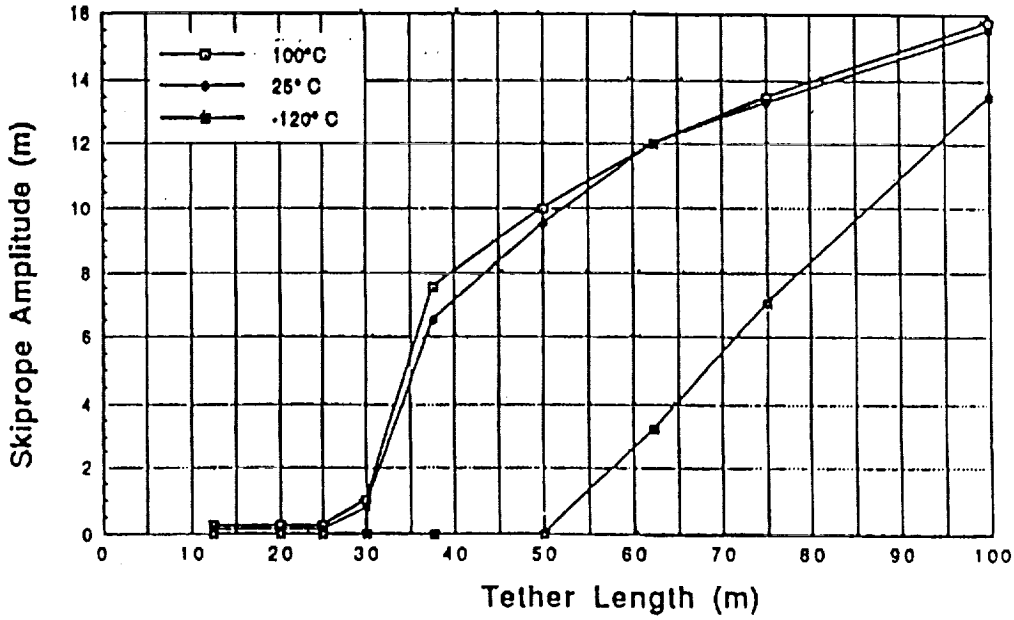

Figure 81. Skiprope damper performance as affected by temperature.

1. Qualification/Acceptance (Negator Motors). The negator motor and yoke had to go through a complete and formal acceptance verification. Figure 82 shows the flow of this formal approach. As shown on the flow diagram, these elements show how the various tests conducted were flowed together to augment final qualification and verification of the performance (damping) under various temperatures and vacuum conditions, including damping determination, before and after random vibration testing. Figures 83 and 84 show the docking ring with negator motor and the test setup, respectively. Two different force motors are shown in figure 84, along with the rotational potentiometer instrumentation.

An alternate damper was designed and tested, but was not selected for incorporation into the hardware (fig. 85, ref. 3).

Table 5 lists the characteristics achieved by each of the negator motors for the various temperatures. All the motors met the qualification acceptance requirements.

F. Other Control Modes

Three other control modes are available to augment the skiprope control plan just presented: (1) programmed current flow, (2) slow retrieval from approximately 1,000 m, and (3) satellite spin. Although not baselined for TSS-1, these approaches were available to help contain skiprope. On future missions, they could be part of the baselined approach.

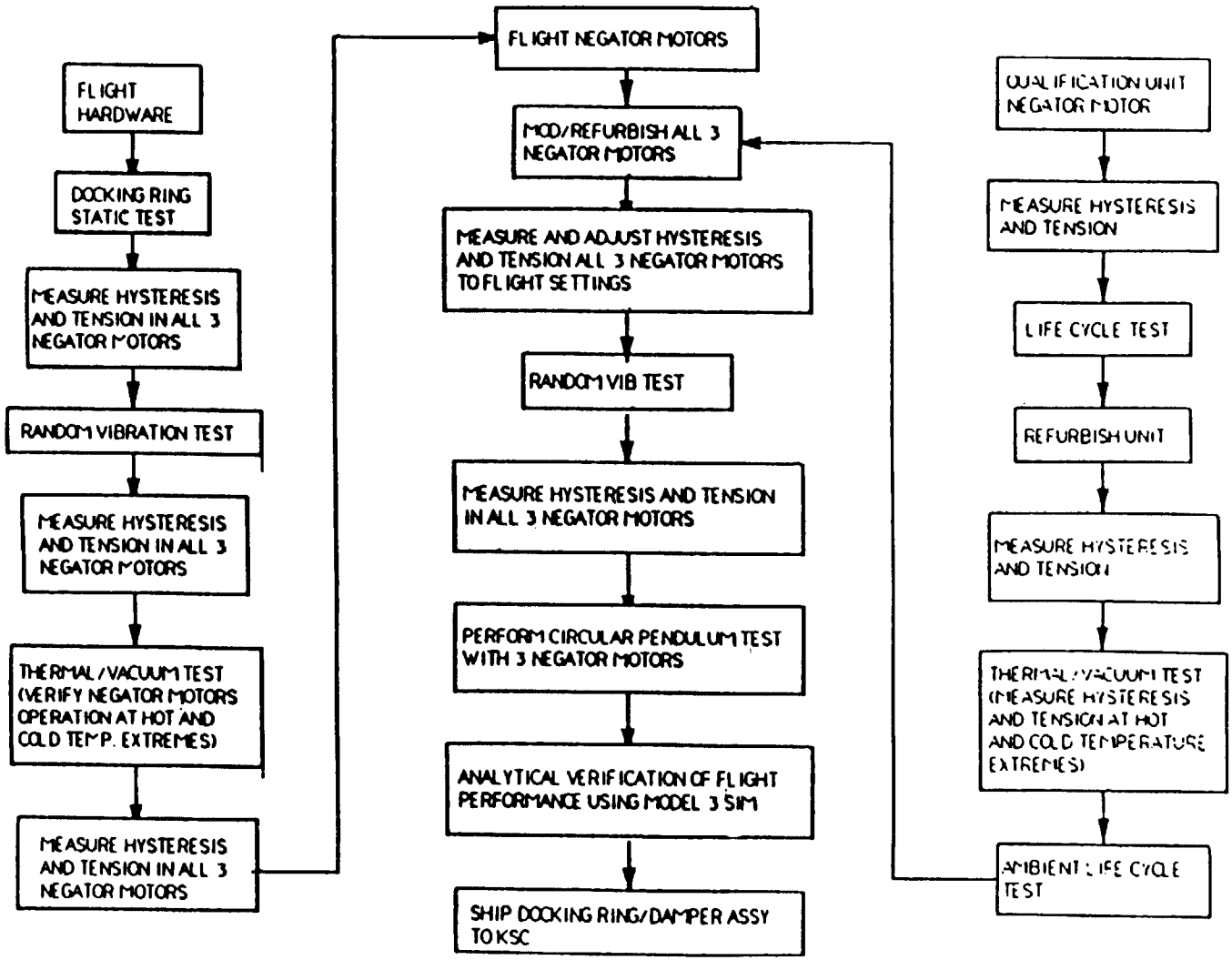

Figure 82. Skiprope damper qualification/acceptance plan.

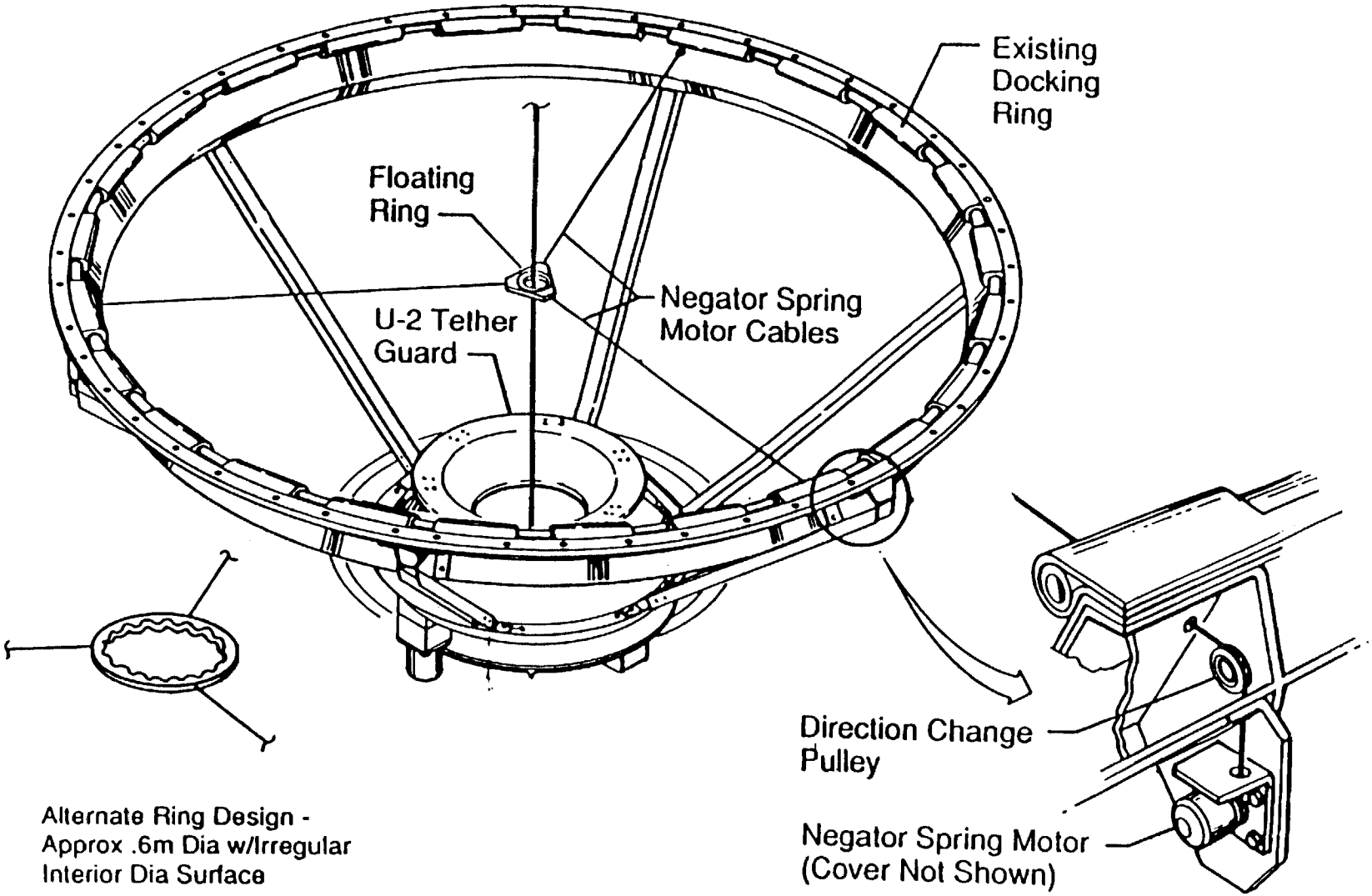

Figure 83. Suspended tether ring damper.

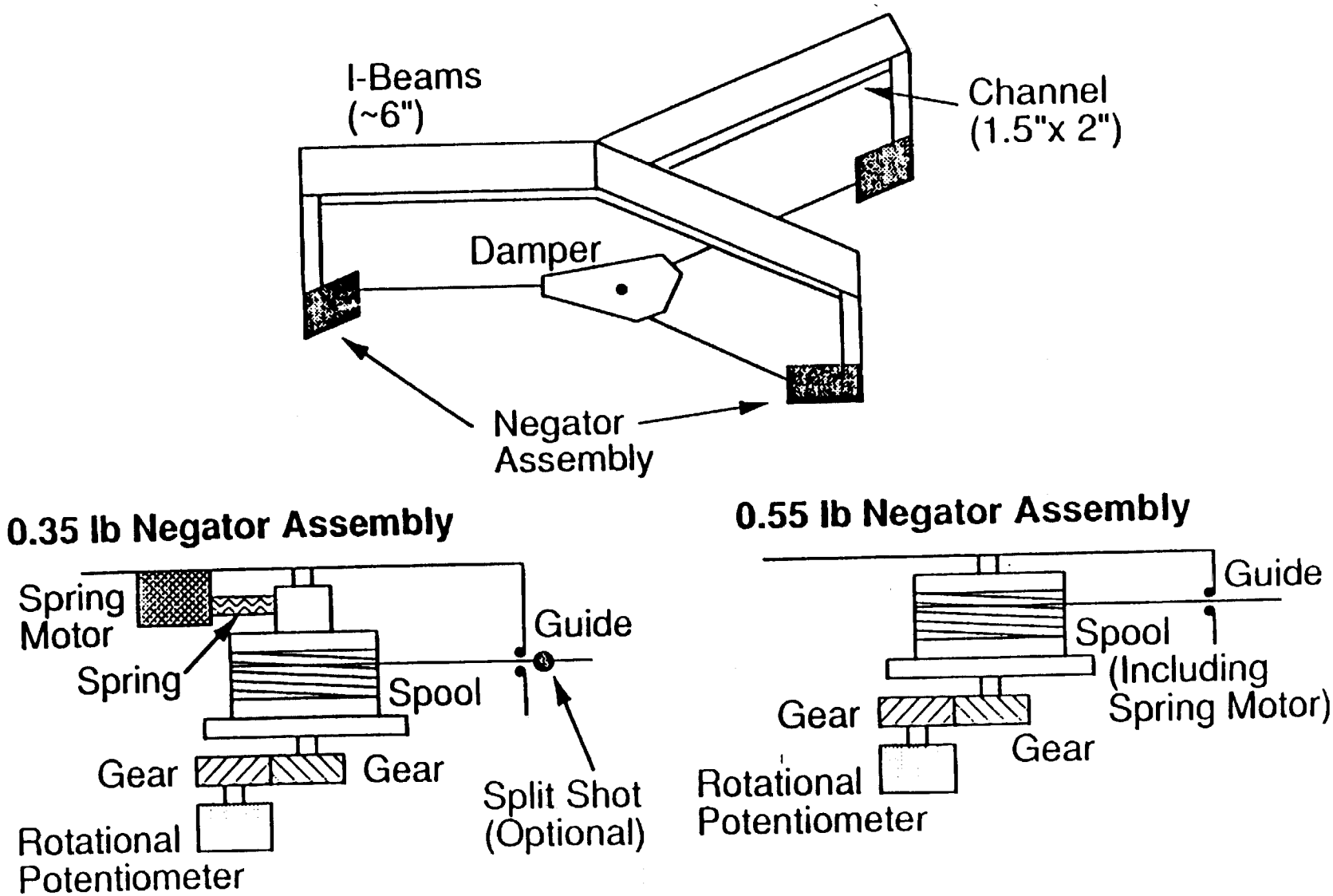

Figure 84. Concentric damper test setup.

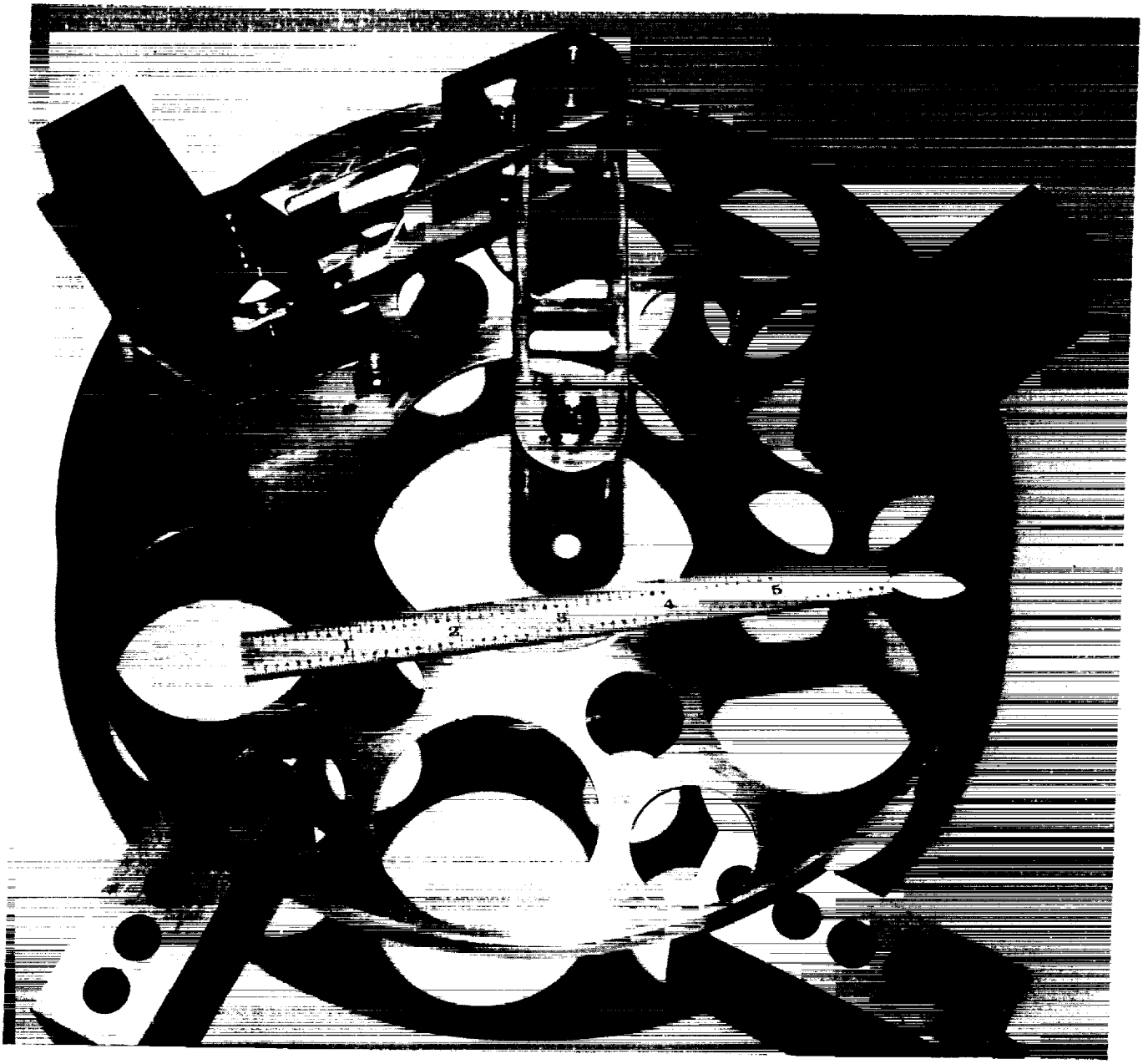

Figure 85. Redmon skiprope damper design.

Table 5. Skiprope damper characteristics.

Flight Negator	−120 °C		25 °C		100 °C	
	Force (lb)	Hysteresis (percent)	Force (lb)	Hysteresis (percent)	Force (lb)	Hysteresis (percent)
A	0.572	12.04	0.458	6.85	0.501	4.61
B	0.594	12.50	0.475	6.68	0.587	4.61
C	0.559	11.46	0.458	6.85	0.583	7.07
Average	0.575	12.00	0.464	6.79	0.542	5.47

1. Programmed Current Flow. Current flow has been shown to excite skiprope or dampen it depending upon its phasing relative to Earth's magnetic field and the skiprope motion. It is particularly effective on station 1 if the skiprope amplitude becomes excessive. To utilize this approach, the time-domain skiprope observer calculates the required parameters. They are:

- Time to start current flow (skiprope phase)
- Duration of current flow (skiprope period).

To demonstrate the effectiveness of this approach, a 35- by 8-m elliptical skiprope case with approximately 4 m of third-string mode amplitude was chosen. The simulation went from 19 hours to 20.5 h. The phased current flow was performed from 19.65 to 20.15 h. Figure 86 shows the current flow profile used from 19 to 20.5 h. Only the current flowing from 19.65 to 20.15 h was phased to dampen skiprope, the rest is normal science. Figure 87 shows the reduction in skiprope amplitude, while figure 88 shows the reduction in skiprope angular momentum. The amplitude was reduced from 35 m to less than 15 m, while the angular momentum approached zero.

2. Slow Retrieval. The mission period of satellite retrieval from approximately 1 km to 20 m is critical to satellite retrieval because this is the region where the satellite's pendulous motion and skiprope resonances coalesce, and the relative skiprope amplitude increases due to angular momentum conservation. The slow retrieval allows more time for satellite attitude control to dampen out satellite motion and skiprope, and for the concentric damper to dampen skiprope. The down side of this approach is longer mission time, which pushes the battery life limit and could interfere with other mission objectives.

To simulate this effect, a case of 50 m of circular skiprope at station 2 (2,400 m) was chosen as the starting point. The satellite was retrieved to a tether length of 20 m. Figure 89 shows the tether length versus time and the tether retrieval rate versus time. Figure 90 plots the skiprope amplitude and angular momentum versus tether length. As is shown on the plots, the slow retrieval was very effective in damping even this large initial skiprope amplitude and angular momentum. Figure 91 shows the satellite pitch attitude and pitch rate versus length, while figure 92 shows roll attitude and rate. Figure 93 shows the control impulse used, while figure 94 shows the α and β satellite docking angles. Here, α is defined to be the angle between the line from the centerline of the

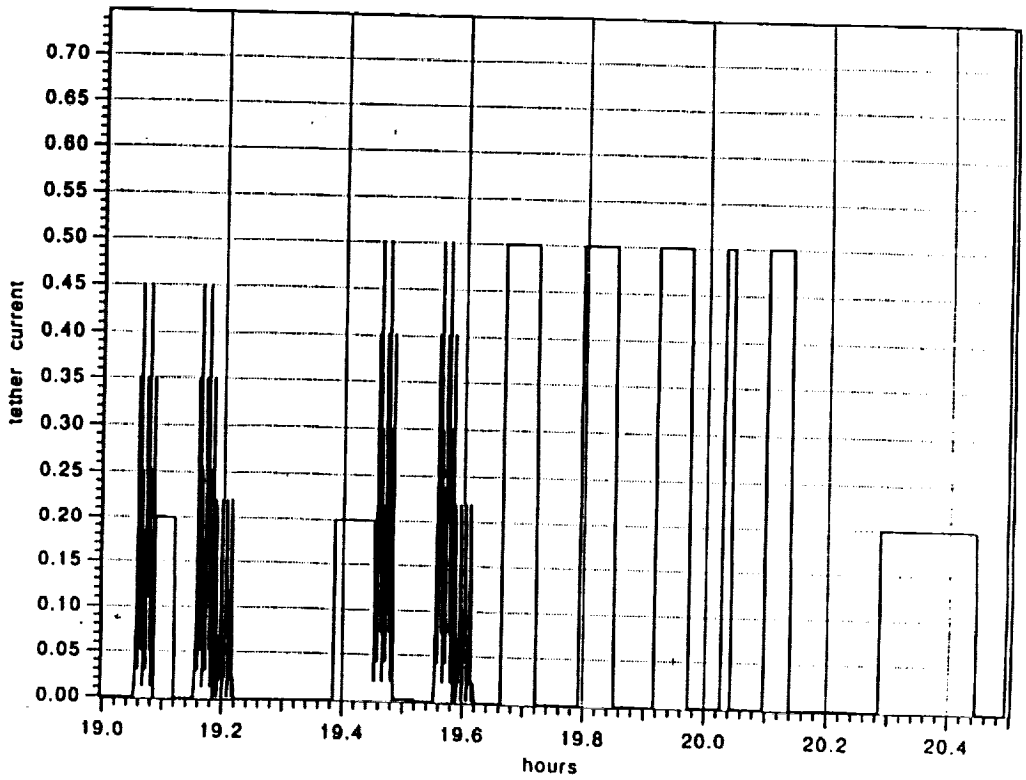

Figure 86. Phased current flow simulation.

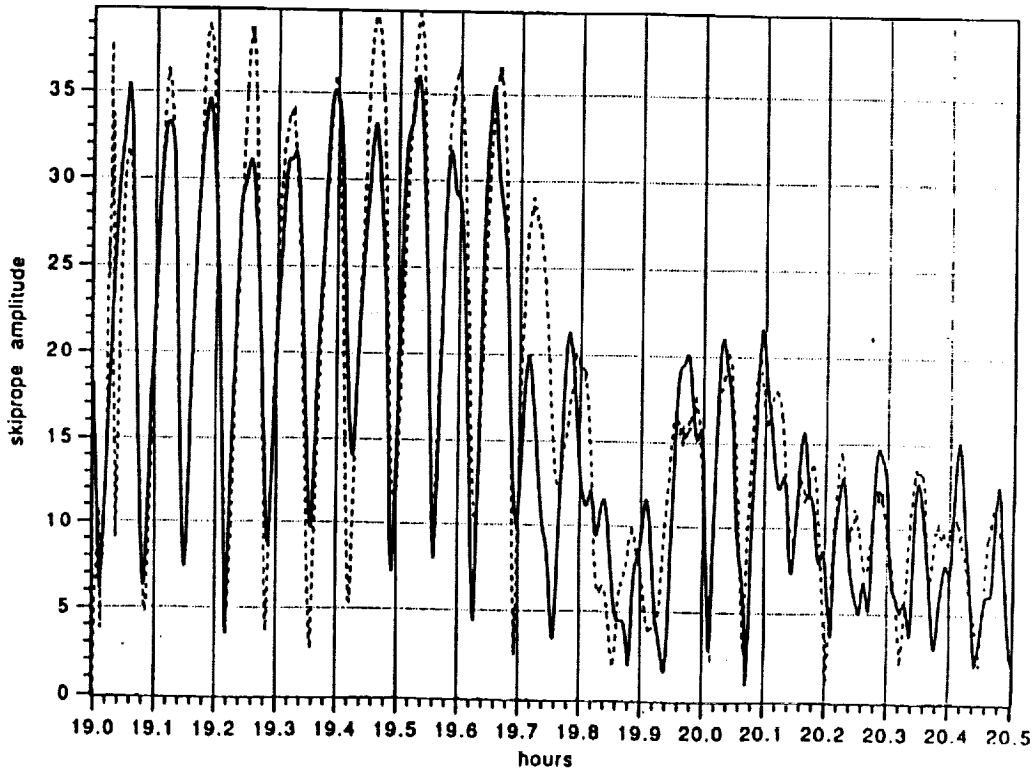

Figure 87. Phased current flow simulation (skiprope amplitude).

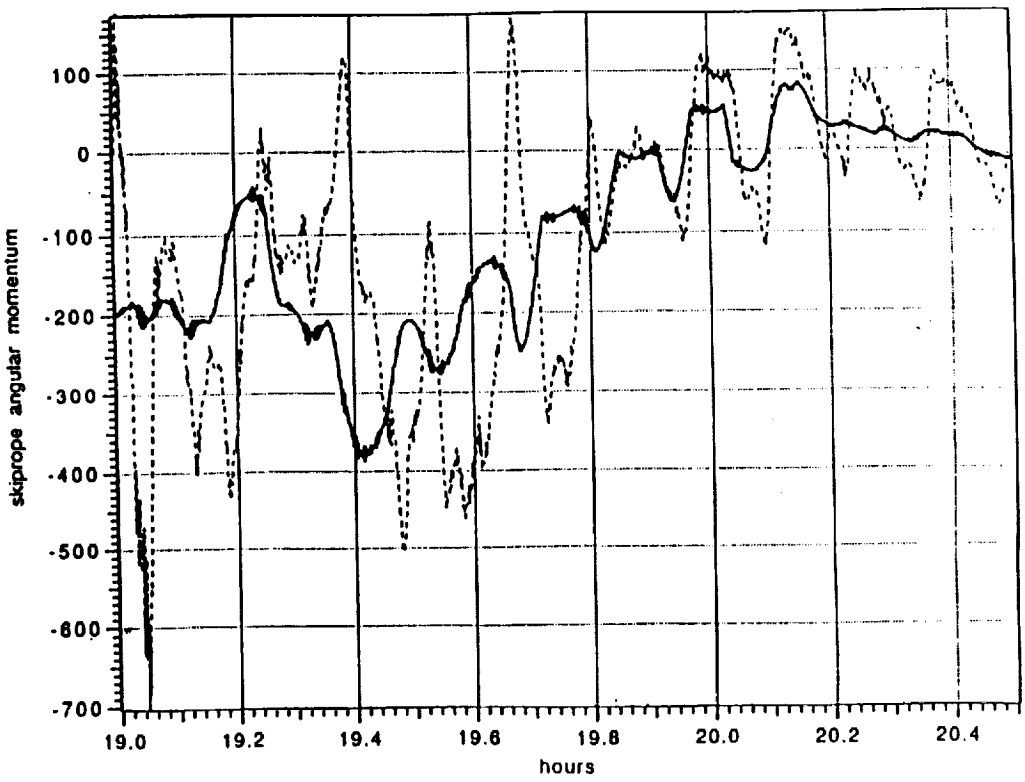

Figure 88. Phased current flow simulation (angular momentum).

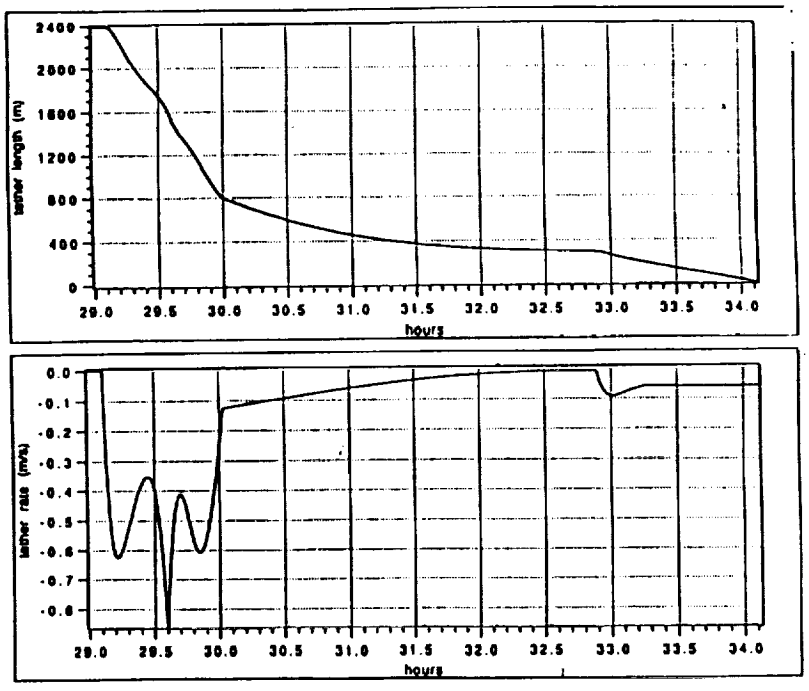

Figure 89. Slow retrieve simulation (tether length and rate).

C-2

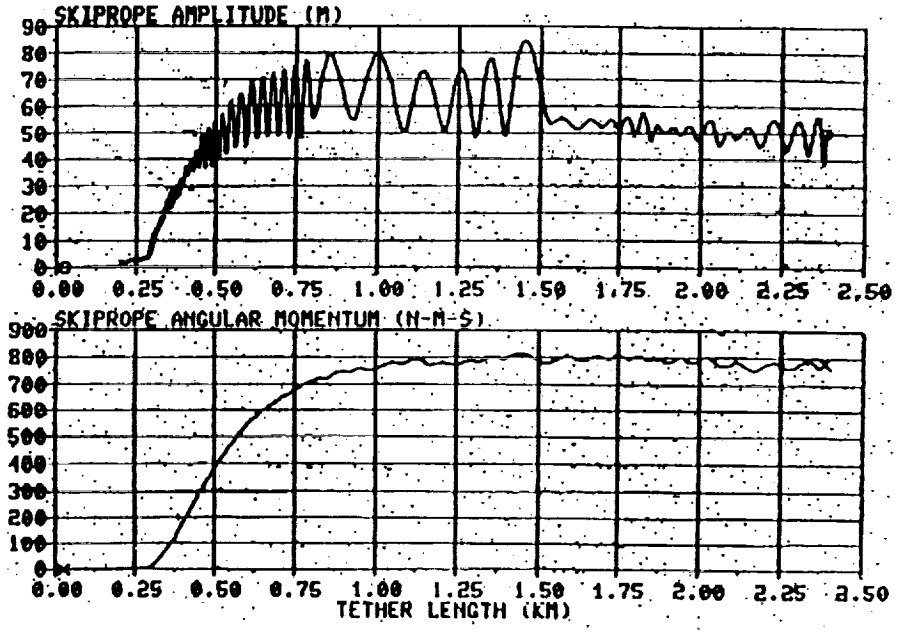

Figure 90. Slow retrieve simulation (amplitude and angular momentum).

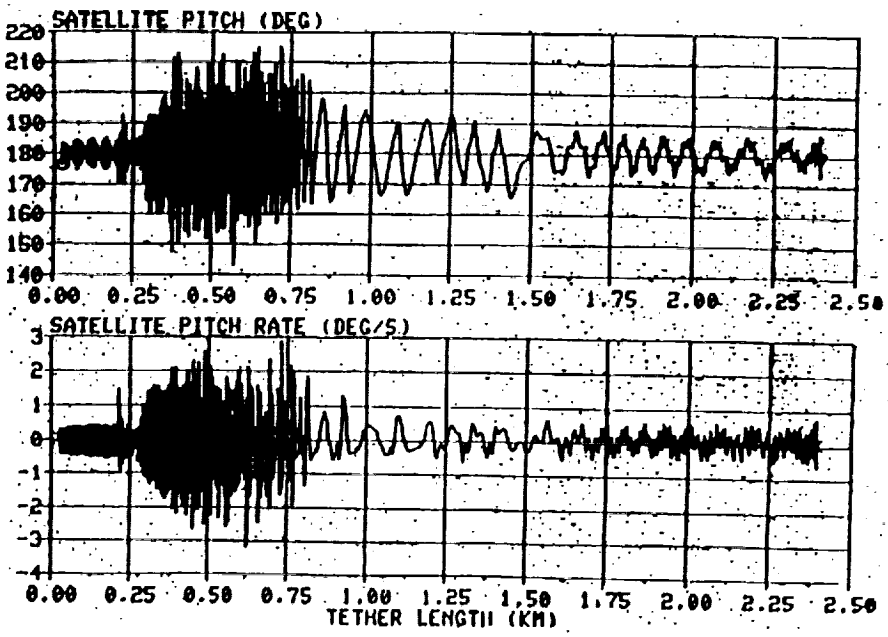

Figure 91. Slow retrieve simulation (satellite pitch attitude and rate).

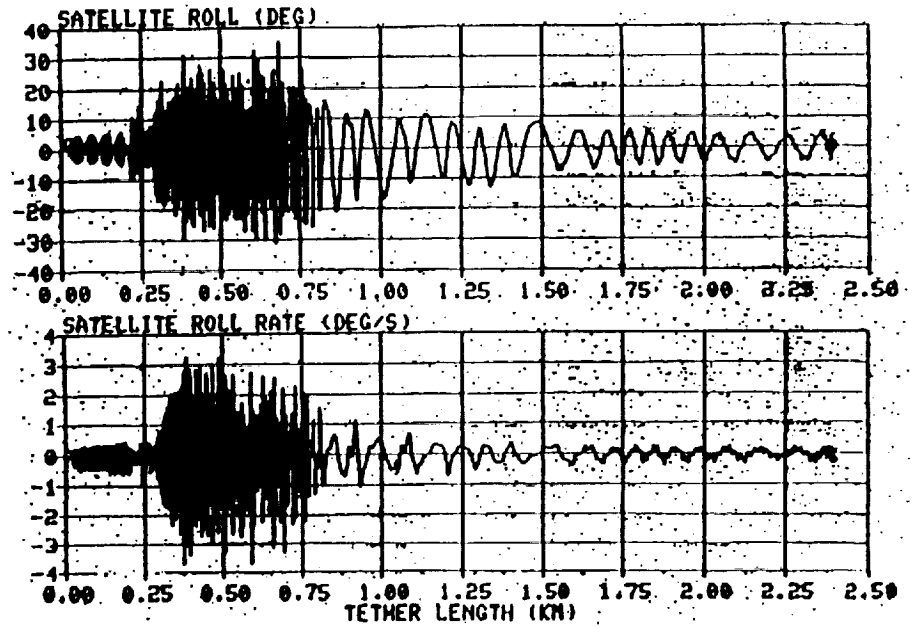

Figure 92. Slow retrieve simulation (satellite roll attitude and rate).

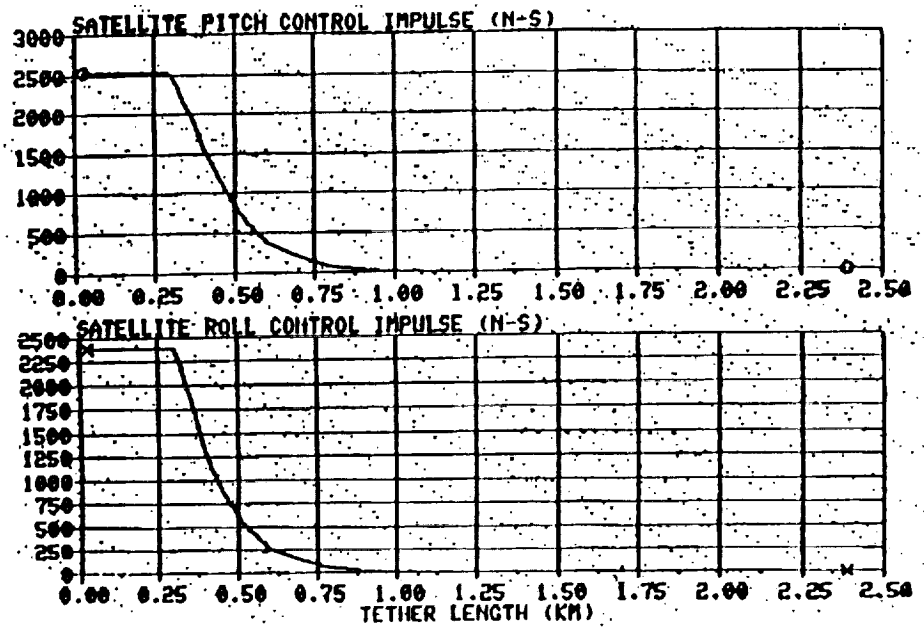

Figure 93. Slow retrieve simulation (satellite pitch and roll control impulse).

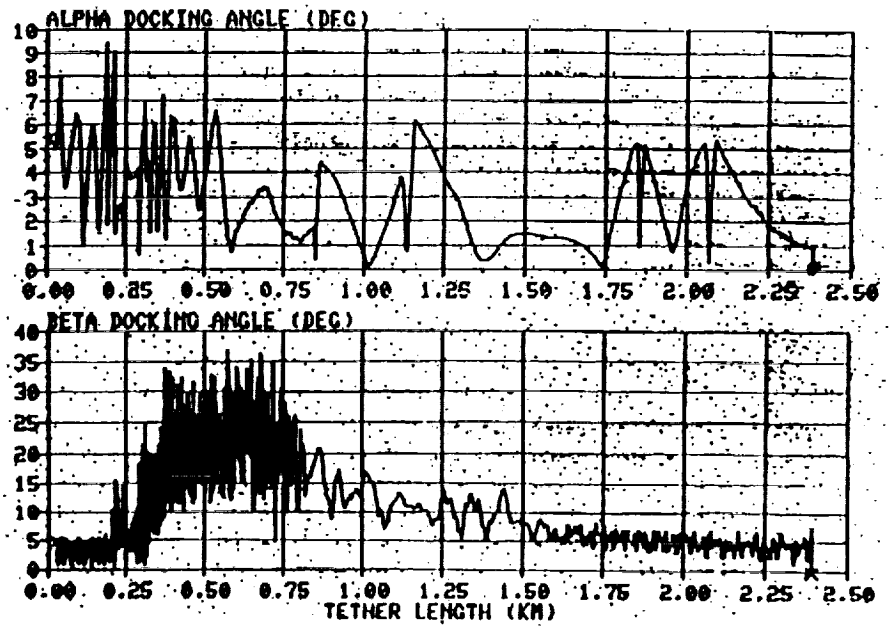

Figure 94. Slow retrieve simulation (satellite docking angles).

boom and the line formed by connecting the bugle head top point to the center of gravity (CG) of the satellite. Likewise, β is the angle between the line from the CG of the satellite to the attach point and the line formed by connecting the bugle head top to the CG of the satellite.

3. Spinning Satellite. Spinning the satellite during this last portion of the retrieval cycle transfers the tether/satellite attitude coalescence to a different length to stabilize the satellite and reduce the attitude control requirement. To demonstrate the effectiveness of this approach, a 20-m circular skiprope simulation (retrieval) was started at 2,400 m. The satellite was retrieved to a length of 20 m at the nominal rate. PCS (satellite attitude control) and the concentric ring damper were active in the later portions (750 m to 180 m). The satellite was spun at 4.2°/s at 950 m and allowed to passively spin for the rest of the simulation. Figure 95 shows the pitch and roll control impulse versus tether length, while figure 96 shows the skiprope amplitude and angular momentum, and figure 97 shows the α and β docking angles. This approach is effective in reducing energy of the system and meeting all docking requirements. The results of this study show that:

- Spinning satellite reduces energy transfer to satellite from skiprope
- Reduces PCS (attitude control) activity required to control satellite attitude
- Reduces satellite attitude excursions during coalescence
- Increases the residual skiprope following coalescent which must be removed by the concentric ring damper
- The concentric ring damper effectively removed this additional skiprope.

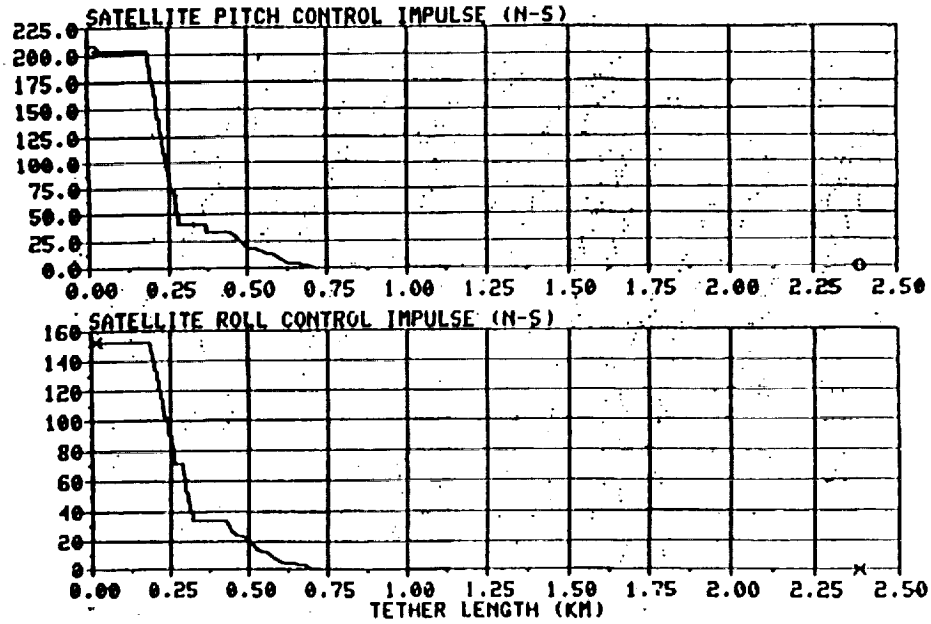

Figure 95. Satellite spinning simulation (satellite pitch and roll control impulse).

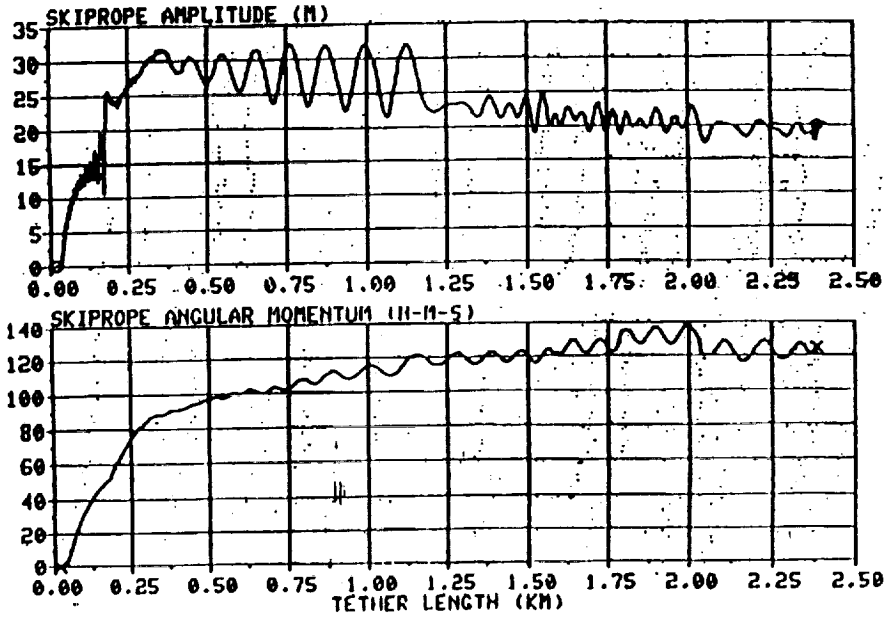

Figure 96. Satellite spinning simulation (skiprope amplitude and angular momentum).

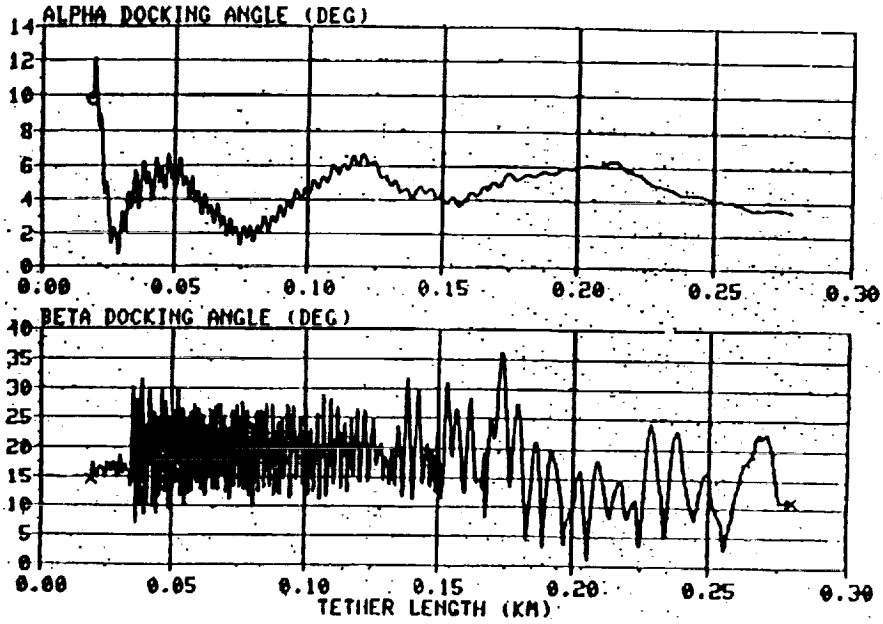

Figure 97. Satellite spinning simulation (docking angles).

G. Operational Procedures

Control of skiprope is managed by using the satellite attitude data telemetered to the ground. In real time, these data are fed to redundant MassComp computers which contain the preprocessor and the time and frequency observers. Using these systems and trained operators to interpret the data, as well as guidelines from procedures developed preflight, the control team/flight crew formulates the necessary operations for the crew to execute in real time.

As in standard-practice mission design, a series of safety gates has been set up for the various mission phases that become decision points for the operational teams. These mission-specific gates are based on the skiprope amplitude and phase as predicted by the observers. Some of the gates were shown in the initial portion of the paper (fig. 42); for example, 20 m is the maximum skiprope allowable to begin retrieve from station 2.

V. END-TO-END SIMULATIONS

End-to-end simulations of the total TSS-1 mission were performed to demonstrate that the proposed skiprope controls will work in an environment which is as close to reality as is available preflight, including higher-order skiprope modes and skiprope observers. The time-domain observer utilized the model certified for flight. Also considered was simulated telemetry data, assumed errors,

and data dropouts. The skiprope controls were in conjunction with the model 3 dynamics (20-bead model of tether). The case that is presented included the following:

- Phased current flow
- Yaw maneuver
- PCS control of satellite using validated PCS models
- Concentric damper using test-verified models and parameters.

Use of the baseline skiprope control operations allows successful retrieval of the satellite. The system meets all docking constraints. It is concluded that the use of the baseline approach (skiprope control) enhances the probability of a successful mission. The results of an end-to-end simulation show the basis for this conclusion.

Table 6 gives the skiprope amplitude at various times of the mission. The maximum skiprope observed during science operations was 55 m. At the start of retrieve 2, the amplitude was 14 m maximum. Figures 98 through 103 show the time-domain (total mission) results for the skiprope amplitude, skiprope angular momentum, satellite pitch (in degrees), satellite pitch rate (degrees/second), satellite roll (degrees), and satellite roll rate (degrees/second). Due to the compression of the time scale, it is difficult to identify the effects of the individual events, although the effects of the yaw maneuver are clear around the 25-h time point. The yaw maneuver and second retrieval events are presented with expanded time scale.

Figure 104 shows the orbiter yaw rate in degrees per second. Figure 105 shows the skiprope amplitude as it is reduced from about 25 m to 10 m. Figure 106 shows the reduction in skiprope angular momentum and indicates a reduction from about –200 N-m-s to approximately –25 N-m-s.

The results during the second retrieval are shown on figures 107 through 118 and include skiprope amplitude (m), skiprope angular momentum, out-of-plane and in-plane skiprope third-mode amplitude (m), satellite attitude pitch (degrees), pitch rate (degrees/second), roll (degrees), roll rate (degrees/second), and pitch control impulse. Satellite docking angles α and β are also included. The effects of resonance between satellite pendulous motion and skiprope dynamics can be clearly seen around the 29-h time period.

The effectiveness of the PCS damping satellite motion is observed from 29.2 to 29.6 h. The effects of the concentric docking ring damper upon the skiprope amplitude can be seen on figure 107 from 29.8 to 30.6 h. It is also effective in damping third mode (figs. 108 and 109). The skiprope angular momentum also approaches zero (fig. 110).

Although limited, end-to-end simulation results demonstrate they can predict the basic capability of the skiprope control approach which has been baselined.

Table 6. Skiprope amplitude during mission from end-to-end simulation results.

	End of Station 1	State of Current Damping	End of Current Damping	Start of Yaw Maneuver	After Yaw Maneuver	Start of Retrieve 2
Skiprope Amplitude (m)	55 by 7	58 by 8	35 by 5	35 by 17	17 by 5	14 by 6

Full Mission Results

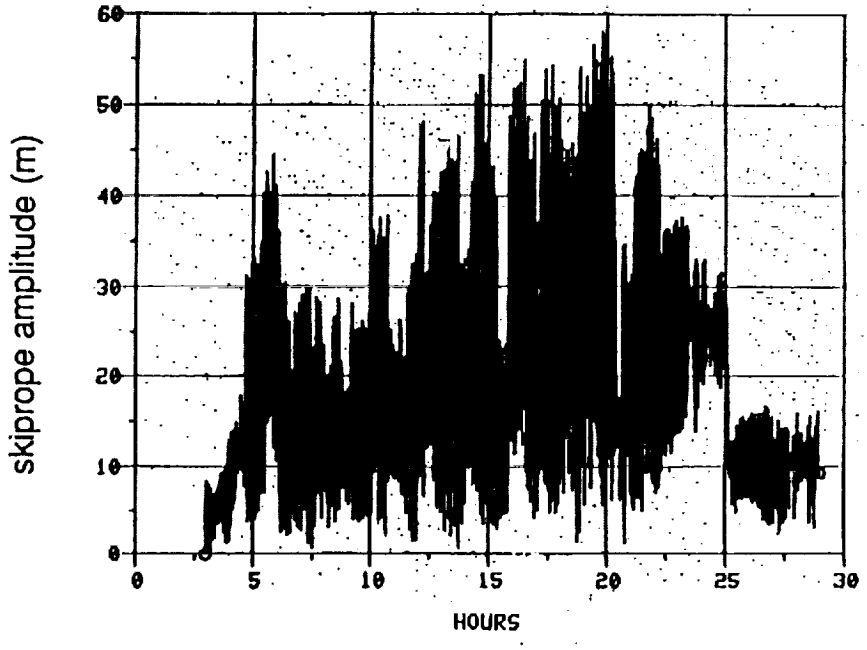

Figure 98. End-to-end simulation results (skiprope amplitude).

Full Mission Results

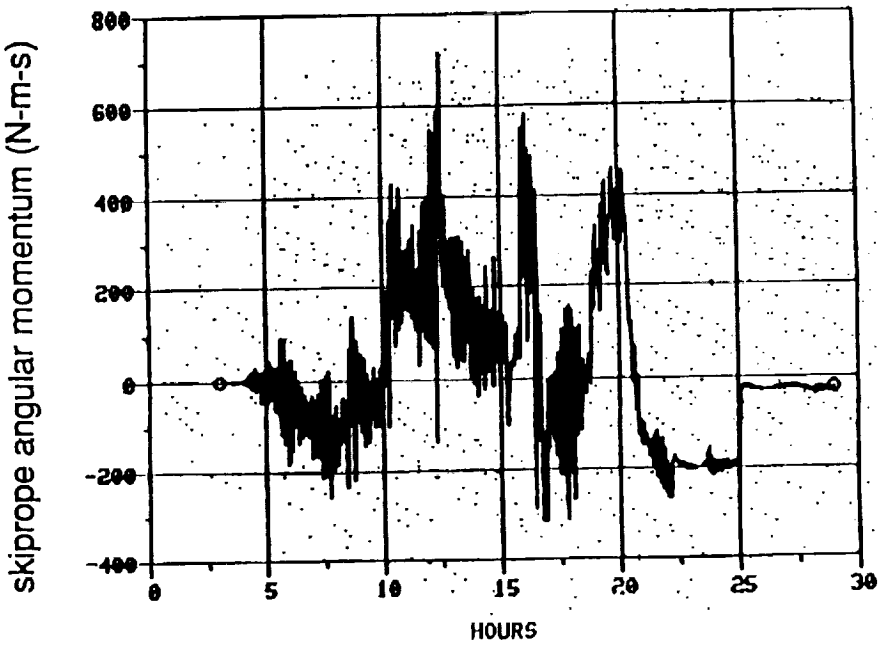

Figure 99. End-to-end simulation results (skiprope angular momentum).

Full Mission Results

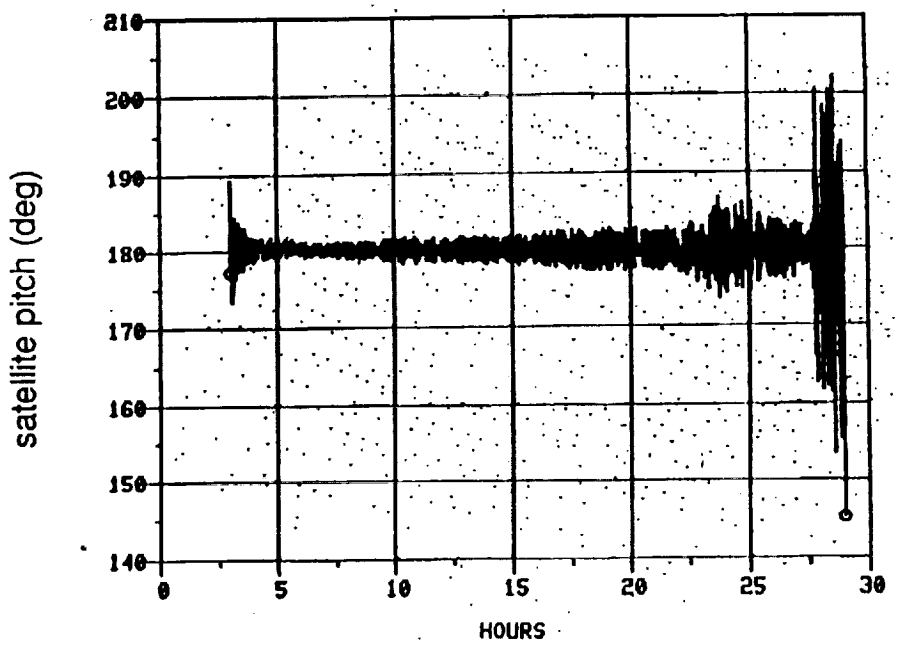

Figure 100. End-to-end simulation results (satellite pitch attitude).

Full Mission Results

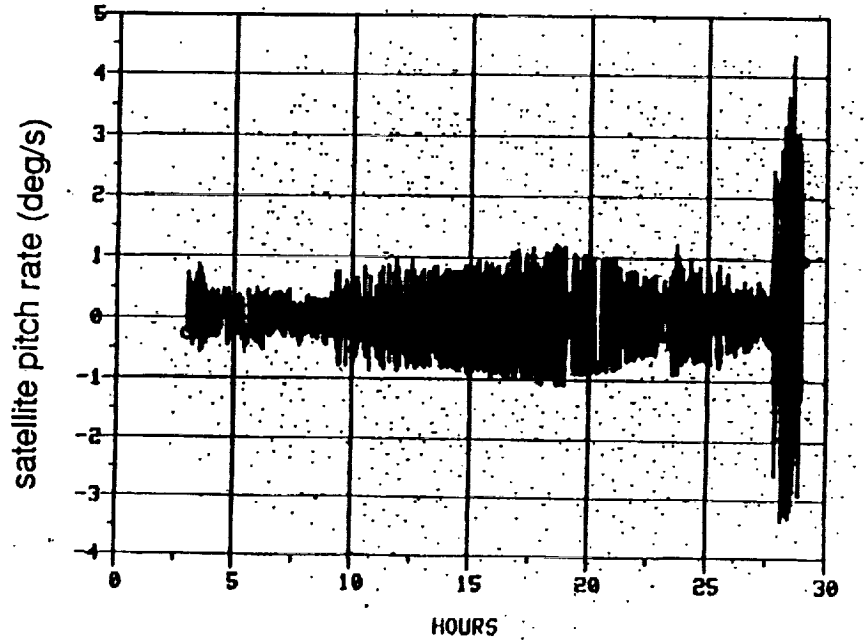

Figure 101. End-to-end simulation results (satellite pitch rate).

Full Mission Results

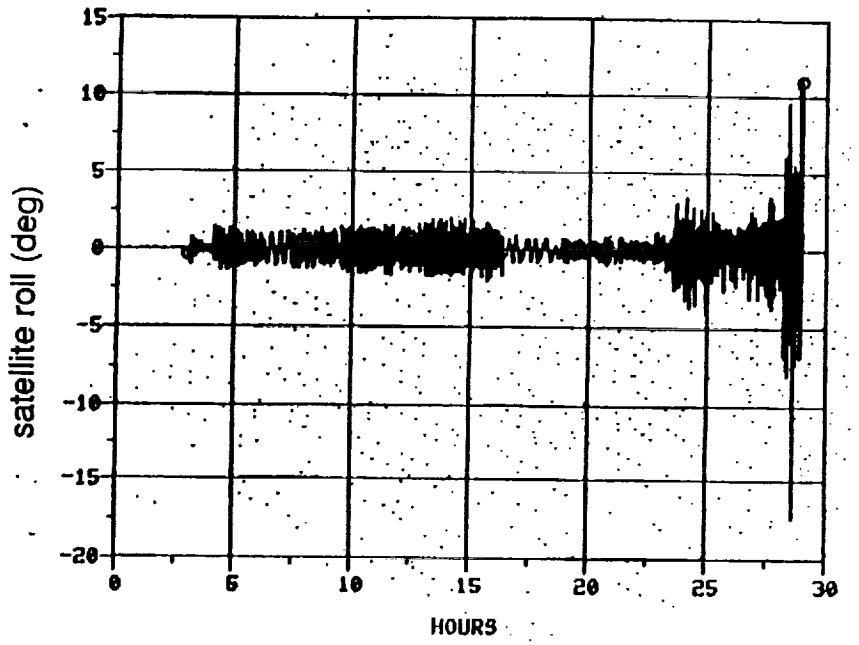

Figure 102. End-to-end simulation results (satellite roll attitude).

Full Mission Results

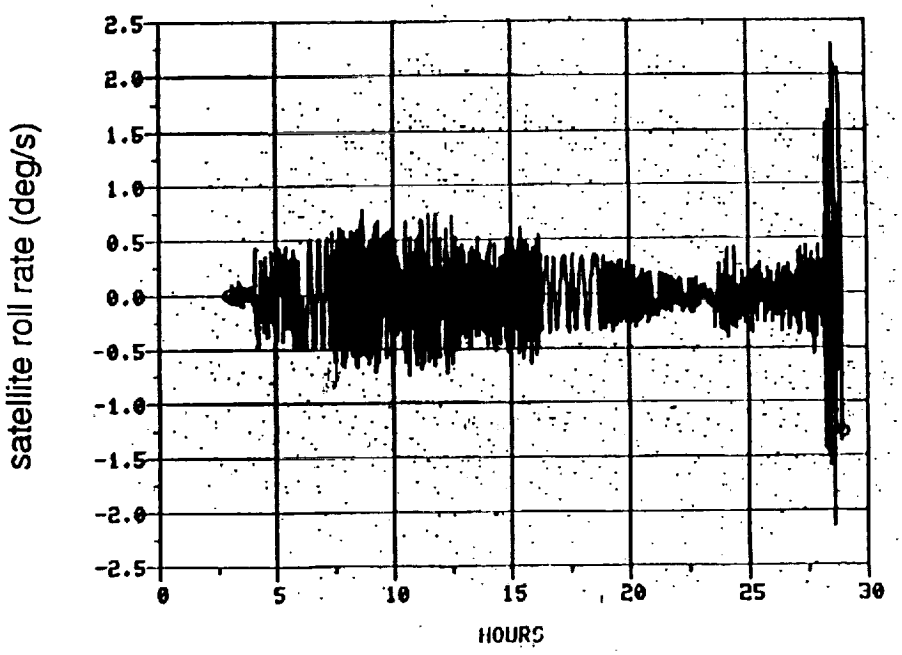

Figure 103. End-to-end simulation results (satellite roll rate).

Yaw Maneuver Results

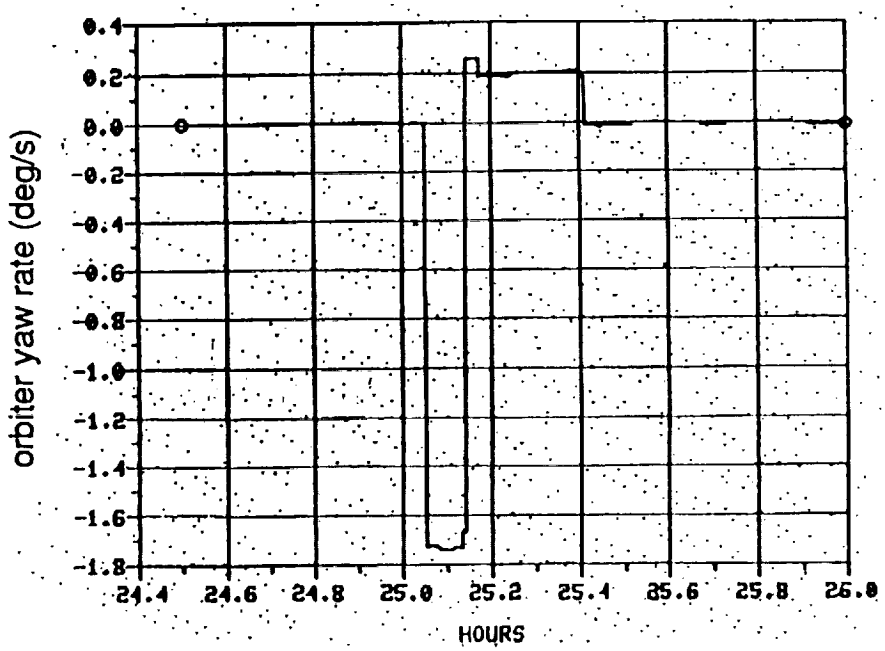

Figure 104. End-to-end simulation results (orbiter yaw rate).

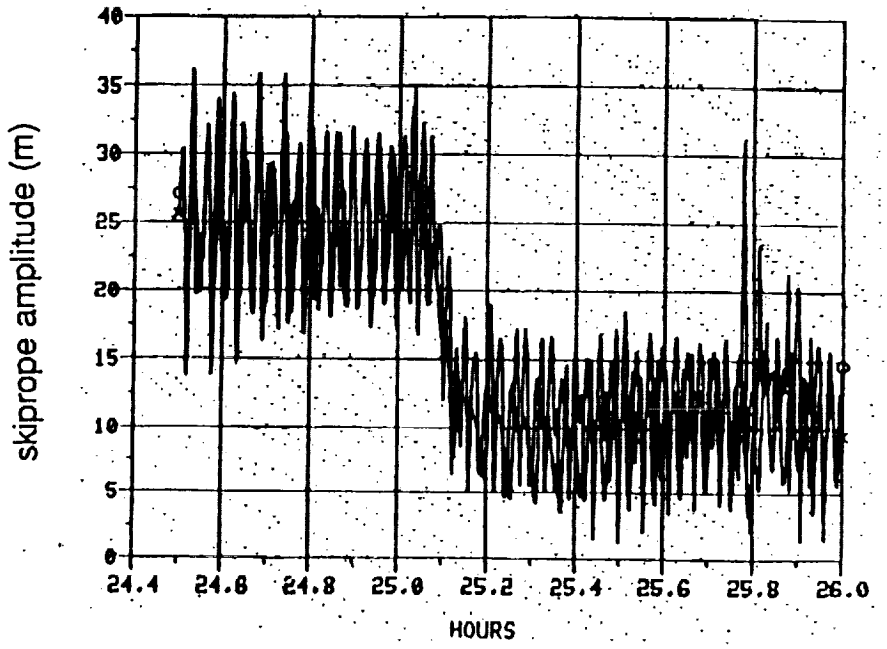

Figure 105. End-to-end simulation results (skiprope amplitude).

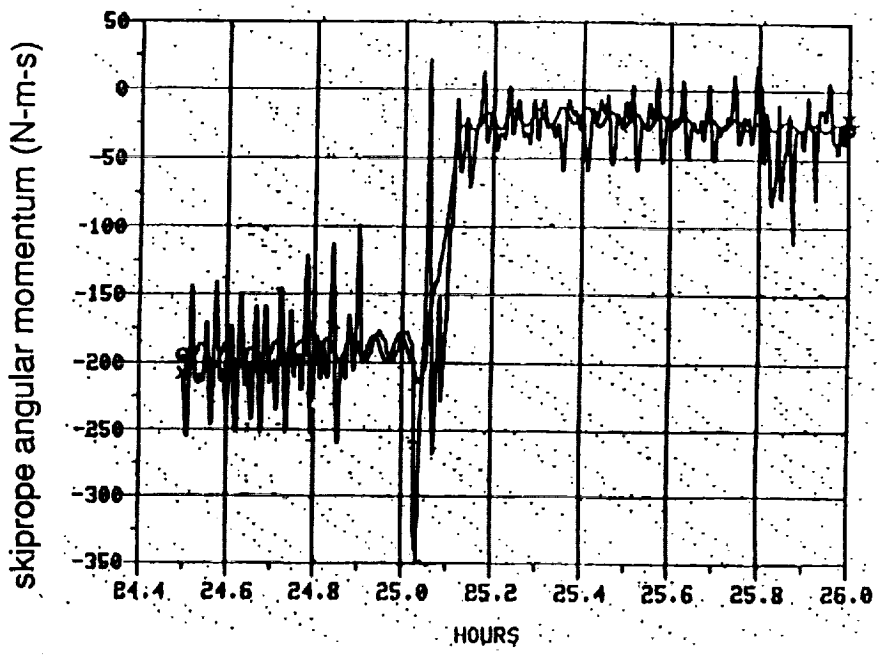

Figure 106. End-to-end simulation results (skiprope angular momentum).

Retrieval 2 Results

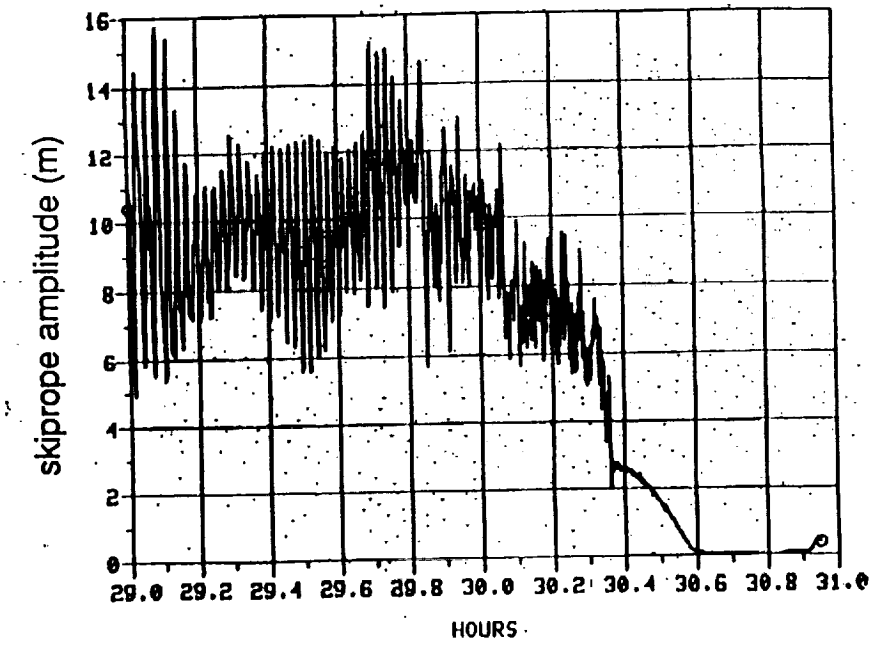

Figure 107. End-to-end simulation results (skiprope amplitude).

Retrieval 2 Results

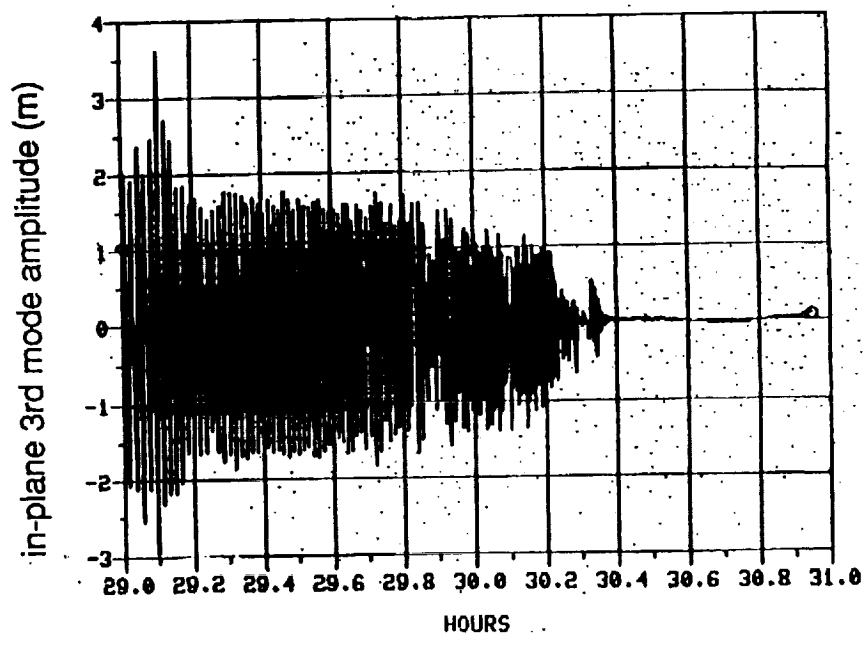

Figure 108. End-to-end simulation results (skiprope third-mode amplitude).

Retrieval 2 Results

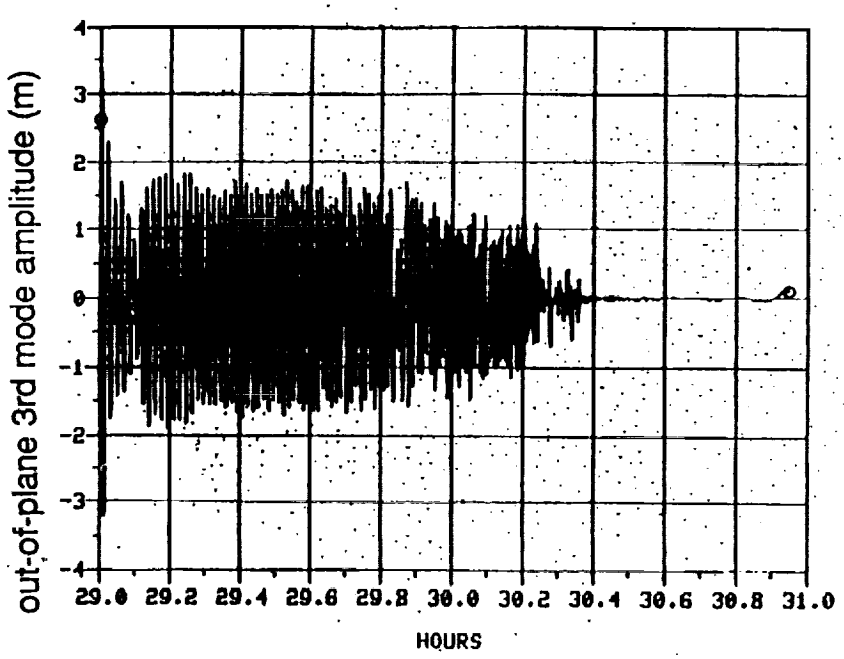

Figure 109. End-to-end simulation results (skiprope third-mode amplitude).

Retrieval 2 Results

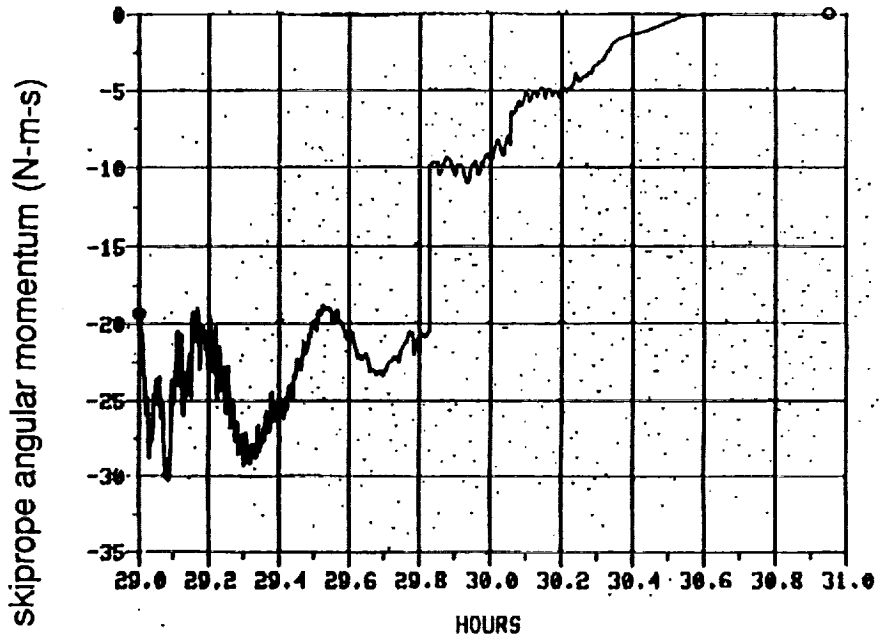

Figure 110. End-to-end simulation results (skiprope angular momentum).

Retrieval 2 Results

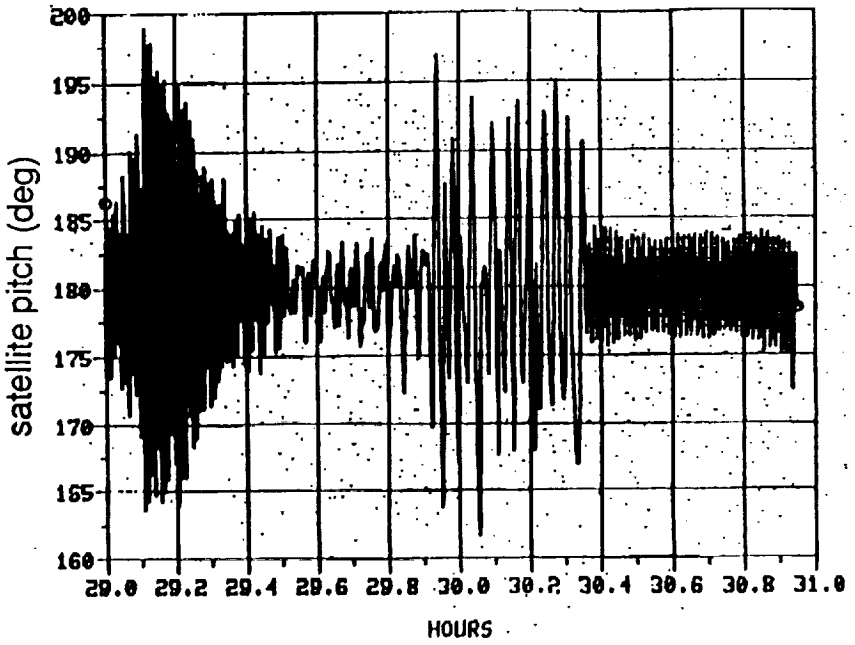

Figure 111. End-to-end simulation results (satellite pitch attitude).

Retrieval 2 Results

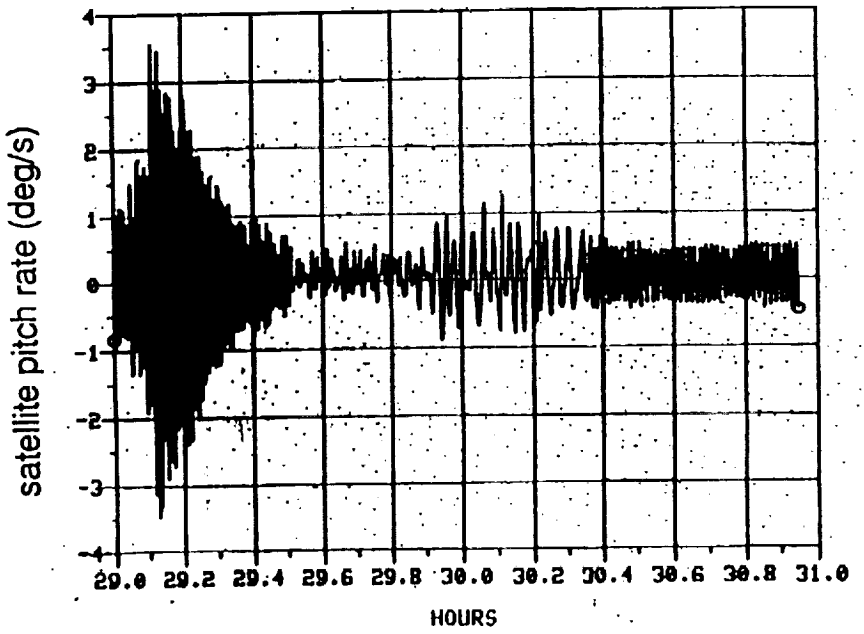

Figure 112. End-to-end simulation results (satellite pitch rate).

Retrieval 2 Results

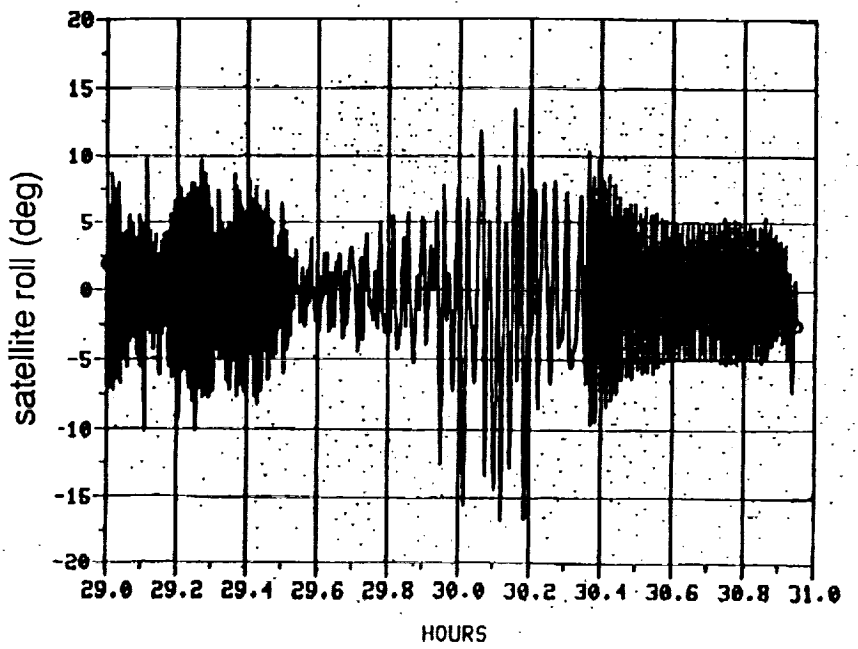

Figure 113. End-to-end simulation results (satellite roll attitude).

Retrieval 2 Results

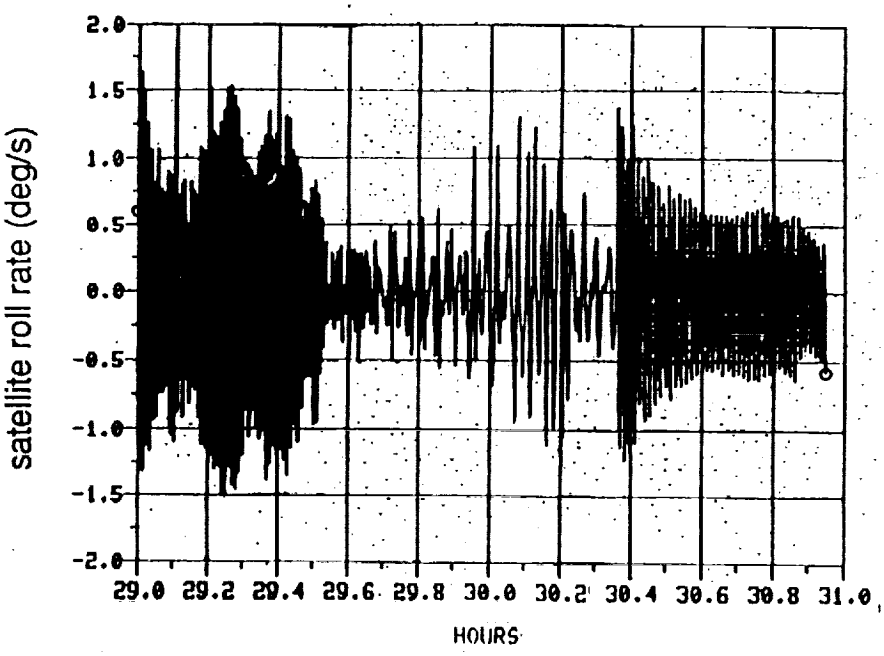

Figure 114. End-to-end simulation results (satellite roll rate).

Retrieval 2 Results

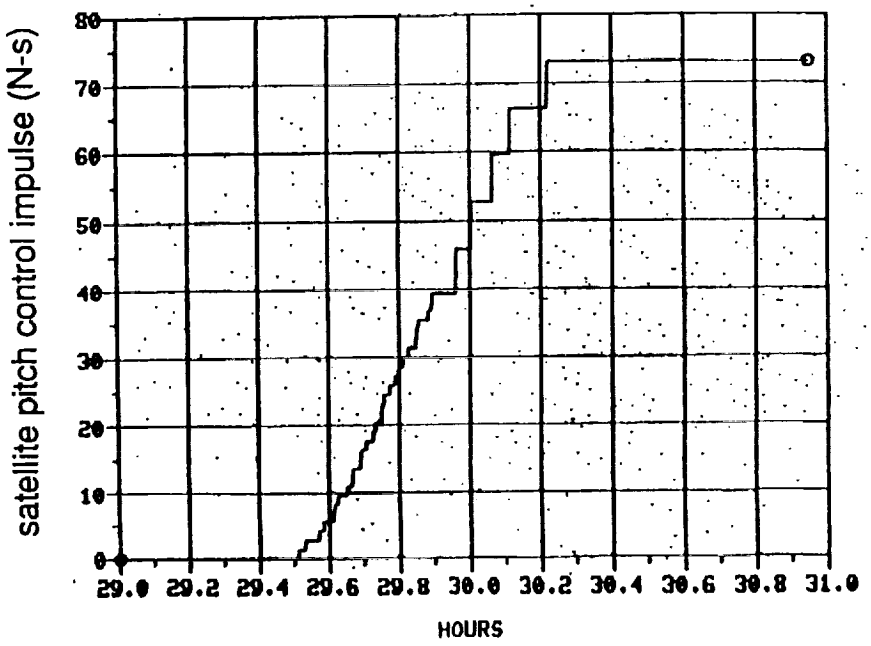

Figure 115. End-to-end simulation results (satellite pitch control impulse).

Retrieval 2 Results

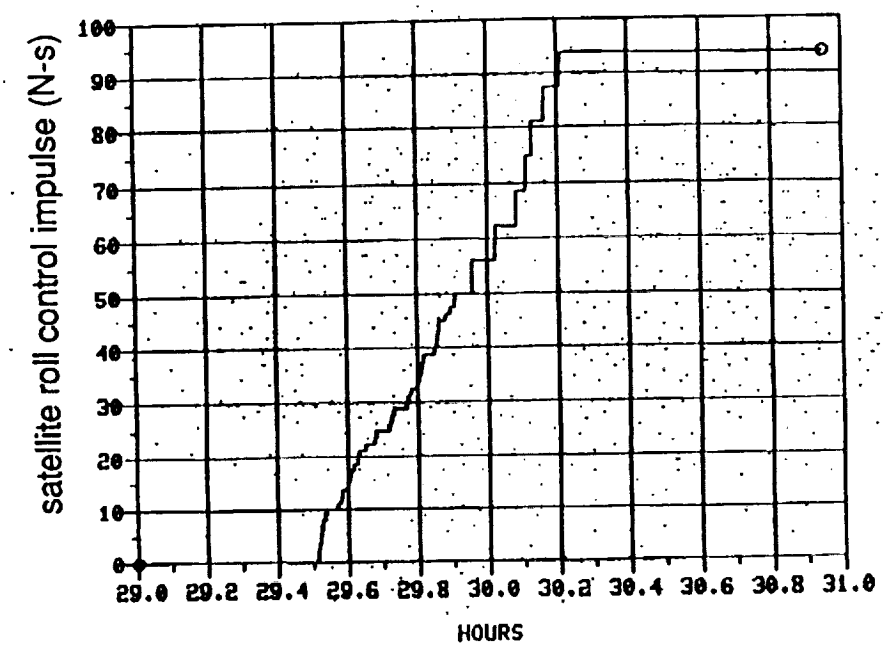

Figure 116. End-to-end simulation results (satellite roll control impulse).

Retrieval 2 Results

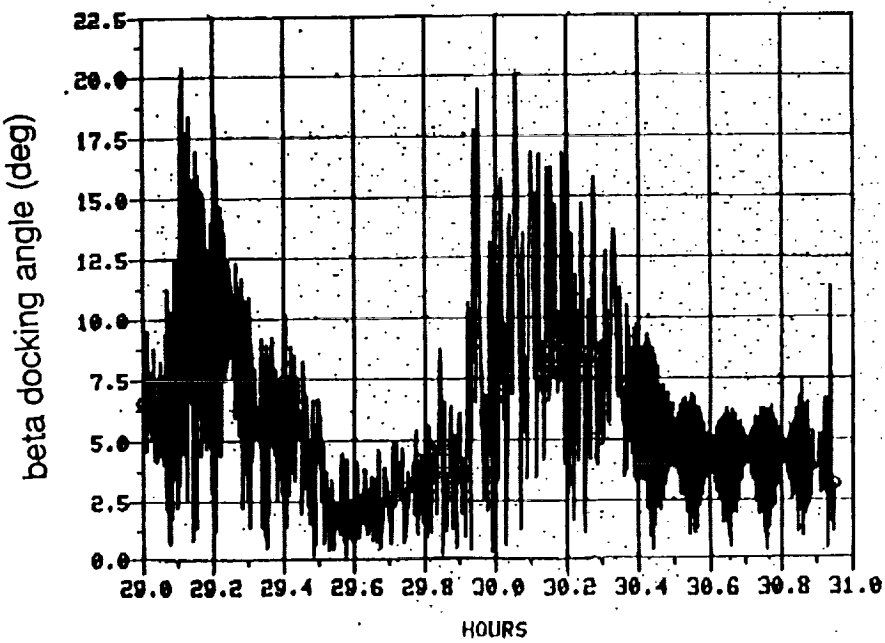

Figure 117. End-to-end simulation results (satellite docking angle).

Retrieval 2 Results

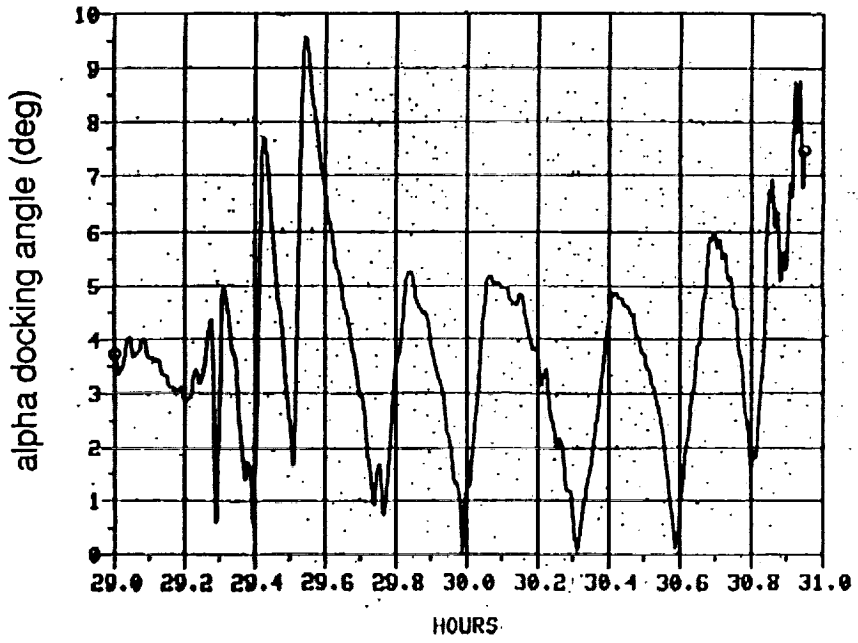

Figure 118. End-to-end simulation results (satellite docking angle).

VI. TSS-1 FLIGHT RESULTS

The tethered satellite flight (TSS-1, STS-46) was launched on July 31, 1992. Mechanical difficulties precluded deployment to planned length. Only 256 m of tether deployment was reached with some difficulty (fig. 119). The satellite stayed at this length for a significant period. At 256 m, only approximately 40 V of EMF and a tether current close to 20 mA were achieved. Tether currents at this level were not great enough to significantly excite the tether string dynamics, however, skiprope amplitudes of less than 1 m due to other excitation sources were observed. Libration modes, satellite pendulous oscillation, and longitudinal slack/taut tether dynamics were experienced. The crew demonstrated that the procedures and controls to control these dynamics were adequate. At 256 m, the system was stable with respect to the orbiter, and the satellite remained at this length and dynamic state with very little maintenance required by the crew. Also, it was demonstrated that in the region of greatest concern from a safety and mission success standpoint (close proximity, both deploying and retrieving), the satellite was well behaved and within flyable envelopes. The crew also had the opportunity to use the manual tether length control mode, which is a contingency mode. The manual mode provided the flexibility needed to deal with the anomalous conditions of this mission.

While little was learned about the skiprope, much was learned concerning the total dynamics of the TSS, and the flight served to whet the appetite of the scientists and the dynamicists alike.

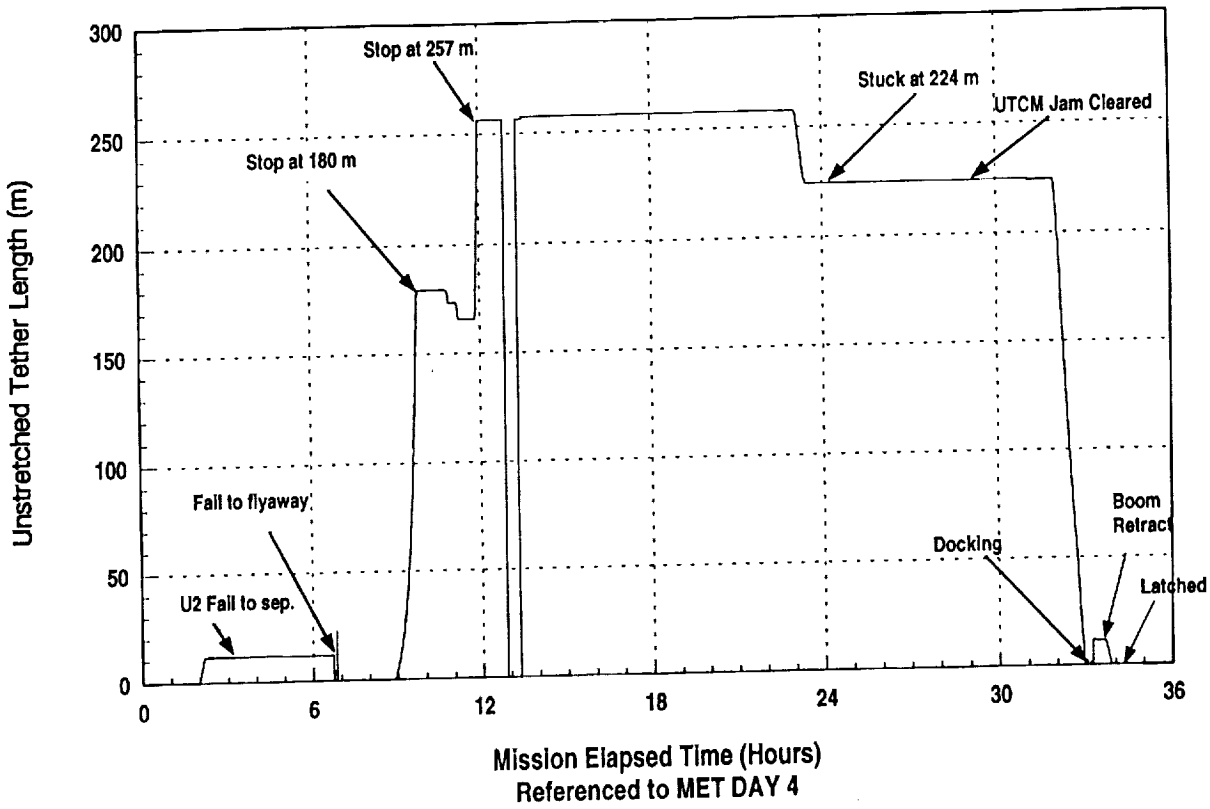

Figure 119. Measured unstretched tether length.

VII. SUMMARY

In summary, the control of tether dynamics, including skiprope containment, has been demonstrated by simulations. The basic understanding of the physics of the problem has been verified to the extent possible on Earth. The tether deployment and docking mechanism was verified and acceptance tested prior to flight. A detailed skiprope control plan was in place, its design completed, and all systems verified. It worked very well during flight. Those include three observers for estimating skiprope data from the satellite telemetry data.

- Time domain
- Frequency domain
- Visual by crew.

For TSS-1, the skiprope control tools for the plan were:

- Orbiter yaw maneuver
- Canted satellite side thrusters
- Payload control supervision or manual control
- Deployer boom tip damper
- Tether current flow
- Contingency maneuvers (slow retrieval and spinning satellite).

All were verified and put in place with proper procedures definition and training (ground and flight crews). All ground and flight equipment were certified. The system worked as expected during TSS-1 flight.

The various simulations used to design, verify, and operate the system went through a rigid verification process to show they all produce comparable results.

The orbiter safety was provided for and verified by using:

- Redundant tether cutters
- Orbiter breakout maneuver
- Completed phase III safety review
- Completed flight operations review.

Although there are risks in flying a system that cannot be totally ground verified, reasonable steps were taken before the system was declared ready for flight. The flight showed no real evidence

of skiprope out to the 256 m of deployment achieved. In fact, most of the tether and end-body dynamics displayed better behavior than expected. Flight evaluation is currently in progress.

It is shown in this report that there is a strong interaction between orbital mechanics of the tethered system, various dynamic modes such as satellite libration, pendulous modes, and tether skiprope—all requiring various control procedures to ensure a successful mission.

TSS-1 design, in the initial phases, concentrated on the various elements, satellite, tether, and deployer/retrieval mechanism design. Only in the later phases did the full system interaction of the tethered system become clear, indicating the various interaction problems discussed in this report. As a result, the solutions to the skiprope control became add-on fixes, emphasizing operational procedures versus the development of an up-front system hardware/software design. Future tethered satellite missions should start with the system understanding developed during TSS-1 and then develop a new set of requirements. The design should be a more integral system for handling all the interactions, particularly satellite modes and skiprope. As an example, fully automatic closed-loop attitude control of the satellite in conjunction with passive dampers could possibly control the modes without the orbiter yaw maneuver. Dampers could be located on the satellite as well as the deployer docking ring. This approach could potentially eliminate the intensive ground operations using the observers, yaw maneuver, and the PCS damping of the satellite pendulous mode.

VIII. CONCLUSION

The first TSS mission did not provide sufficient experience to verify the total adequacy of the system; however, the lessons learned in designing and verifying this system provide a sound basis for design of future tethered satellite missions. These lessons learned will allow possible simplification of the system such as full closed-loop satellite attitude control and a more refined deployer tip damper. These improvements will, in all likelihood, eliminate the orbiter yaw maneuver requirement, and could eliminate the need for the skiprope observer, though, for other reasons, they may still be required.

The overall skiprope management could therefore be simplified, depending on future flight experience.

REFERENCES

1. National Aeronautics and Space Administration: "Tethers In Space Handbook—Second Edition."

2. Glaese, J.R., and Pastrick, H.L.: "Modal Synthesis Simulation of the Shuttle Orbiter Tethered Satellite System." AIAA/AAS, Astrodynamics Conference, August 9–11, 1982, San Diego, CA.

3. Redmon, J.W. Jr.: "Novel Aerospace Mechanisms: A Passive Tether Damping Device for Tethered Satellite, and a Pin/Latch Structural Interface System." NASA, Marshall Space Flight Center, Huntsville, AL.

4. Rockwell International: "Space Shuttle Orbiter Operational Level C Functional Subsystem Software Requirements, Guidance, Navigation, Control, Part C, Flight Control Orbit Digital Autopilot." STS-83-009B dated June 30, 1987.

5. Mowery, D.K.: "TSS Simulation Plan." ED13-08-88(MSFC), February 3, 1988.

6. Galaboff, Z.J.: "TSS Simulation Validation Report." ED13-44-91, September 3, 1991.

7. Lunsford, V.: "Skiprope Containment Damping Development Test Report, R." MCR-91-1348, Martin Marietta Astronautics Group, Denver, CO, October, 1991.

8. Bodley, C., Flanders, H., Grosserode, P., and Paquette, K.: "Tethered Satellite System Orbital Dynamics Model 3." TSS-ODM3-01, Martin Marietta, Astronautics Group, Denver, CO, August 1988.

*U.S. GOVERNMENT PRINTING OFFICE: 1993-728-150-60044

REPORT DOCUMENTATION PAGE

Form Approved
OMB No 0704-0188

1. AGENCY USE ONLY (Leave blank)	2. REPORT DATE	3. REPORT TYPE AND DATES COVERED
	May 1993	Technical Paper

4. TITLE AND SUBTITLE

The Dynamic Phenomena of a Tethered Satellite
NASA's First Tethered Satellite Mission (TSS-1)

5. FUNDING NUMBERS

6. AUTHOR(S)

R.S. Ryan, D.K. Mowery, and D.D. Tomlin

7. PERFORMING ORGANIZATION NAME(S) AND ADDRESS(ES)

George C. Marshall Space Flight Center
Marshall Space Flight Center, Alabama 35812

8. PERFORMING ORGANIZATION REPORT NUMBER

M-719

9. SPONSORING/MONITORING AGENCY NAME(S) AND ADDRESS(ES)

National Aeronautics and Space Administration
Washington, DC 20546

10. SPONSORING/MONITORING AGENCY REPORT NUMBER

NASA TP-3347

11. SUPPLEMENTARY NOTES

Prepared by Structures and Dynamics Laboratory, Science and Engineering Directorate.

12a. DISTRIBUTION/AVAILABILITY STATEMENT

Unclassified — Unlimited

Subject Category: 18

12b. DISTRIBUTION CODE

13. ABSTRACT *(Maximum 200 words)*

The tethered satellite system (TSS) was envisioned as a means of extending a satellite from its base (space shuttle, space station, space platform) into a lower or higher altitude in order to more efficiently acquire data and perform science experiments. This is accomplished by attaching the satellite to a tether, deploying it, then reeling it in. When its mission is completed, the satellite can be returned to its base for reuse. If the tether contains a conductor, it can also be used as a means to generate and flow current to and from the satellite to the base. When current is flowed, the tether interacts with the Earth's magnetic field, deflecting the tether. When the current flows in one direction, the system becomes a propulsive system that can be used to boost the orbiting system. In the other direction, it is a power generating system. Pulsing the current sets up a dynamic oscillation in the tether, which can upset the satellite attitude and preclude docking. A basic problem occurs around 400-m tether length, during satellite retrieval when the satellite's pendulous (rotational) mode gets in resonance with the first lateral tether string mode. The problem's magnitude is determined by the amount of skiprope present coming into this resonance condition. This paper deals with the tethered satellite, its dynamic phenomena, and how the resulting problems were solved for the first tethered satellite mission (TSS-1). Proposals for improvements for future tethered satellite missions are included. Results from the first tethered satellite flight are summarized.

14. SUBJECT TERMS	15. NUMBER OF PAGES
Dynamics Control Tether	120
	16. PRICE CODE: A06

17. SECURITY CLASSIFICATION OF REPORT	18. SECURITY CLASSIFICATION OF THIS PAGE	19. SECURITY CLASSIFICATION OF ABSTRACT	20. LIMITATION OF ABSTRACT
Unclassified	Unclassified	Unclassified	Unlimited